

FOREWORD

The work described in this report was carried out by personnel of the Astronuclear Laboratory and the Research Laboratories of the Westinghouse Electric Corporation under USAF Contract AF 33(616)-6258. This contract was initiated under Project No. 7351, "Metallic Materials", Task No. 735101, "Refractory Metals". The contract was administered under the direction of the Materials Central, Directorate of Materials and Processes, Aeronautical Systems Division, with Lt. W. E. Smith and Mr. J. T. Gow serving as project engineers.

This report describes the results of research conducted during the period 1 January 1962 to 1 March 1963.

Contrails

ABSTRACT

The influence of carbon additions on the properties of a complex columbium alloy, Cb-10W-5V-1Zr (B-77), was investigated. Carbon additions of 0.077 and 0.15 w/o refined the as-cast grain size and increased hardness. For the conditions of heat treatment investigated, the carbon level had no effect on the 1205 °C (2200 °F) stress rupture strength of B-77, but the carbon containing alloys had higher rupture strains than low carbon B-77. Heat treatment studies did not show any evidence of precipitation hardening effects, however solution annealed and cold rolled B-77 + 0.15 C material gave significantly higher hot hardness values than solution annealed material, suggesting that carbide precipitation on dislocations was contributing to high temperature strength. Preliminary data showed grain boundary sliding occurred in B-77 during creep testing at 1205 °C (2200 °F).

The Cb rich corner of the Cb-V-Mo ternary system was studied by means of metallography, lattice parameter measurements, and melting point determinations. The system was single phase under all conditions of heat treatment. Classical precipitation hardening behavior was exhibited by Cb-Hf-N and Cb-W-Hf-N alloys. The precipitation of HfN constituted the hardening mechanism in these alloys. The effect of heat treatment in high temperature strength was evaluated by means of hot hardness measurements. The hot hardness values for these alloys were much superior to those of B-66 at temperatures up to 1315 °C (2400 °F).

This technical documentary report has been reviewed and is approved.



I. PERLMUTTER
Chief, Physical Metallurgy Branch
Metals and Ceramics Division
AF Materials Laboratory

TABLE OF CONTENTS

	<u>Page</u>
I. INTRODUCTION	1
II. GENERAL EXPERIMENTAL PROCEDURE	2
III. INFLUENCE OF CARBON ADDITIONS ON THE PROPERTIES OF B-77	7
INTRODUCTION	7
MELTING AND FABRICATION	7
EFFECTS OF HEAT TREATMENT	15
MECHANICAL PROPERTIES	23
GRAIN BOUNDARY SLIDING	40
IV. CONSTITUTION AND PROPERTIES OF Cb-V-Mo ALLOYS	48
LITERATURE	48
EXPERIMENTAL PROCEDURE	48
RESULTS	50
V. STUDIES OF Cb-Hf-N ALLOYS	57
ALLOY PREPARATION	57
EFFECTS OF HEAT TREATMENT	58
Cb-W-Hf-N ALLOYS	78
VI. REFERENCES	91

LIST OF FIGURES

<u>No.</u>		<u>Page</u>
1	Vacuum Hot Hardness Tester.	6
2	Macrostructure of B-77 Arc Melted Ingots. As Cast.	10
3	Processing of Low Interstitial B-77, Heat VAM-57.	11
4	Processing of Low Interstitial B-77, Heat VAM-68.	12
5	Processing of B-77 + 0.075C, Heat VAM-61.	13
6	Processing of B-77 + 0.15C, Heat VAM-69.	14
7	Microstructure of B-77 Solution Annealed 4 Hours at 1800 °C.	16
8	Microstructure of B-77 Solution Annealed 4 Hours at 1800 °C. Aged 2 Hours at 1200 °C.	17
9	Microstructure of B-77 Solution Annealed 4 Hours at 1800 °C. Aged 2 Hours at 1400 °C.	18
10	Effect of Aging Temperature on the Hardness of B-77. (1 Hour Anneals).	19
11	Effect of Aging Temperature on the Hardness of B-77. (1 Hour Anneals).	22
12	Effect of Temperature on the Hardness of Recrystallized B-77.	26
13	Correlation of Hot Hardness with Tensile Strength for Columbium Alloys.	27
14	Hot Hardness of B-77 as a Function of Heat Treatment.	29
15	Effect of Prior Treatment on the Hot Hardness of B-77 Alloys.	31
16	Microstructure of B-77 Sheet. Recrystallized 1 Hour at 2700 °F (1480 °C).	34
17	1205 °C (2200 °F) Stress Rupture Data for B-77 with Varying Carbon Levels.	36

<u>No.</u>		<u>Page</u>
18	Photographs of Fractured B-77 Stress Rupture Specimens	38
19	Microstructure of Low Carbon B-77 (VAM-57) Annealed 1 Hour at 2700 °F (1480 °C). Prior to Stress Rupture Testing at 2200 °F (1205 °C).	39
20	Fixture Used to Scribe Lines on the Surface of Creep Specimens.	42
21	Microstructure of VAM-68 (B-77) Showing the Scribe Lines Intersecting Grain Boundaries. Prior to Creep Straining.	43
22	Microstructure of VAM-68 (B-77) Showing Grain Boundary Sliding. After Creep Straining at 1205 °C (2200 °F).	44
23	Microstructure of VAM-68 (B-77) Showing Grain Boundary Sliding as Evidenced by the Displacement at the Triple Point.	45
24	Microstructure of VAM-61 (B-77 + 0.077C) Showing Grain Boundary Sliding. After Creep Straining at 1205 °C (2200 °F).	47
25	Variation of Lattice Parameter with Composition for Cb-V-Mo Alloys.	51
26	Variation of Melting Point with Composition for Cb-V-Mo Alloys.	52
27	Effect of Composition on the Hardness of Cb-V-Mo Alloys.	53
28	Hot Hardness of Cb-V-Mo Alloys.	54
29	Correlation of Hot Hardness with Change in Lattice Parameter for Cb-V-Mo Alloys.	56
30	Dynapak Extruded Cb-5Hf-0.2 N Alloy.	59
31	Effect of Aging Temperature on the Hardness of a Cb-5Hf-0.1 N Alloy.	60
32	Microstructure of Cb-5Hf-0.1 N Alloy (NC-370). Aged 4 Hours at 1800 °C.	62
33	Effect of Aging Temperature on the Hardness of a Cb-5Hf-0.2 N Alloy (Aged 1 Hour).	63

<u>No.</u>		<u>Page</u>
34	Microstructure of Cb-5Hf-0.2 N Alloy (VAM-73). Solution Annealed 2 Hours at 1800 °C and Quenched.	64
35	Microstructure of Cb-5Hf-0.2 N (VAM-73). Solution Annealed 2 Hours at 1800 °C and Quenched. Aged 48 Hours.	66
36	Extraction Replica of Cb-5Hf-0.2 N Alloy. Aged 1 Hour at 1200 °C.	67
37	Extraction Replica of Cb-5Hf-0.2 N Alloy. Aged 1 Hour at 1400 °C	68
38	Extraction Replica of Cb-5Hf-0.2 N Alloy. Aged 1 Hour at 1600 °C.	68
39	Electron Micrograph of Bulk Extracted Residue from Cb-5Hf-0.2 N Alloys. Aged 1 Hour at 1200 °C.	73
40	Electron Micrograph and Diffraction Pattern of Bulk Extracted Residue from Cb-5Hf-0.2 N Alloys in Solution for 23 Hours. Aged 1 Hour at 1400 °C.	74
41	Electron Micrograph and Diffraction Pattern of Bulk Extracted Residue from Cb-5Hf-0.2 N Alloys in Solution for 71 Hours. Aged 1 Hour at 1400 °C.	75
42	Electron Micrograph and Diffraction Pattern of Bulk Extracted Residue from Cb-5Hf-0.2 N Alloys. Aged 1 Hour at 1600 °C.	76
43	Effect of Temperature on the Hot Hardness of Cb-5Hf and Cb-5Hf-0.2 N Alloys.	77
44	Microstructure of Cb-10W-5Hf-0.15 N (NC 385-1). Solution Annealed 2 Hours at 1800 °C and Quenched.	80
45	Microstructure of Cb-10W-5Hf-0.07 N (NC-385-2). Solution Annealed 2 Hours at 1800 °C and Quenched.	80
46	Microstructure of Cb-10W-5Hf-0.15 N (NC 385-1). Solution Annealed 2 Hours at 1800 °C and Quenched. Aged 1 Hour at 1400 °C.	81
47	Microstructure of Cb-10W-5Hf-0.07 N (NC 385-2). Solution Annealed 2 Hours at 1800 °C and Quenched. Aged 1 Hour at 1400 °C.	82

Contrails

<u>No.</u>		<u>Page</u>
48	Microstructure of Cb-10W-5Hf-0.15 N (NC 385-1). Solution Annealed 2 Hours at 1800 °C and Quenched. Aged 1 Hour at 1400 °C.	83
49	Effect of Aging Temperature on the Hardness of Cb-W-Hf-N Alloys. Aged 1 Hour.	84
50	Effect of Temperature on the Hot Hardness of Cb-W-Hf-N Alloys.	86
51	Effect of Temperature on the Hot Hardness of Cb-W-Hf-N Alloys.	87
52	Effect of Temperature on the Hot Hardness of Cb-W-Hf-N Alloys.	88
53	Effect of Heat Treatment on the Hot Hardness of a Cb-10W 5Hf-0.07 N Alloy.	89
54	Effect of Heat Treatment on the Hot Hardness of a Cb-10-W-5Hf-0.15 N Alloy.	90

LIST OF TABLES

<u>No.</u>		<u>Page</u>
1	Chemical Analysis of Columbium	3
2	Source and Form of Alloy Additions	4
3	Chemical Analysis and Hardness of B-77 Ingots	8
4	Effect of Heat Treatment on the Hardness of B-77 Alloys	20
5	Tensile Data for Low Carbon B-77 (VAM-57)	24
6	Bend Transition Temperature for B-77 Alloys	25
7	Elevated Temperature Tensile Data for B-77 Alloys	33
8	1205 °C (2200 °F) Stress Rupture Data for B-77 with Varying Carbon Levels	37
9	Creep Data for B-77 Alloys at 1205 °C (2200 °F)	41
10	Chemical Analyses of Cb-Hf and Cb-Hf-N Alloys	58
11	Hardness of Solution Annealed Cb-5Hf-0.2 N Alloy	61
12	Transmission Electron Diffraction Data Cb-5Hf-0.2 N Alloy	70
13	X-ray Diffraction Data Cb-5Hf-0.2 N Alloy (VAM-73)	71
14	Diffraction Results on Bulk Extracted Residues of Aged Cb-5Hf-0.2 N Alloy (VAM-73)	72
15	Chemical Analysis of Cb-W-Hf-N Alloys	79

Contrails

I. INTRODUCTION

This report summarizes research conducted on columbium alloys during the period 1 January 1962 to 1 March 1963. The work described in this report is an extension of earlier research (1 January 1956 through 31 December 1961) described in WADC-TR-57-344, Parts I, II, IV, V, and VI. 1, 2, 3, 4, 5.

At the present time, a number of attractive columbium alloys are being evaluated for applications in the nuclear and aerospace fields. However, considerable interest exists in the development of higher strength columbium-base alloys which possess adequate fabricating characteristics. In particular, attention is being focused on alloys optimized with respect to creep strength rather than short time tensile properties. It is apparent that significant improvement in refractory metal alloys will largely be realized through a better understanding of the physical metallurgy of the alloy systems. Studies of strengthening mechanisms, with emphasis on dispersed phase strengthening effects, must be extended to provide the fundamental background necessary to fully realize the potential of refractory metals as high temperature structural materials.

The present investigation was undertaken primarily to explore the effects of dispersed phases on the properties of several columbium alloys. In an earlier phase of this program⁵, studies of the effect of oxygen, nitrogen and carbon additions on the microstructure and properties of Cb-Hf and Cb-Zr alloys were conducted. The objective of this prior study was to provide data concerning the interaction of Group IVa solute elements with interstitial additions. In the present program, research was extended to establish the effect of composition and prior thermal-mechanical treatments on carbon containing B-77 (Cb-10W-5V-1Zr) and Cb-Hf-N alloys. In addition, earlier work on the constitution of the Cb rich corner of the Cb-V-Mo ternary system was completed.

Manuscript released by the authors 1 April 1963, for publication as a WADC Technical Report

II. GENERAL EXPERIMENTAL PROCEDURE

Alloy Preparation. All of the alloys were prepared by either AC consumable electrode arc melting in vacuum, or by conventional DC non-consumable arc melting in an argon atmosphere. For the consumable electrode melting, high purity electron beam melted columbium, having a total interstitial impurity level less than 150 ppm was used as the starting material. The chemical analyses of the various lots of columbium are listed in Table 1. Alloy additions were of good commercial purity. The source and form of the alloy additions are given in Table 2.

Ingot breakdown was accomplished by Dynapak extrusion or by forging. Secondary working was by rolling in all instances. When rolling at temperatures above approximately 260 °C (500 °F) was required, the alloys were jacketed in stainless steel, and the assembly was evacuated and then sealed off. Detailed descriptions of the processing procedures used for particular alloys are listed in the appropriate subsequent sections of this report.

Heat Treatment. High temperature annealing (to 2200 °C) was accomplished in either a vacuum induction furnace or a tantalum tube resistance furnace. In the induction furnace the samples were wrapped in columbium foil and placed in a molybdenum susceptor. Temperature readings were taken with a calibrated optical pyrometer through a Pyrex sight port located above the susceptor. Corrections were made for emissivity and the transmittance of the Pyrex. Three different cooling rates were used in this furnace. Furnace cooling merely involved turning off the power and allowing the samples to cool in the susceptor. The specimens cooled to below red heat in less than three minutes. Radiation cooling involved turning off the power and simultaneously removing the samples from the susceptor by means of a wire actuated through a vacuum seal. Using this technique, specimen cooling was quite rapid dropping below red heat in less than a minute. Finally, samples were quenched by dropping them from the hot zone onto a copper plate externally cooled with liquid nitrogen. Samples annealed in the tantalum tube furnace were also quenched in the same manner. Temperatures were also measured by an optical pyrometer. All annealing was done in vacuum at pressures below 5×10^{-5} Torr. Both furnaces incorporated liquid nitrogen traps to minimize back diffusion of pump oil. Periodically, pure recrystallized columbium samples were annealed in the furnaces to determine if minor contamination was occurring during heat treatment. Microhardness traverses of the check samples showed no evidence of contamination.

Mechanical Property Testing. Sheet tensile specimens, 0.050 inch thick, having a 1-inch gage length and a 0.250-inch gage width were used for most of the mechanical property testing. Low temperature tensile tests were conducted in a "hard" tensile machine of the type described by Manjoine, Wessel, and Pryle.⁶ All tests were run at a strain rate of $1 \times 10^{-3} \text{ sec}^{-1}$ (360%/hr) and the load and deformation were recorded autographically. Temperatures below ambient were obtained using the technique of Wessel and Olleman.⁷

TABLE I. CHEMICAL ANALYSIS OF COLUMBIUM

Lot No.	Form	Source	Analysis (w/o)							
			O	N	C	Ta	Ti	Zr	Fe	Si
WWC-5	Bar*	Wah Chang	0.008	0.006	0.004	< 0.05	< 0.015	< 0.01	< 0.01	< 0.01
1074	Bar*	Haynes	0.0009	0.011	0.01	0.06	< 0.002	< 0.01	< 0.01	< 0.005

*Produced from Electron Beam Melted Ingot

TABLE 2 - Source and Form of Alloy Additions

Alloying Element	Form	Source
Carbon	Graphite Cloth	National Carbon
Hafnium	Crystal Bar	Westinghouse
Tantalum	Powder	National Research Corporation
Tungsten	Sheet	Fansteel
Vanadium	Sheet	Haynes Stellite
Zirconium	Crystal Bar	Foote Mineral

Bend tests were made on specimens 1 inch long, 0.250 inch wide, and 0.050 inch thick, using a bend deflection rate of 0.1 in/min. The samples were tested with the bend axis perpendicular to the rolling direction.

Elevated temperature tensile and stress rupture tests were carried out in spring machines similar to those described by Lawthers and Manjoine.⁸ The heating unit was a tungsten wound furnace located within an Inconel vacuum chamber. Pressure during testing was generally well below 1×10^{-4} Torr. The gage length of the specimen was loosely wrapped in columbium foil to minimize contamination. The strain rate was maintained at $1 \times 10^{-3} \text{ sec}^{-1}$, the same as that used for the low temperature tests.

Hot Hardness Testing. Hot hardness tests were conducted in a vacuum hot hardness machine utilizing a sapphire pyramid indenter mounted in a molybdenum extension shaft. The furnace is a cylindrical chamber 1-1/2 inches in diameter and 6 inches long, heated by Mo resistance elements. Tantalum radiation shields surround the furnace assembly. The sample rests on a molybdenum anvil located inside the furnace. Temperature is measured by means of Pt + Pt/Rh thermocouples placed inside the furnace in close proximity to the test specimen. To carry out testing, a series of samples are placed on a loading tray. The system is then evacuated and the furnace power turned on. After stabilizing the furnace at the desired test temperature, a sample is inserted into the hot zone of the furnace by means of a push rod actuated through an O-ring seal. The specimen is stabilized on the anvil inside the furnace for 15 minutes. Hardness impressions are then made, and the sample is removed from the furnace hot zone by means of the push rod and the next specimen inserted. At the termination of a run, the specimens are removed from the machine and the impressions measured. The samples are then reloaded and the next series of hardness impressions made. The load on the indenter is generally 2.5 kg. Pressure during testing is maintained below 5×10^{-5} Torr, and a liquid nitrogen cold trap is incorporated in the pumping system to minimize back diffusion of pump oil. A photograph of the hot hardness tester with its associated controller and power supply is shown in Figure 1.

Electron Metallography and Phase Identification. Data on the distribution and structure of dispersed phases were obtained using extraction replicas. Samples were polished and etched using standard metallographic procedures. A carbon film was vapor deposited on the surface of the sample, which was then etched in a 10% Br₂ - CH₃ OH solution containing 10% tartaric acid until the carbon film could be floated off. Electron transmission micrographs and selected area electron diffraction patterns were obtained from the extraction replicas. All diffraction patterns were calibrated with Al as a standard. A thin layer of aluminum was vapor deposited on part of the specimen. Dispersed phases were also extracted from the matrix using the bromine-methanol-tartaric acid solution⁴ and the extracted residues identified by x-ray analysis using the Debye-Scherrer technique.

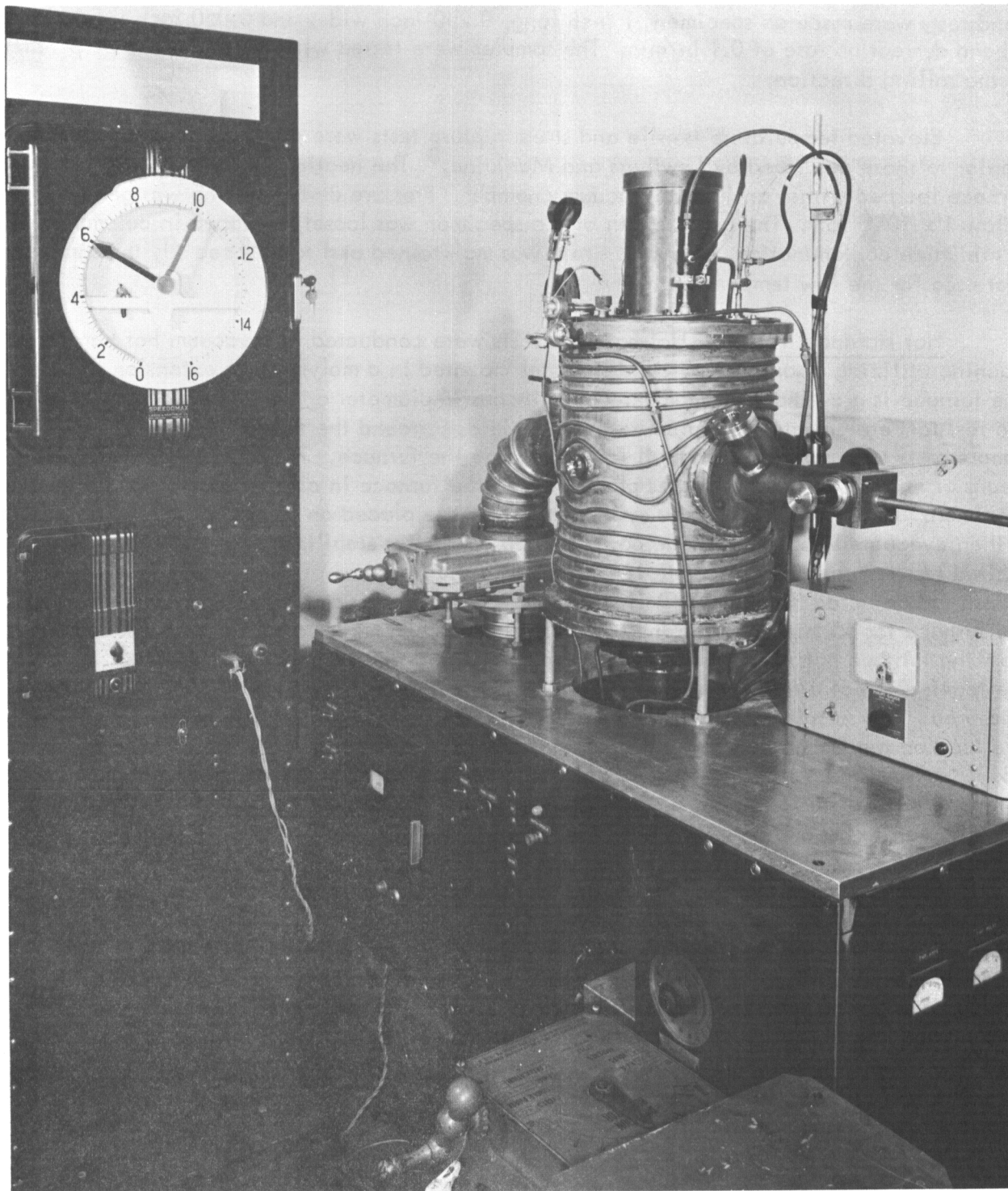


FIGURE 1 - VACUUM HOT HARDNESS TESTER

III. INFLUENCE OF CARBON ADDITIONS ON THE PROPERTIES OF B-77

Introduction

Strengthening of refractory metal alloys by carbide dispersions is an area of active investigation at the present time. Chang has studied the effect of carbide dispersions on the mechanical properties and microstructure of both molybdenum-base and columbium-base alloys.⁹ In the presence of interstitial elements the complex Cb-base alloys F-48 and F-50 exhibit typical precipitation hardening phenomena. The precipitation of a Zr-rich (Zr, Cb) C monocarbide constitutes the strengthening mechanism in these alloys. In the Mo-TZC alloy Chang has shown that strain induced precipitation of TiC has a very pronounced effect on high temperature strength. Recent studies^{10, 11} have shown that carbon additions have a significant strengthening effect in several tantalum base alloys.

In the present investigation the effects of carbon additions on the properties of a fairly high strength solid solution alloy, B-77 (Cb-10W-5V-1Zr), were evaluated. The objective was to determine the influence of carbon level and prior mechanical and thermal history on microstructure and mechanical properties. High purity columbium was used as the base material in preparing the B-77 alloys to eliminate, insofar as possible, the complexities introduced by the presence of other interstitial elements. Two carbon levels, selected to provide carbon contents slightly deficient and slightly in excess of that required to provide stoichiometric ZrC were investigated.

Melting and Fabrication

Four heats of B-77 of varying carbon content were prepared by AC consumable electrode arc melting. High purity electron beam melted columbium was cold rolled to 3/4" wide strip. Vanadium, tungsten, and zirconium sheets of the appropriate thickness were sandwiched between the columbium strip, and the assembly was riveted together with Cb rivets to provide electrodes for melting. Carbon was added by placing the proper quantity of high purity graphite cloth in the electrode assembly. The electrodes were melted into a 1-7/8 inch diameter water-cooled copper mold, at currents ranging from 2300 to 2800 amps. Arc voltage varied from 24 to 28 volts. With AC power, electrode melting is quite uniform even when composite electrodes containing elements of widely differing melting points are used. The uniform "melt off" and vigorous stirring action in the molten pool provided very homogeneous ingots with only a single AC melt.

The chemical analyses and as-cast hardness of the four B-77 ingots are listed in Table 3. Heats VAM-57 and VAM-68 were prepared, without intentional carbon additions, to provide reference data on low interstitial B-77. The nominal carbon contents of heats VAM-61 and VAM-69 were 0.075 w/o and 0.15 w/o respectively. As can

TABLE 3. CHEMICAL ANALYSIS AND HARDNESS OF B-77 INGOTS

Heat No.	Nominal Composition (w/o)	Analysis (w/o)					As-Cast Hardness (VPN)
		W	V	Zr	O	N	
VAM-57	Cb-10W-5V-1Zr	9.59	4.39	0.87	0.0066	0.0025	231
VAM-68	Cb-10W-5V-1Zr	11.3	4.53	1.39	0.0059	0.0043	260
VAM-61	Cb-10W-5V-1Zr-0.075C	10.1	4.59	1.13	0.009	0.003	265
VAM-69	Cb-10W-5V-1Zr-0.15C	9.55	4.69	0.89	0.0073	0.0046	313

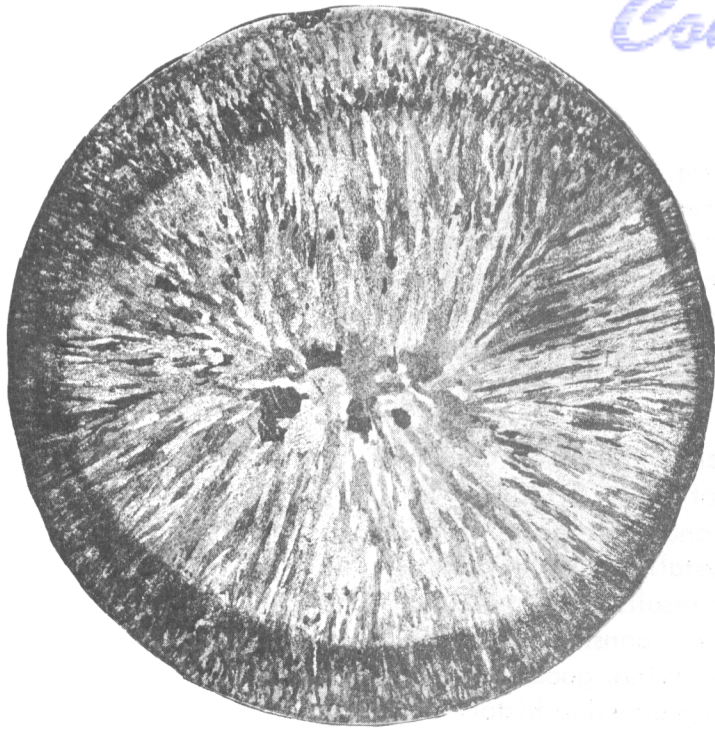
be seen from Table 3, recovery of carbon was excellent. The oxygen and nitrogen levels of all the heats were very low. The low interstitial heat VAM-68 had somewhat higher tungsten and zirconium concentrations than the other alloys in this series. The hardness data listed in Table 3 show that carbon additions significantly increase the as-cast hardness of B-77. Sections of the as-cast ingots were polished and macro-etched to reveal the ingot structure. Figure 2 shows the rather pronounced effect of carbon in refining the as-cast grain size.

One-inch thick sections were taken from each of the ingots and upset forged. The first low interstitial heat (VAM-57) was forged at 1095 °C (2000 °F) to 50% reduction in thickness. The forged plate was conditioned and recrystallized by annealing 1 hour at 1480 °C (2700 °F) in vacuo. The recrystallized material was then rolled at 260 °C (500 °F) to 0.05 inch sheet with excellent results. The remaining portion of heat VAM-57 was side forged at 1205 °C (2200 °F), but considerable edge cracking occurred. However, after conditioning and stress-relieving, good quality sheet was obtained from this portion of the ingot. The detailed processing history of VAM-57 is shown in the flow chart of Figure 3.

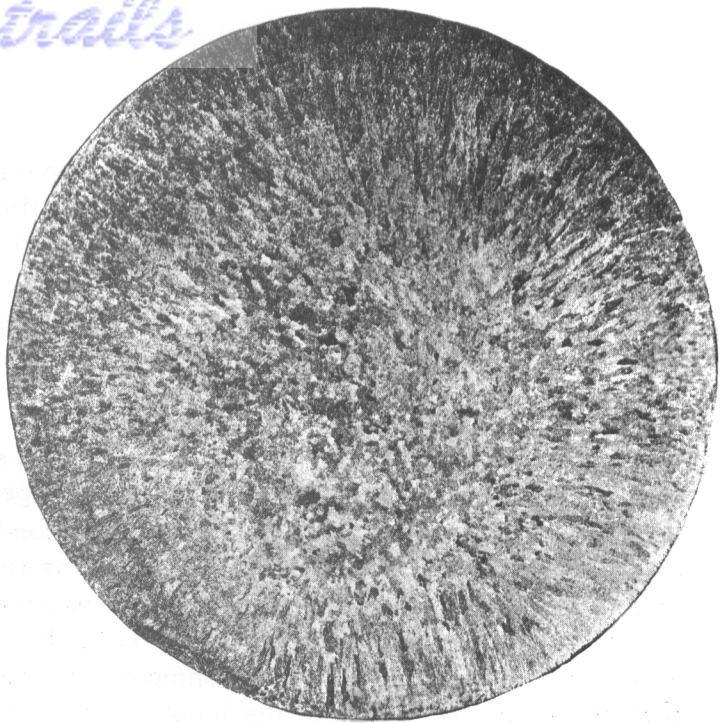
The second low interstitial ingot (VAM-68) was also upset forged at 1205 °C (2200 °F) with very good results. The forged slab was then given a stress-relief anneal of 1 hour at 1095 °C (2000 °F) and subsequently rolled at 260 °C (500 °F). However, a longitudinal split occurred after the first several rolling passes. The material was conditioned to remove the defect and re-rolled at 260 °C without difficulty. The remaining portion of VAM-68 was Dynapak extruded to sheet bar at 1650 °C (3000 °F), using an extrusion ratio of 4:1. The extrusion techniques were the same as those described in an earlier report.⁴ The sheet bar was conditioned, stress-relieved 1 hour at 1205 °C (2200 °F) and rolled at 260 °C (500 °F). Lateral cracking occurred after 12% reduction, hence the slab was reconditioned, canned in an evacuated stainless steel jacket, and rolled at 1095 °C (2000 °F). Rolling characteristics at the higher temperatures were satisfactory, but the stainless steel can fractured after 37% reduction and rolling was terminated at this point. The poorer fabricating characteristics of heat VAM-68 are evidently a reflection of its higher zirconium and tungsten content. The processing data of this heat are summarized in Figure 4.

A one-inch thick section of the B-77 + 0.077 C heat (VAM-61) was also upset forged at 1205 °C (2200 °F) with good results. However, it was necessary to can the forged slab in stainless steel and roll at 1095 °C (2000 °F) to provide sheet stock. The remaining portion of this ingot was Dynapak extruded to sheet bar at 1540 °C (2800 °F), using established procedures. The extruded material was successfully rolled to sheet as outlined in Figure 5.

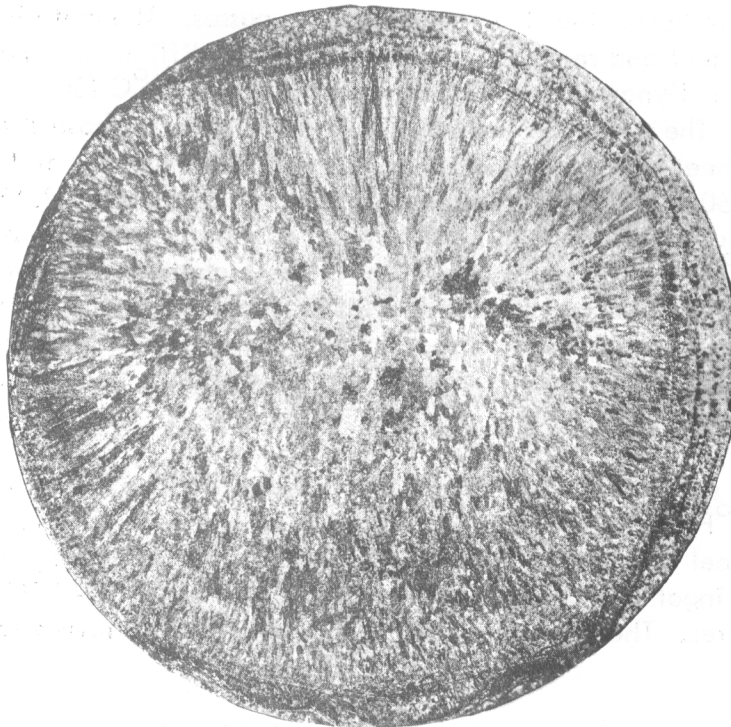
Considerable difficulty was encountered in upset forging the high carbon B-77 ingot (VAM-69) and the ultimate yield of sheet was fairly low. The remaining portion of this ingot was also Dynapak extruded to sheet bar which was subsequently rolled to sheet stock. The detailed processing history is shown in Figure 6.



B-77 + 0.0056 C
(VAM 57)



B-77 + 0.15 C
(VAM-69)



B-77 + 0.077 C
(VAM-61)

FIGURE 2 - MACROSTRUCTURE OF B-77 ARC MELTED INGOTS. AS CAST. 2X

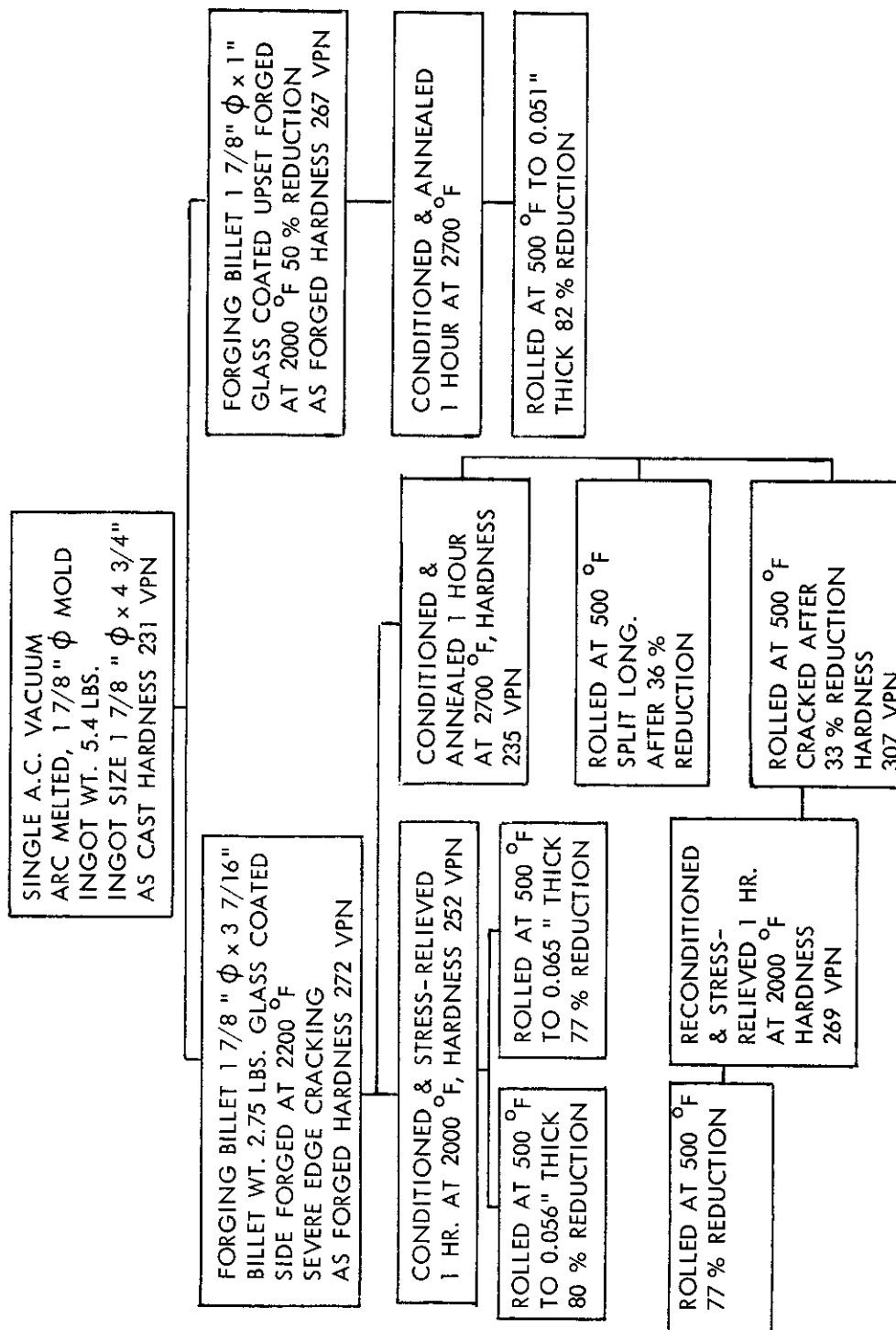


FIGURE 3 - PROCESSING OF LOW INTERSTITIAL B-77, HEAT VAM 57

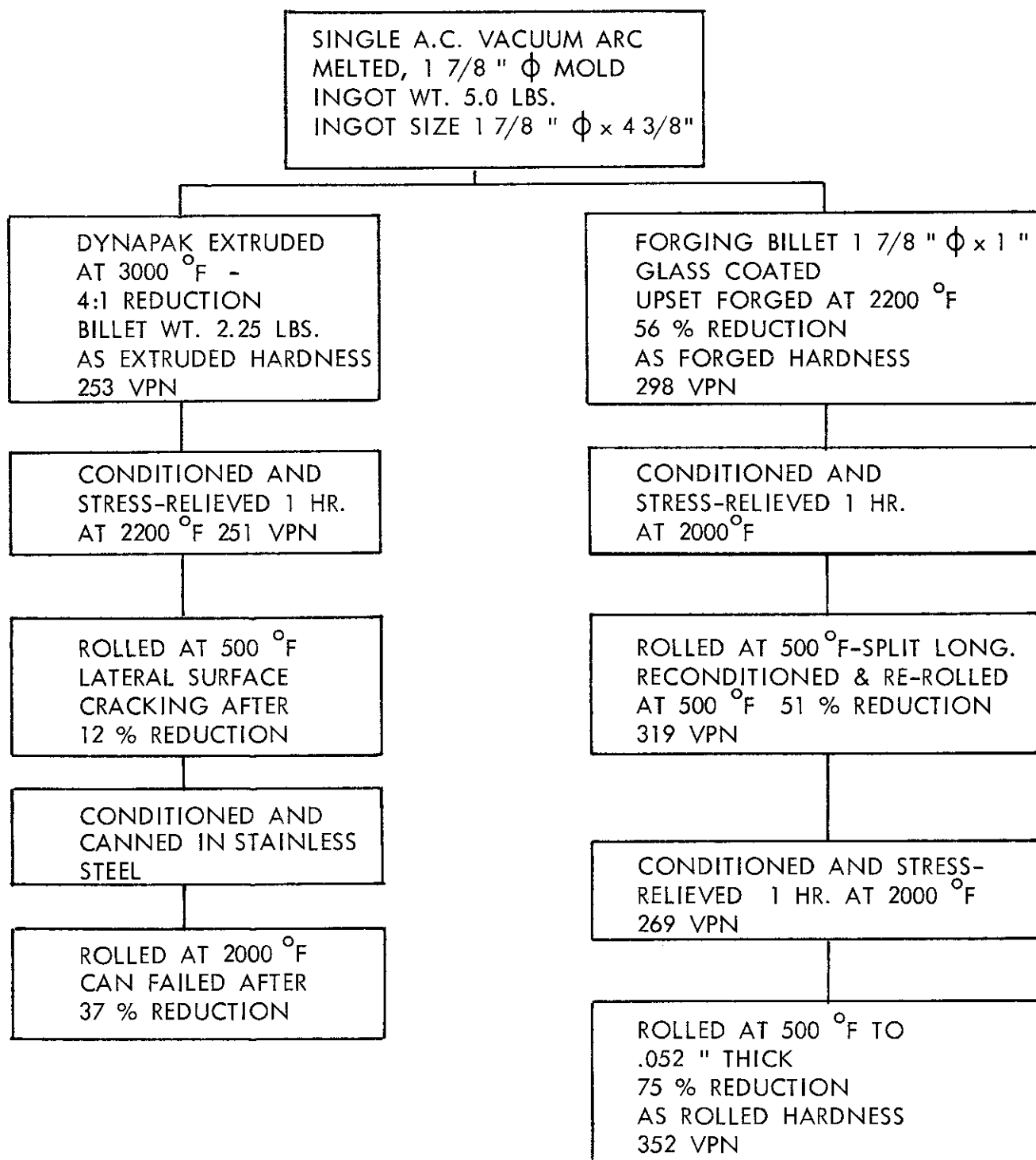


FIGURE 4 - PROCESSING OF LOW INTERSTITIAL B-77, HEAT VAM 68

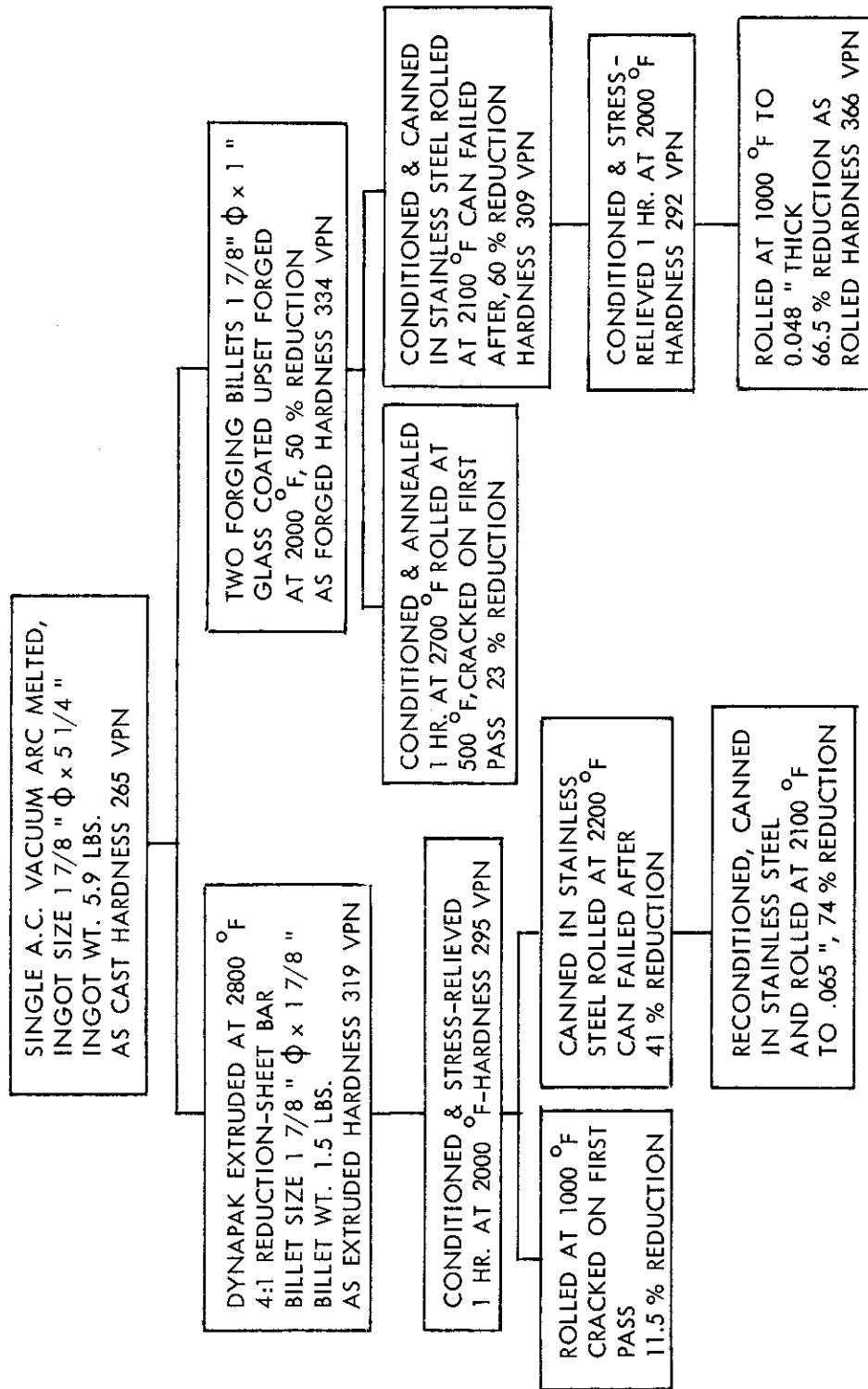


FIGURE 5 - PROCESSING OF B-77 + .075C, HEAT VAM 61

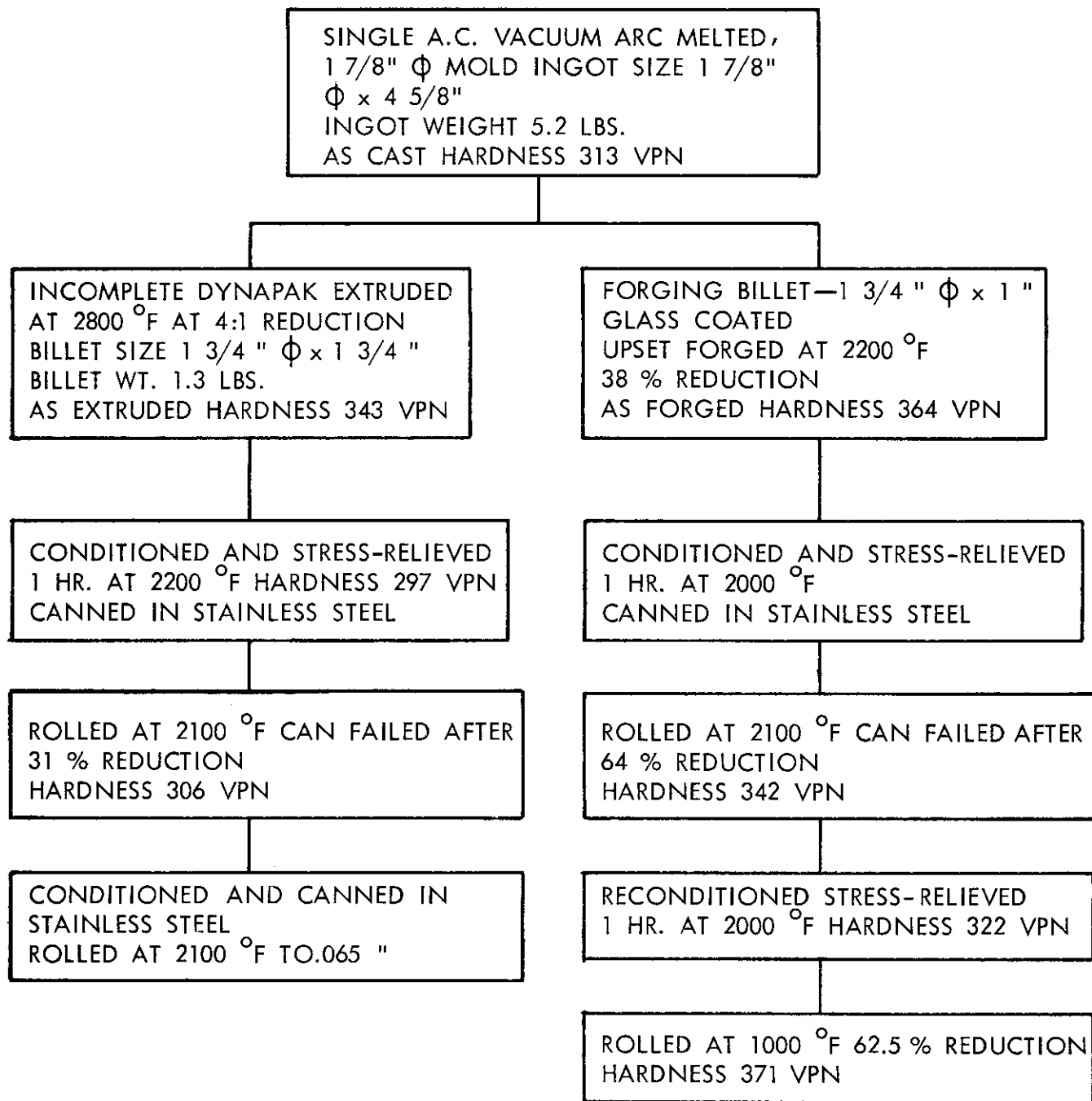


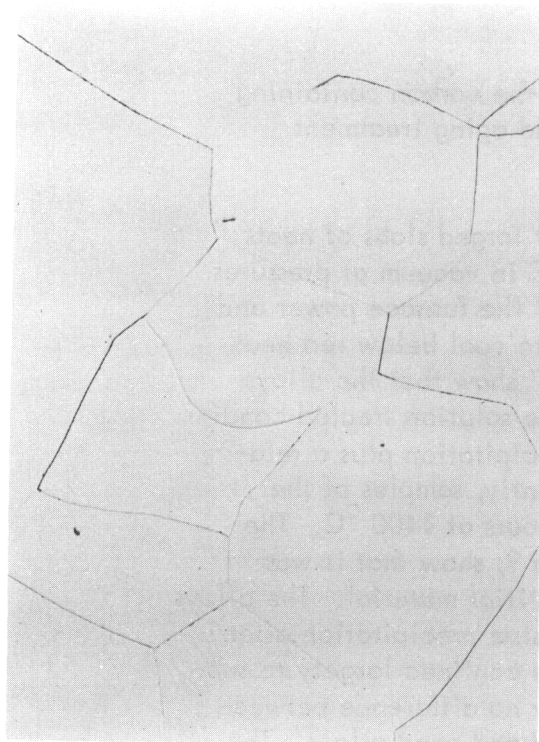
FIGURE 6 - PROCESSING OF B-77 + 0.15C, HEAT VAM 69

Effects of Heat Treatment

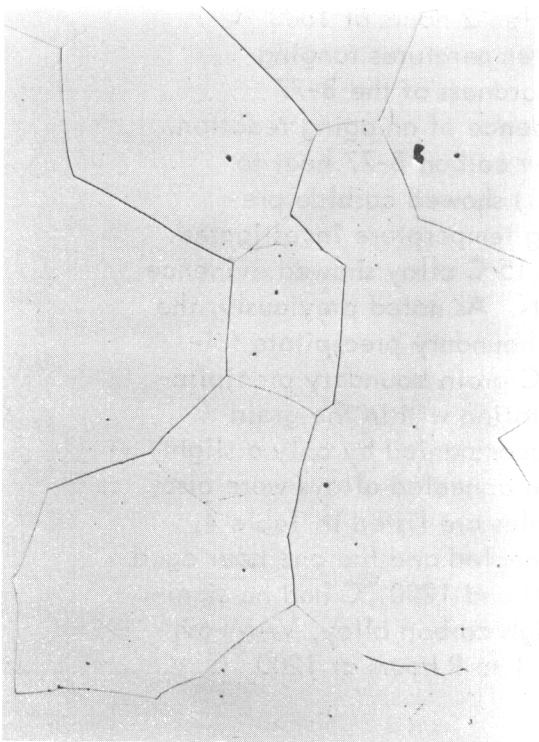
Heat treatment studies were undertaken to determine if the carbon containing B-77 alloys would exhibit the response to solution annealing and aging treatment typical of precipitation hardened alloys.

Solutioning and Aging Reactions. Sections of the upset forged slabs of heats VAM-57, 61, and 69 were solution annealed 4 hours at 1800 °C in vacuum at pressures below 5×10^{-5} Torr. The specimens were cooled by turning off the furnace power and allowing them to cool in the molybdenum susceptor. The time to cool below red heat was approximately 3 minutes. The photomicrographs of Figure 7 show that the alloys of low and intermediate carbon content were single phase in the solution treated condition. The B-77 + 0.15 C alloy showed some grain boundary precipitation plus a relatively minor amount of precipitate within the grains. Subsequently, samples of the solution treated material were aged 2 hours at 1200 °C and 2 hours at 1400 °C. The microstructures of the low carbon heat (VAM-57), Figures 8 and 9, show that it was single phase after aging as would be expected of the low interstitial material. The alloys of intermediate and high carbon content exhibited fairly extensive precipitation after aging at 1200 °C and 1400 °C. The precipitate appeared to be confined largely to sub-boundaries. Room temperature hardness data showed essentially no difference between the hardness of the solution annealed and the solution annealed and aged alloys. The hardness values in all conditions of heat treatment were essentially the same as those of the as-cast ingots listed in Table 3.

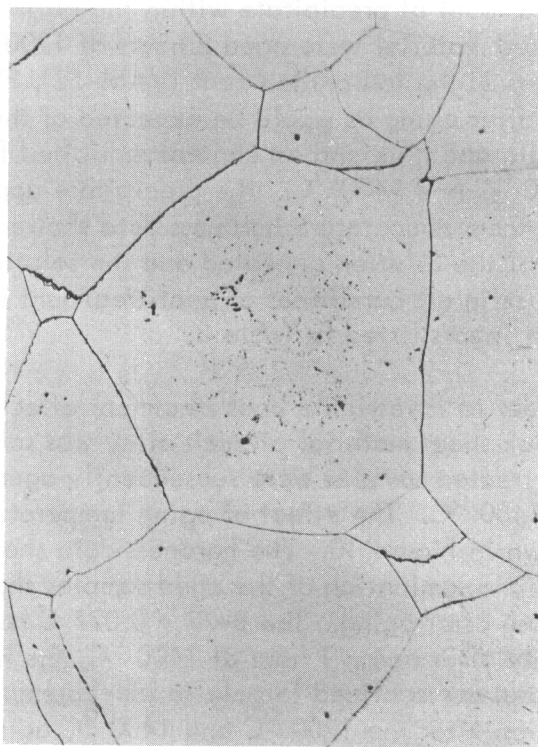
In order to investigate heat treatment effects in the B-77 alloys in more detail, 0.05 inch thick sheet material of each alloy was solution annealed 2 hours at 1800 °C. The solution treated samples were subsequently aged 1 hour at temperatures ranging from 600 to 1400 °C. The effect of aging temperature on the hardness of the B-77 alloys is shown in Figure 10. The hardness data showed no evidence of an aging reaction. Metallographic examination of the aged samples showed the low carbon B-77 heat to be single phase after aging. The B-77 + 0.077 C heat (VAM-61) showed carbide precipitation only after aging 1 hour at 1400 °C, the highest aging temperature investigated. The precipitate was confined largely to sub-boundaries. The 0.15 C alloy showed evidence of precipitation after the 1200 °C and 1400 °C aging treatments. As noted previously, the high carbon B-77 contained a relatively small amount of grain boundary precipitate following solution annealing at 1800 °C. During aging at 1400 °C grain boundary precipitation became more extensive. This was accompanied by precipitation within the grain volumes. However, as shown in Figure 10, precipitation was accompanied by only a slight decrease in room temperature hardness. Sections of the solution annealed alloys were also aged 9 hours at 800 and 1200 °C. Hardness data for these samples are listed in Table 4, which includes comparative hardness values for the solution annealed and the one hour aged conditions. As shown in Table 4, aging for longer times at 800 and 1200 °C had no significant effect on the hardness of heats VAM-57 and 61. The high carbon alloy, VAM-69, showed some softening when the aging time was increased from 1 to 9 hours at 1200 °C.



B-77 + 0.077 C (VAM-61)

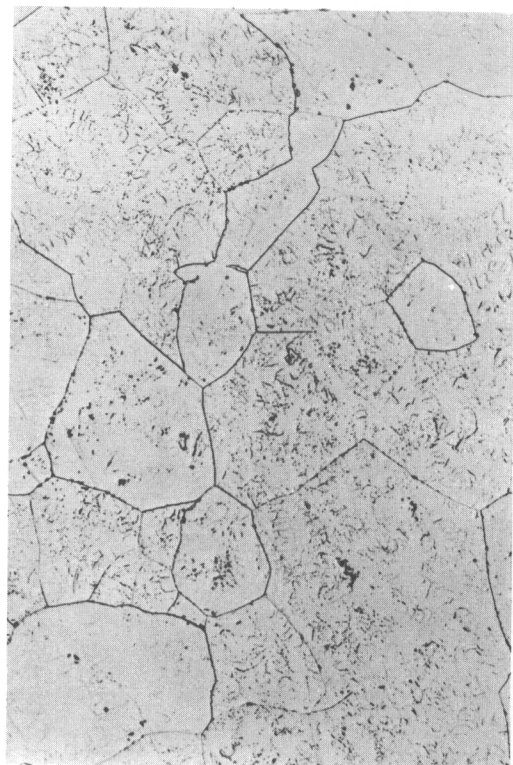


B-77 + 0.0056 (VAM-57)

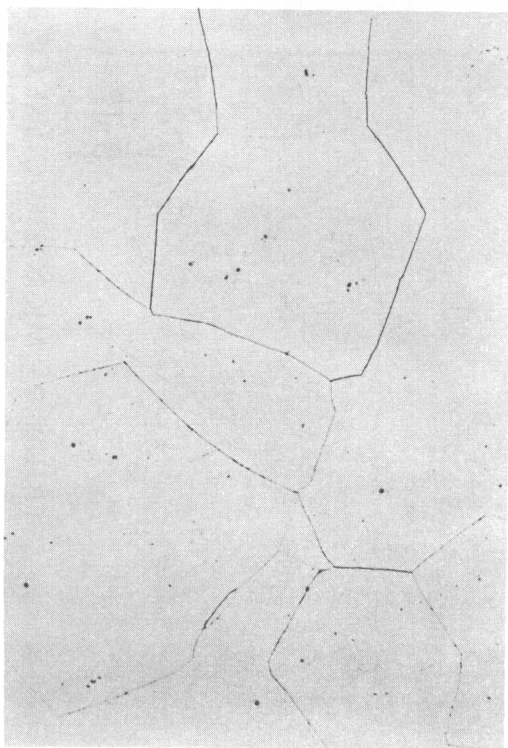


B-77 + 0.15 C (VAM-69)

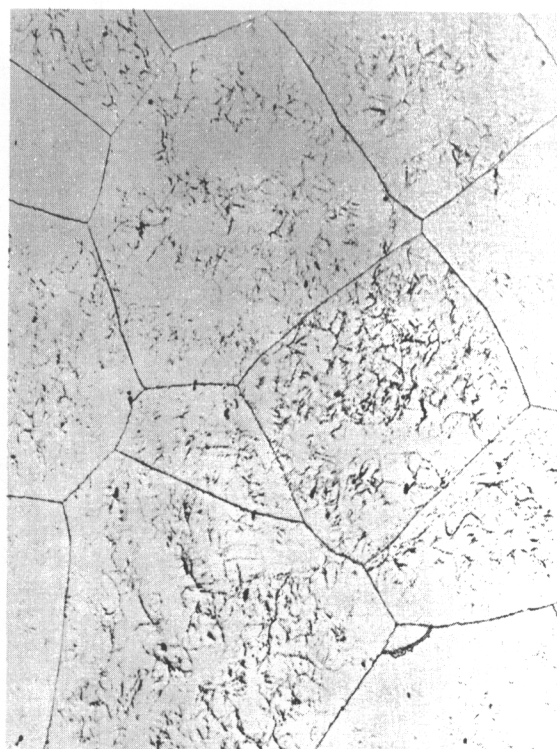
FIGURE 7 - MICROSTRUCTURE OF B-77 SOLUTION ANNEALED 4 HOURS AT 1800 °C. 200X



B-77 + 0.077 C (VAM-61)

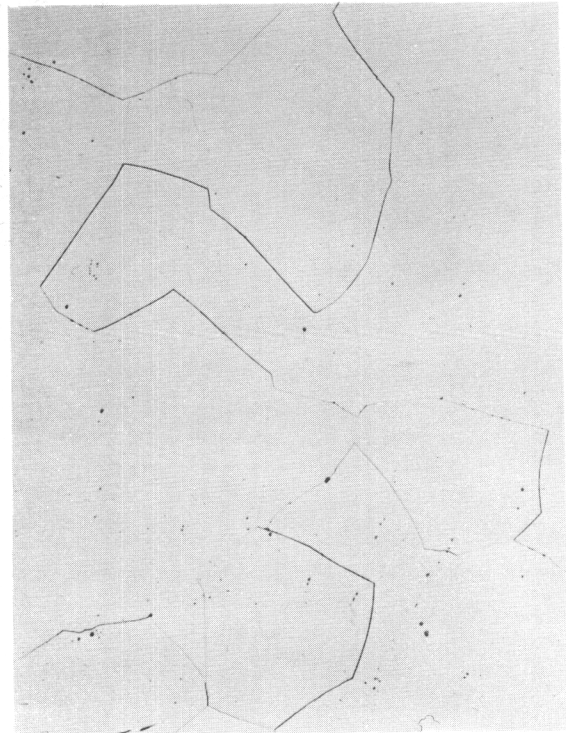


B-77 + 0.0056 C (VAM-57)

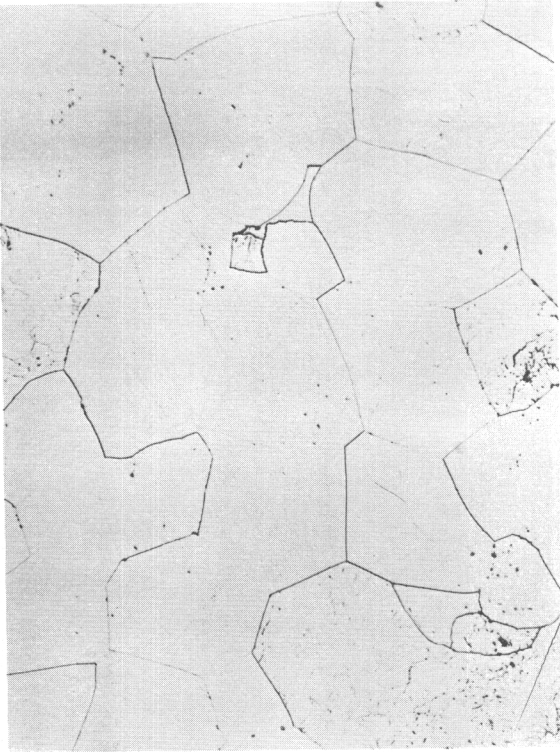


B-77 + 0.15 C (VAM-69)

**FIGURE 8 - MICROSTRUCTURE OF B-77 SOLUTION ANNEALED 4 HOURS
AT 1800 °C. AGED 2 HOURS AT 1200 °C. 200X**



B-77 + 0.0056 C (VAM-57)



B-77 + 0.077 C (VAM-61)



B-77 + 0.15 C (VAM-69)

**FIGURE 9 - MICROSTRUCTURE OF B-77 SOLUTION ANNEALED 4 HOURS
AT 1800 °C. AGED 2 HOURS AT 1400 °C. 200X**

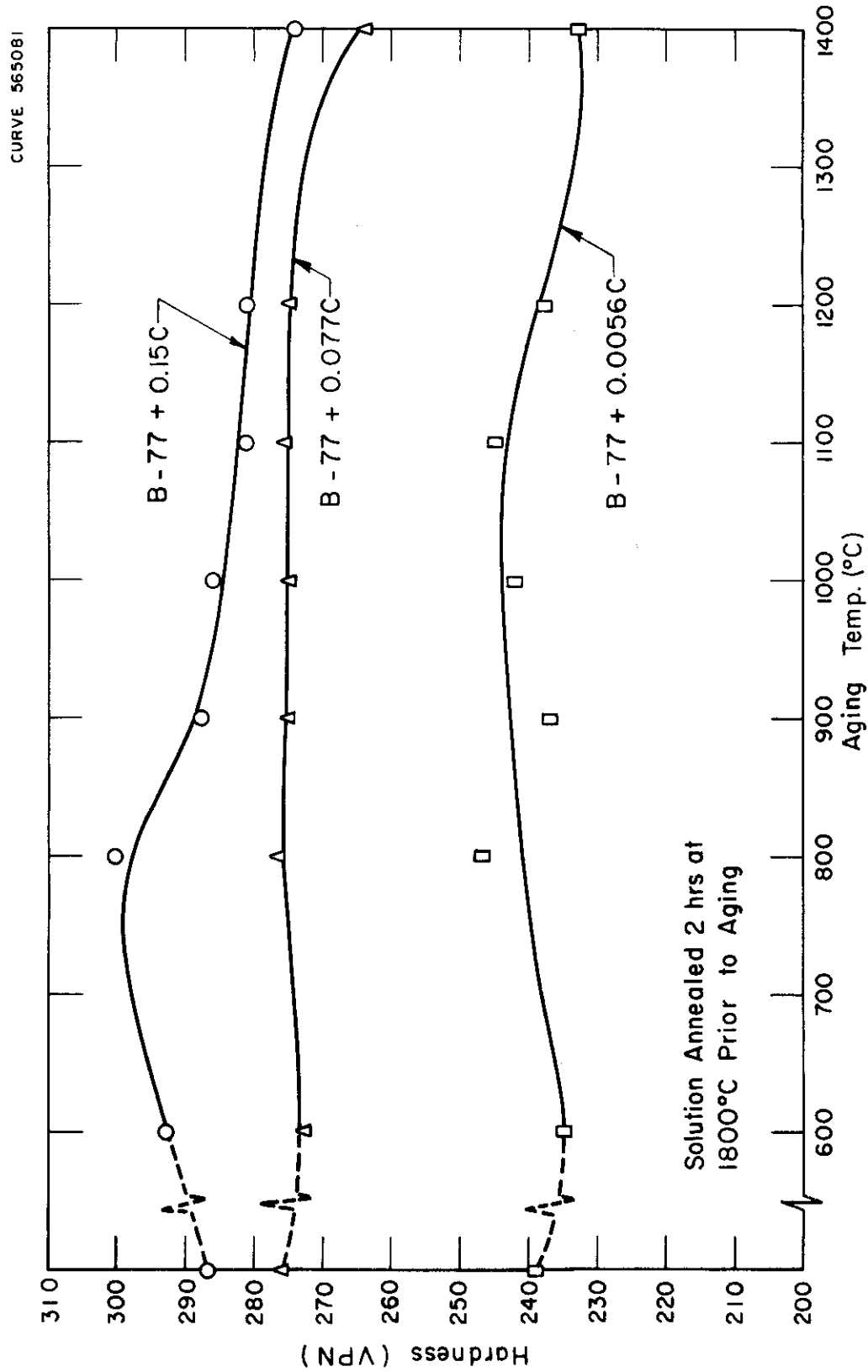


FIGURE 10 - EFFECT OF AGING TEMPERATURE ON THE HARDNESS OF B-77 (1 HR. ANNEALS)

TABLE 4. EFFECT OF HEAT TREATMENT ON THE HARDNESS OF B-77 ALLOYS

Condition	Hardness (VPN)		
	VAM-57 (B-77, low carbon)	VAM-61 (B-77 + 0.077C)	VAM-69 (B-77 + 0.15C)
A. As-cast	231	265	313
B. Annealed 2 hours at 1800°C	239	276	286
C. Annealed 2 hours at 1800°C + 1 hour at 800°C	247	276	300
D. Annealed 2 hours at 1800°C + 9 hours at 800°C	234	270	285
E. Annealed 2 hours at 1800°C + 1 hour at 1200°C	237	276	282
F. Annealed 2 hours at 1800°C + 9 hours at 1200°C	236	267	267

The lack of response to aging of the carbon containing B-77 is quite different than the results obtained by Chang⁹ on the F-48 alloy (Cb-15W-5Mo-1Zr-0.1C). Chang observed a moderate but distinct hardness peak in F-48 aged 1 hour at 1205 °C (2200 °F), following solution annealing at 1925 and 2205 °C (3500 and 4000 °F). F-48 and B-77 are essentially similar, in that they are solid solution alloys containing Zr and C. The obvious differences between the two alloys are the presence of 5 w/o V in B-77 and the fact that Chang's material contained approximately 0.03 w/o oxygen and nitrogen in addition to carbon. Earlier work in this program⁴ indicated that vanadium increases the solubility of carbon in columbium. If it is assumed that the carbon solubility is greater in B-77 than in F-48, then the supersaturation at any given temperature (at equivalent carbon content) is less in B-77. The stable precipitate nucleus size depends on the degree of supersaturation, the stable nucleus size decreasing with increasing supersaturation. Thus, in B-77 the precipitate nuclei would be larger than in F-48. Continued aging of the alloys would favor fewer, larger precipitates in B-77 with respect to F-48. The larger precipitates and their smaller volume fraction would provide much less effective strengthening in B-77. The other factor which may contribute to the difference in aging behavior of the two materials is the much higher oxygen and nitrogen level of Chang's F-48. The presence of other interstitials could modify the carbide morphology by effects on carbon solubility in the matrix, and by substituting for carbon in the monocarbide precipitate.

The carbon containing B-77 alloys (heats VAM-61 and 69) are supersaturated with respect to carbon at the aging temperatures investigated (600 to 1400 °C), as witnessed by the carbide precipitation observed metallographically after aging at the higher temperatures. However, precipitation appears to be confined to grain boundaries and subgrain boundaries, with no accompanying effect on room temperature hardness. Earlier work⁵ on Cb-Hf-C and Cb-Zr-C alloys showed that cold working prior to aging resulted in precipitation hardening effects; whereas, material solution treated and aged without intermediate cold working showed no response to aging. Transmission electron micrographs revealed that in the case of the cold worked and aged alloys, very small particles precipitated on dislocations. The alloys aged without prior working exhibited considerably larger precipitates, which were ineffective strengtheners. In view of these results, it was decided to plastically deform the B-77 alloys prior to aging to determine if cold working would provide more favorable sites for precipitate nucleation, and thus promote finer precipitates within the grain volumes. Consequently, small sections of sheet from heats VAM-61 and 69 were solution annealed 2 hours at 1800 °C and rolled to 25% reduction at 260 °C (500 °F). Rolling was carried out at slightly elevated temperatures to minimize the danger of cracking the large grained solution annealed material. The rolled material was then annealed 1 hour at temperatures ranging from 800 to 1100 °C. Hardness data are shown as a function of annealing temperature in Figure 11. Pronounced recovery occurred as a result of annealing at 800 °C. Hardness decreased slightly thereafter with increasing annealing temperature. However, annealing at temperatures up to 1100 °C did not result

CURVE 565832

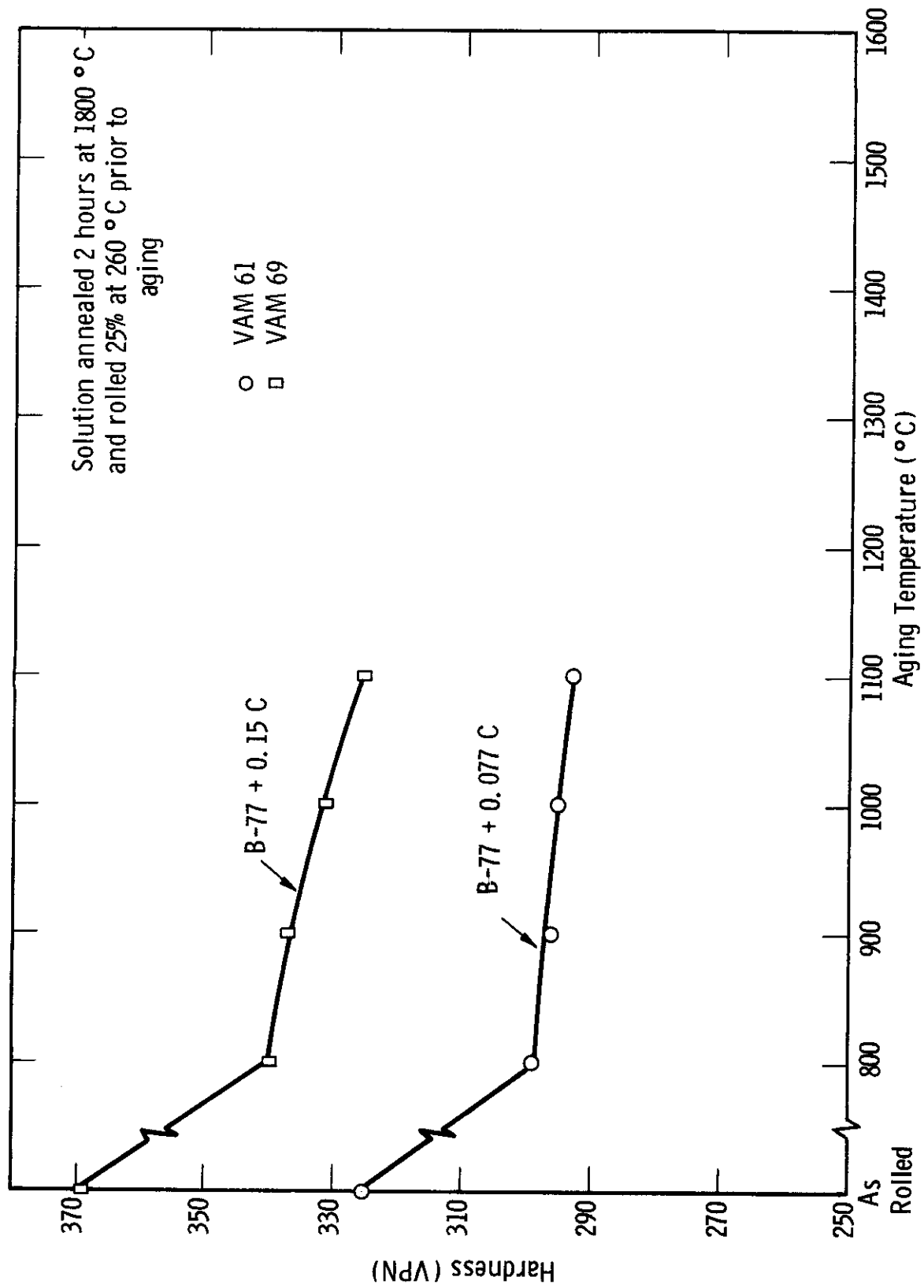


FIGURE 11 - EFFECT OF AGING TEMPERATURE ON THE HARDNESS OF B-77 (1HR, ANNEALS)

in full recovery of the solution annealed hardness. The lack of material precluded annealing at higher temperatures. The hardness data of Figure 11 appear to merely reflect a recovery process and show no evidence of an aging reaction. However, as will be shown in a subsequent section of this report, prior deformation had a substantial effect in increasing the hot hardness of the high carbon B-77.

Phase Identification. Attempts were made to obtain residues from the B-77 alloys for phase identification using bromine extraction techniques. However, insufficient material was obtained for x-ray diffraction analysis. Phase identification work carried out by Cuff¹² on a very similar alloy, B-66 (Cb-5V-5Mo-1Zr), revealed the presence of ZrC or (Zr, Cb) C. This identification was confirmed by additional work at Westinghouse. As noted previously, Chang⁹ also observed a zirconium rich (Zr, Cb) C phase in F-48. The monocarbide was stable below 1650 °C (3000 °F), and the hexagonal dicarbide above this temperature. It thus appears quite likely that the precipitate observed in the carbon containing B-77 alloys is a monocarbide based on ZrC.

Mechanical Properties

Tensile, hot hardness, and stress rupture data were obtained for the B-77 alloys in several conditions of heat treatment.

Low Temperature Properties. Base line tensile data for low interstitial B-77 in the recrystallized and stress-relieved conditions are listed in Table 5. The test specimens were stress-relieved 1 hour at 1095 °C (2000 °F) and recrystallized by annealing 1 hour at 1480 °C (2700 °F). The as-recrystallized grain size was ASTM 5. The data of Table 5 show that in the stress-relieved condition low interstitial B-77 had excellent ductility at temperatures as low as -196 °C. However, in the recrystallized condition the tensile transition temperature was approximately -100 °C. At temperatures below room temperature the recrystallized specimens exhibited transgranular cleavage failures. Because of limited material low temperature tensile data were not obtained for the carbon containing alloys.

Bend ductility data were obtained for the low and intermediate carbon alloys. The specimens were tested with the bend axis perpendicular to the rolling direction. Bend deflection rate was 0.1 inch/min. Bend transition data are listed in Table 6. The bend data show that the recrystallized B-77 had a much higher bend transition temperature than the stress-relieved material.

The B-77 + 0.077 carbon alloy in the stress-relieved condition was ductile below -130 °C (-200 °F).

Wessel, France, and Begley¹³ have shown a very good correlation between flow stress and low temperature hardness for pure columbium. Consequently, low temperature hardness measurements were conducted in the range 25 °C to -196 °C in order to provide some data on the effect of carbon additions on the low temperature strength of B-77. The low temperature hardness apparatus has been described by France, et al.¹⁴

TABLE 5. TENSILE DATA FOR LOW CARBON B-77 (VAM-57)

Specimen No.	Test Temp.		0.2% Yield Strength (psi)	Ultimate Strength (psi)	Elongation (%)		Red. in Area (%)	Condition
	(°C)	(°F)			Unif.	Total		
VAM-57-1	-196	-320	155,300	175,700	20.6	25.8	29	Cold rolled 80-90% and stress-relieved one hour at 1095 °C. " " " "
VAM-57-2	-100	-150	113,500	132,000	23.1	31.2	48	
VAM-57-3	RT	RT	87,600	103,700	20.5	27.8	72	
VAM-57-4	260	500	60,600	80,600	19.5	25.5	62	
VAM-57-11	-130	-200	-----	98,200*	--	--	--	Recrystallized one hour at 1480 °C. " " " "
VAM-57-13	-73	-100	100,200	103,200	--	.5	2	
VAM-57-14	-18	0	90,000	122,000	--	11.2	11	
VAM-57-10	RT	RT	79,200	100,700	22.0	35.5	51.4	

*True stress at fracture.

TABLE 6. BEND TRANSITION TEMPERATURE FOR B-77 ALLOYS

Heat No.	Composition	Bend Radius	Bend Transition Temperature	Condition
VAM-57	B-77	2t	$< -196^{\circ}\text{C} (-320^{\circ}\text{F})$	Stress-relieved*
VAM-57	B-77	2t	$-100^{\circ}\text{C} (-150^{\circ}\text{F})$	Recrystallized**
VAM-61	B-77 + 0.077C	4t	$-130^{\circ}\text{C} (-200^{\circ}\text{F})$	Stress-relieved

*Stress-relieved 1 hour at $1095^{\circ}\text{C} (2000^{\circ}\text{F})$

**Recrystallized 1 hour at $1480^{\circ}\text{C} (2700^{\circ}\text{F})$

The low temperature hardness data are plotted as a function of temperature in Figure 12. The samples were recrystallized by annealing 1 hour at $1480^{\circ}\text{C} (2700^{\circ}\text{F})$ before testing. All the samples show the characteristic rapid increase in flow stress (hardness) with decreasing test temperature. The hardness values increased with increasing carbon content over the entire temperature range. A considerable difference in grain size was observed in the alloys, the grain size decreasing with increasing carbon level. Since it has been observed that grain size has no significant effect on the low temperature yield strength of pure Cb⁴, and several Cb alloys⁵, it may be assumed that the variation in grain size per se is not responsible for the difference in low temperature hardness values for the sample.

Hot Hardness. Hot hardness testing was relied on extensively in this program to provide data on the effect of compositional and thermal treatment variables on high temperature strength properties. Earlier work had established a very good correlation between hot hardness and tensile properties for columbium alloys. The hot hardness - tensile strength correlation for columbium alloys at 1095 and $1205^{\circ}\text{C} (2000$ and $2200^{\circ}\text{F})$ is shown in Figure 13. Subsequent studies have indicated the correlation to be valid over a considerably broader temperature range than that listed above. The obvious disadvantage of hot hardness tests is that they provide no information on ductility or fracture behavior. However, as a screening technique they have proven to be extremely useful.

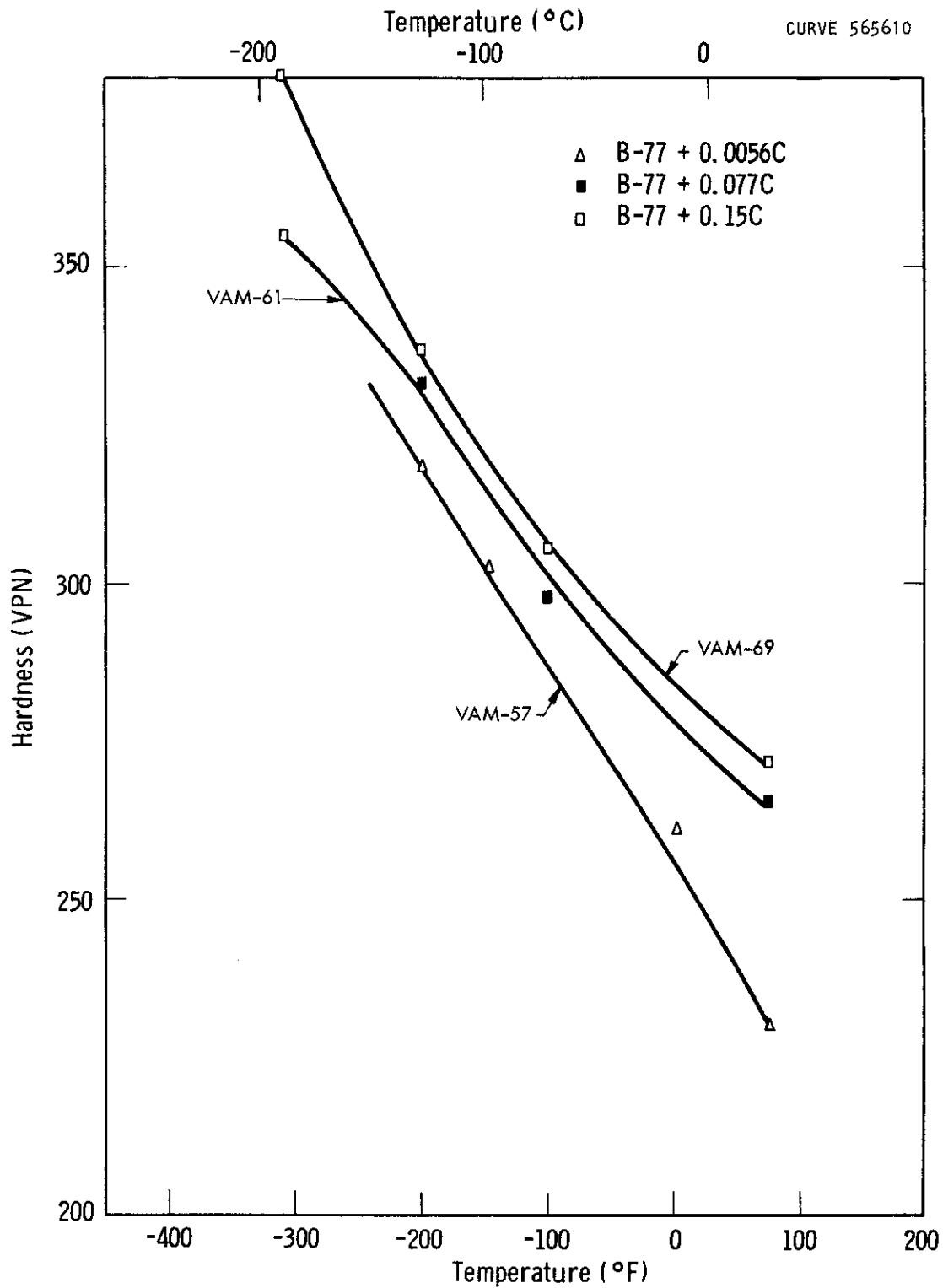


FIGURE 12 - EFFECT OF TEMPERATURE ON THE HARDNESS OF RECRYSTALLIZED B-77

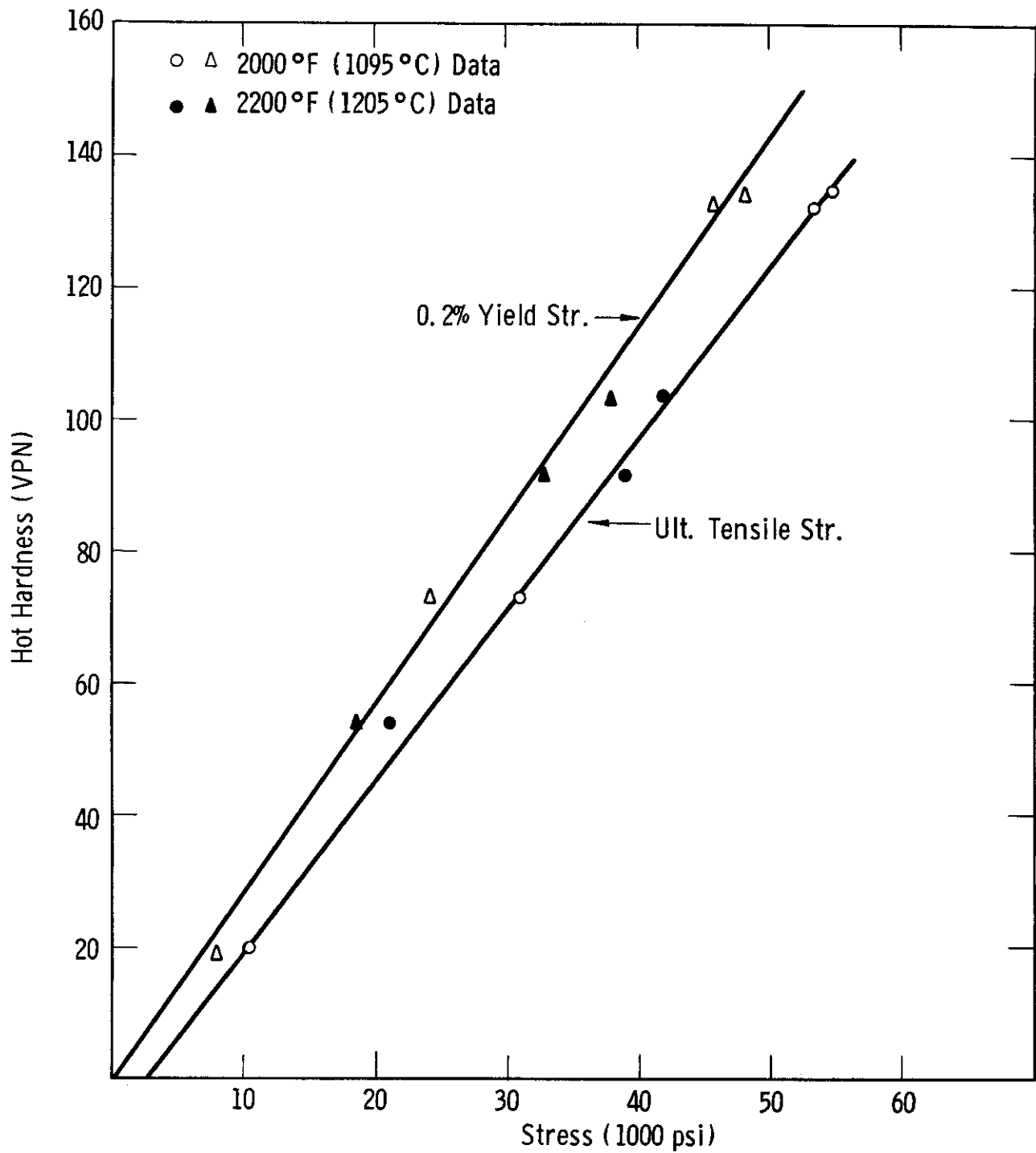


FIGURE 13 - CORRELATION OF HOT HARDNESS WITH TENSILE STRENGTH FOR COLUMBIUM ALLOYS

The first series of hot hardness tests were conducted using specimens machined from upset forged slabs of heats VAM-57, 61, and 69. Material was evaluated in these conditions of heat treatment:

- A. Annealed 4 hours at 1800 °C and radiation cooled.
- B. Annealed 4 hours at 1800 °C and radiation cooled. Aged 2 hours at 1200 °C.
- C. Annealed 4 hours at 1800 °C and radiation cooled. Aged 2 hours at 1400 °C.

Tests were carried out in order of increasing test temperature using a 2.5 kg load on the indenter. The data of Figure 14 show that the low carbon B-77 (VAM-57) had the lowest hot hardness values over the entire temperature range 870 - 1205 °C (1600 - 2200 °F). Prior heat treatment had little effect on the hot hardness of low carbon B-77 except at 1095 °C (2000 °F); where the sample, aged at 1400 °C, had somewhat superior properties. The intermediate and high carbon alloys (VAM-61 and 69) had fairly comparable hardness values at 1205 °C (2200 °F). However, at lower temperatures considerable variation in hardness values was observed. The B-77 + 0.077 carbon alloy exhibited the highest hardness values over most of the test temperature range. Aging this alloy 2 hours at 1200 °C resulted in a significant decrease in hot hardness. Increasing the aging temperature to 1400 °C resulted in a further shift of the hardness-temperature curve to lower hot hardness values.

As shown previously, aging the intermediate carbon B-77 alloy at 1200 and 1400 °C resulted in the precipitation of carbides which were easily resolvable by optical metallography. The hot hardness data show clearly that precipitation of fairly large carbides on aging substantially lowers the elevated temperature strength of B-77. The strength decrease presumably arises from the depletion of zirconium and carbon from the matrix during precipitation of a zirconium rich monocarbide. In the solution annealed condition heat VAM-61 exhibited high hot hardness values up to 1095 °C (2000 °F), and a rapid decrease in hardness when the test temperature was increased to 1205 °C (2200 °F). Based upon the hot hardness - strength correlation shown in Figure 13, the hot hardness of VAM-61 at 1095 °C (2000 °F) corresponds to an ultimate tensile strength of approximately 75,000 psi. It is unlikely that the high strength of the solution annealed material can be attributed entirely to solution hardening by carbon. It appears more reasonable to suggest that carbide precipitation occurred during the hot hardness testing thermal cycle, and at temperatures up to 1095 °C (2000 °F) the precipitates were still sufficiently fine to exert some strengthening. Above this temperature the precipitates became larger and strength decreased rapidly. Metallographic examination of the solution annealed hot hardness specimen showed that carbide precipitation had occurred during the testing thermal cycle.

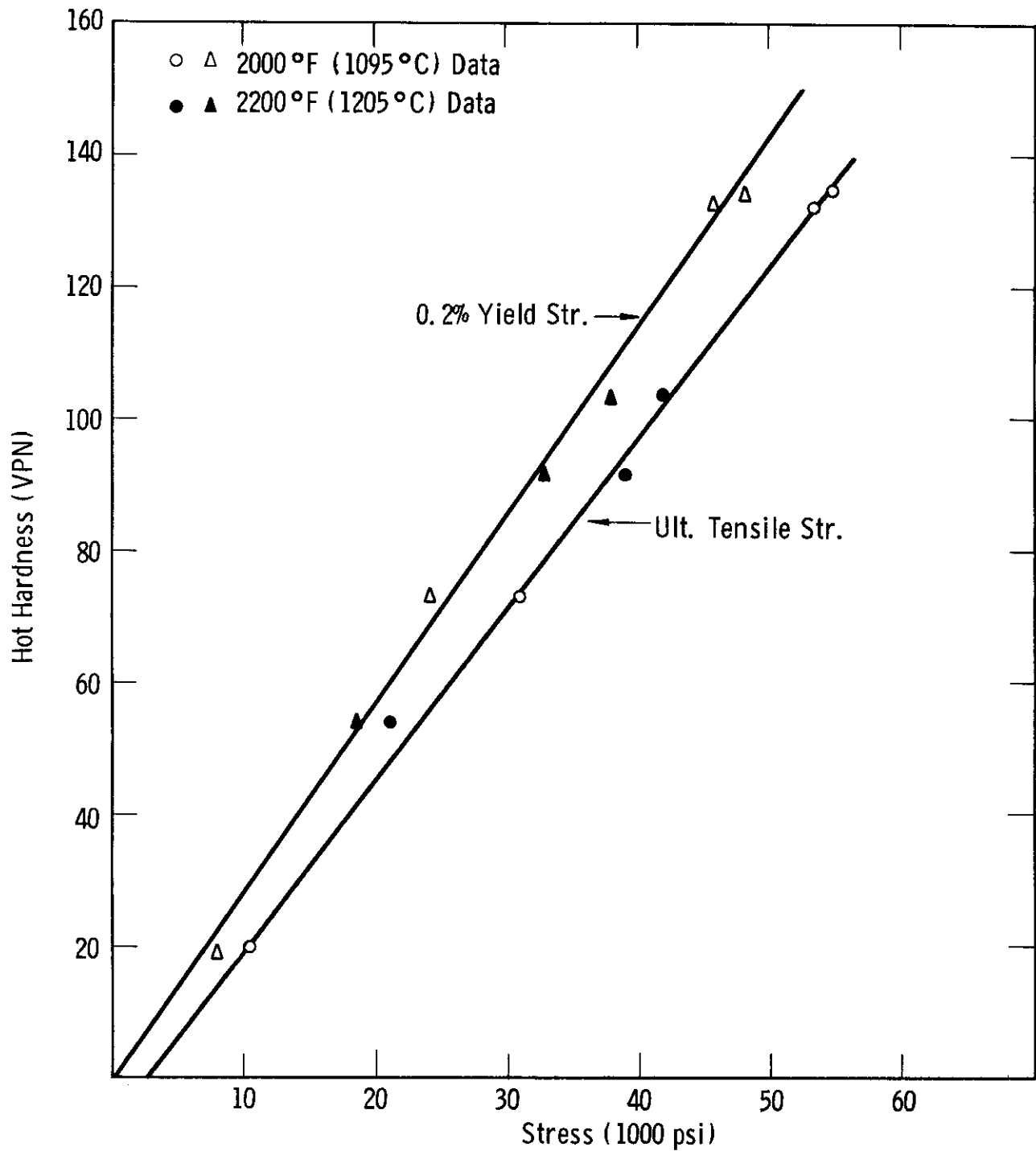


FIGURE 13 - CORRELATION OF HOT HARDNESS WITH TENSILE STRENGTH FOR COLUMBIUM ALLOYS

The first series of hot hardness tests were conducted using specimens machined from upset forged slabs of heats VAM-57, 61, and 69. Material was evaluated in these conditions of heat treatment:

- A. Annealed 4 hours at 1800 °C and radiation cooled.
- B. Annealed 4 hours at 1800 °C and radiation cooled. Aged 2 hours at 1200 °C.
- C. Annealed 4 hours at 1800 °C and radiation cooled. Aged 2 hours at 1400 °C.

Tests were carried out in order of increasing test temperature using a 2.5 kg load on the indenter. The data of Figure 14 show that the low carbon B-77 (VAM-57) had the lowest hot hardness values over the entire temperature range 870 - 1205 °C (1600 - 2200 °F). Prior heat treatment had little effect on the hot hardness of low carbon B-77 except at 1095 °C (2000 °F); where the sample, aged at 1400 °C, had somewhat superior properties. The intermediate and high carbon alloys (VAM-61 and 69) had fairly comparable hardness values at 1205 °C (2200 °F). However, at lower temperatures considerable variation in hardness values was observed. The B-77 + 0.077 carbon alloy exhibited the highest hardness values over most of the test temperature range. Aging this alloy 2 hours at 1200 °C resulted in a significant decrease in hot hardness. Increasing the aging temperature to 1400 °C resulted in a further shift of the hardness-temperature curve to lower hot hardness values.

As shown previously, aging the intermediate carbon B-77 alloy at 1200 and 1400 °C resulted in the precipitation of carbides which were easily resolvable by optical metallography. The hot hardness data show clearly that precipitation of fairly large carbides on aging substantially lowers the elevated temperature strength of B-77. The strength decrease presumably arises from the depletion of zirconium and carbon from the matrix during precipitation of a zirconium rich monocarbide. In the solution annealed condition heat VAM-61 exhibited high hot hardness values up to 1095 °C (2000 °F), and a rapid decrease in hardness when the test temperature was increased to 1205 °C (2200 °F). Based upon the hot hardness - strength correlation shown in Figure 13, the hot hardness of VAM-61 at 1095 °C (2000 °F) corresponds to an ultimate tensile strength of approximately 75,000 psi. It is unlikely that the high strength of the solution annealed material can be attributed entirely to solution hardening by carbon. It appears more reasonable to suggest that carbide precipitation occurred during the hot hardness testing thermal cycle, and at temperatures up to 1095 °C (2000 °F) the precipitates were still sufficiently fine to exert some strengthening. Above this temperature the precipitates became larger and strength decreased rapidly. Metallographic examination of the solution annealed hot hardness specimen showed that carbide precipitation had occurred during the testing thermal cycle.

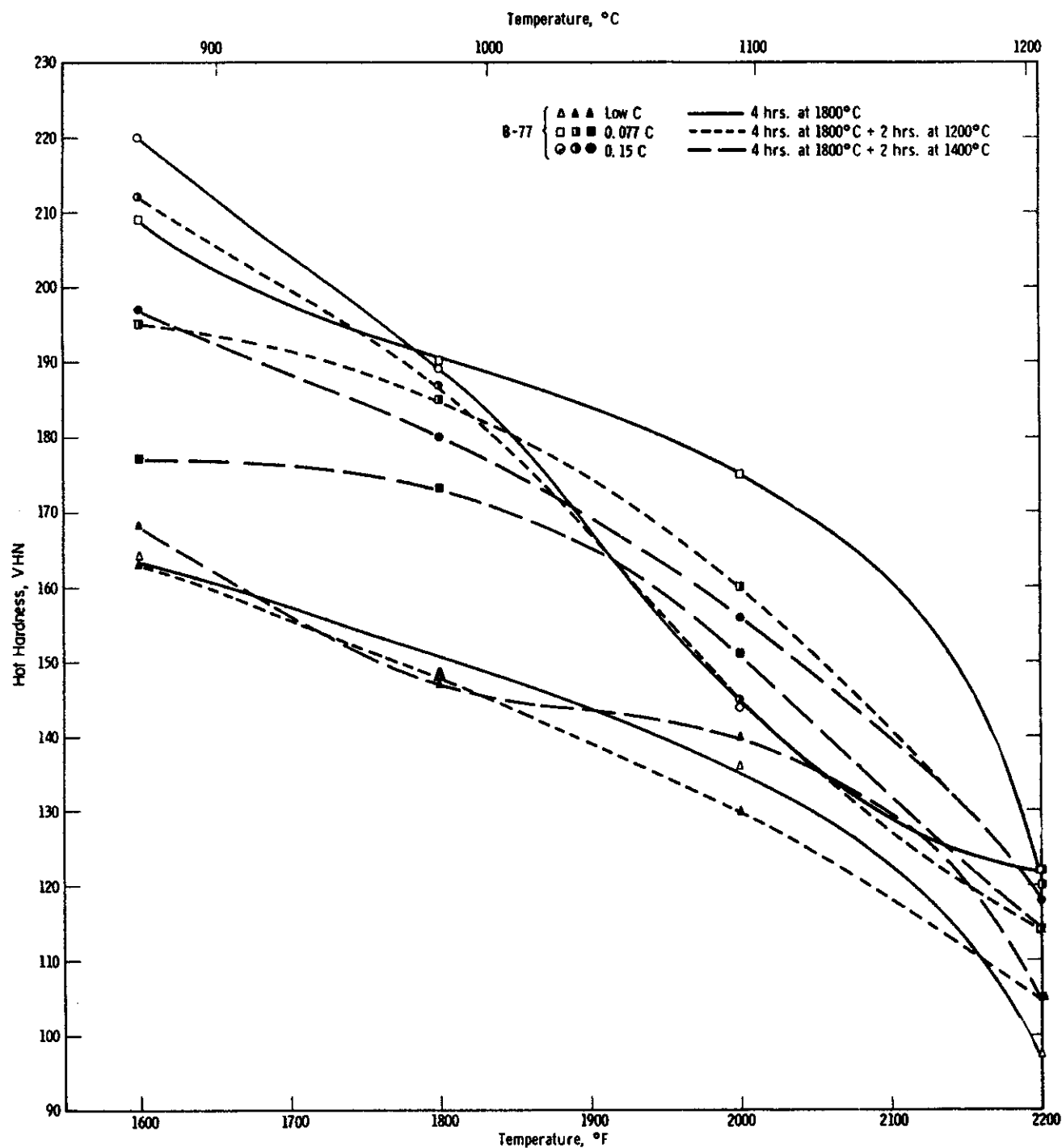


FIGURE 14 - HOT HARDNESS OF B-77 AS A FUNCTION OF HEAT TREATMENT

The high carbon B-77 (VAM-69) did not show the same behavior as the intermediate carbon heat. The explanation for the difference is not apparent at the present. It is, however, interesting to note that the only significant deviation from the behavior of the B-77 + 0.077 alloy is the low 1095 °C (2000 °F) hardness values of the solution annealed and solution annealed + 1200 °C aged samples. If these two data points were shifted to higher hardness values, the same trend of decreasing hot hardness with increasing aging temperature pertains.

Additional hot hardness data were obtained on sheet material prepared from heats VAM-68 (low carbon B-77) and VAM-69 (B-77 + 0.15C). As pointed out previously in this report, sections of VAM-69 solution annealed 4 hours at 1800 °C and radiation cooled showed a small amount of grain boundary precipitate. The sheet material was quenched from the solution annealing temperature to inhibit grain boundary precipitation. The high carbon B-77 was tested in the following conditions of heat treatment:

- A. Annealed 2 hours at 1800 °C and quenched.
- B. Annealed 2 hours at 1800 °C and quenched. Aged 1 hour at 900 °C.
- C. Annealed 2 hours at 1800 °C and quenched. Rolled to 25% reduction at 260 °C.

The low interstitial heat (VAM-68) was annealed 2 hours at 1800 °C and quenched. Sheet samples were fastened to cylindrical molybdenum mounts by means of small pins peened in the edges of the specimens. The mounts were surface ground to assure that the surface of the test samples was flat, and perpendicular to the axis of the indenter.

Hot hardness data are shown as a function of temperature in Figure 15. The solution annealed, and the solution annealed plus aged conditions gave essentially the same results. However, the hot hardness data shown in Figure 14 for the solution annealed and quenched VAM-69 material gave consistently higher hot hardness data over the entire temperature range than the radiation cooled samples. Furthermore, low hot hardness values at 1095 °C (2000 °F) were not observed in the quenched material. The higher hardness values reflect the higher carbon supersaturation of the quenched samples, since grain boundary precipitation did not occur on cooling from the solution annealing temperature. The solution annealed and rolled specimen gave much higher hot hardness results than the solution annealed and solution annealed plus aged alloys at temperatures up to 980 °C (1800 °F). Hardness decreased fairly rapidly above this temperature, but the data for the deformed sample were still significantly higher than the solution annealed material at 1205 °C (2200 °F). As shown previously, pronounced recovery of hardness occurred when deformed VAM-69 was annealed 1 hour at 800 °C (Figure 11). The higher hot hardness values for the deformed B-77 alloy cannot

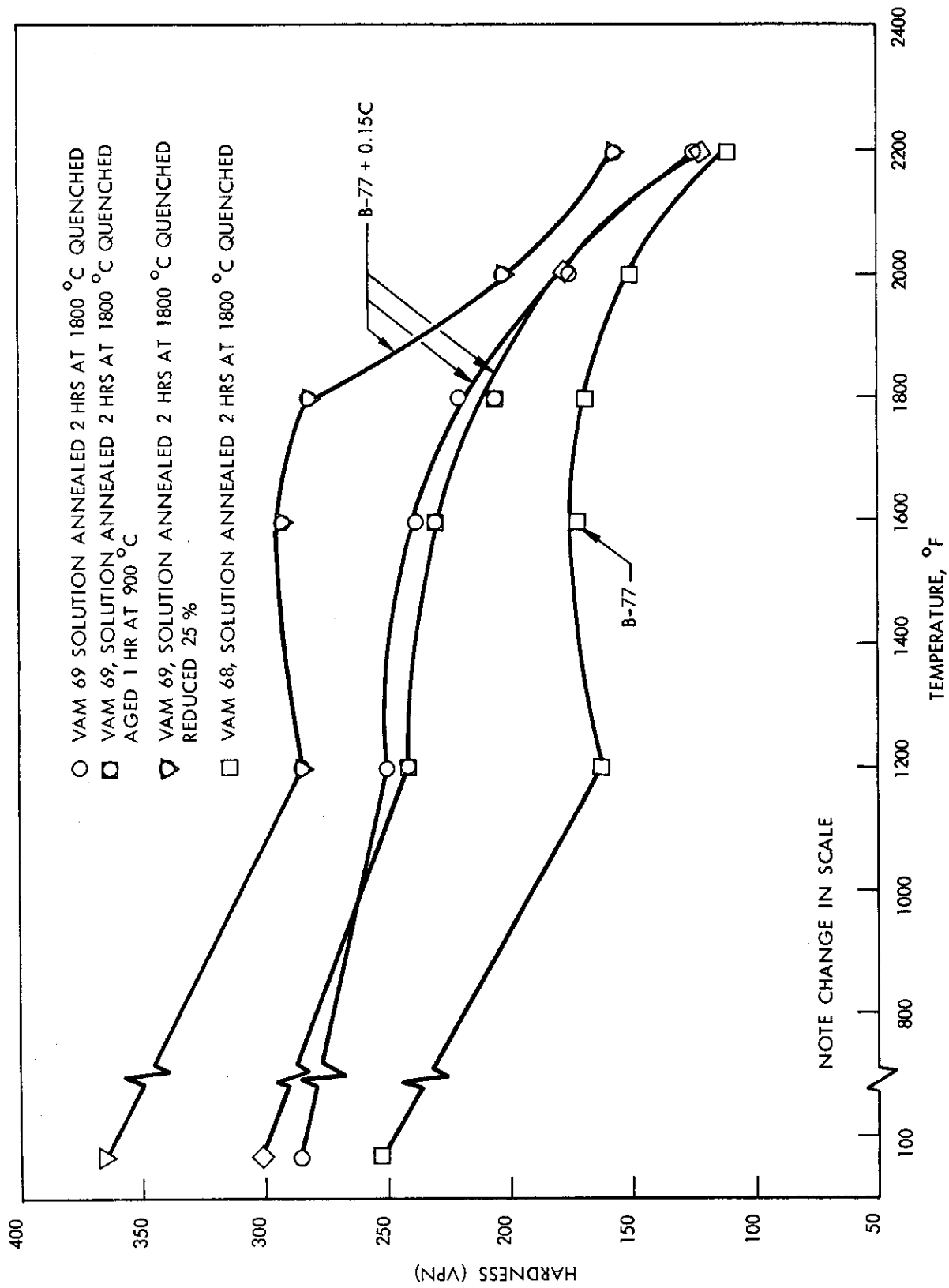


FIGURE 15 - EFFECT OF PRIOR TREATMENT ON THE HOT HARDNESS OF B-77 ALLOYS

be attributed merely to a strain hardening effect, since this sample was exposed to the entire hot hardness thermal cycle, which should have provided sufficient thermal activation for recovery. It appears quite likely that carbide precipitation on dislocations is contributing to the high strength of the deformed B-77 + 0.15 C alloy, similar to results obtained earlier on Cb-Hf-C alloys. Transmission electron micrographic studies are required to determine the interaction of precipitates with dislocations in this alloy, but difficulties in preparing thin films have precluded such studies to date.

Elevated Temperature Tensile Properties. Limited elevated temperature tensile data were obtained on the B-77 alloys to supplement hot hardness tests. The results are summarized in Table 7. It was initially intended to quench the carbon containing B-77 tensile specimens after solution annealing on a cold copper block in order to duplicate the thermal treatment of the hot hardness specimens. However, the available annealing furnaces were not capable of quenching a sample the size of a tensile specimen. As an alternate, helium was admitted to the furnace chamber at the conclusion of the 1800 °C solution annealing treatment to provide as rapid a cooling rate as possible. The test specimens cooled to below red heat in less than 3.5 minutes.

The low interstitial B-77 tensile properties are somewhat lower than the data reported originally for B-77 bar stock containing 0.06 O₂, 0.03 C, and 0.03 nitrogen⁴. Tensile results for the intermediate and high carbon B-77 show a marked improvement in 1205 °C (2200 °F) tensile properties with respect to low interstitial B-77. The B-77 + 0.077 C alloy had the highest strength properties and excellent ductility. The tensile strength of the high carbon material was slightly lower than VAM-61, and the fracture strain was significantly reduced. The tensile properties of low carbon and high carbon alloys cannot be compared directly because the low carbon specimens were tested in the stress-relieved rather than the solution annealed condition. However, the hot hardness data for solution annealed low carbon B-77 (Figure 14) indicate that the 1205 °C (2200 °F) tensile properties of the solution annealed and the stress-relieved low carbon B-77 are essentially identical. At the present time studies of the effect of prior deformation on the high temperature tensile properties of solution annealed B-77 + C alloys are in progress.

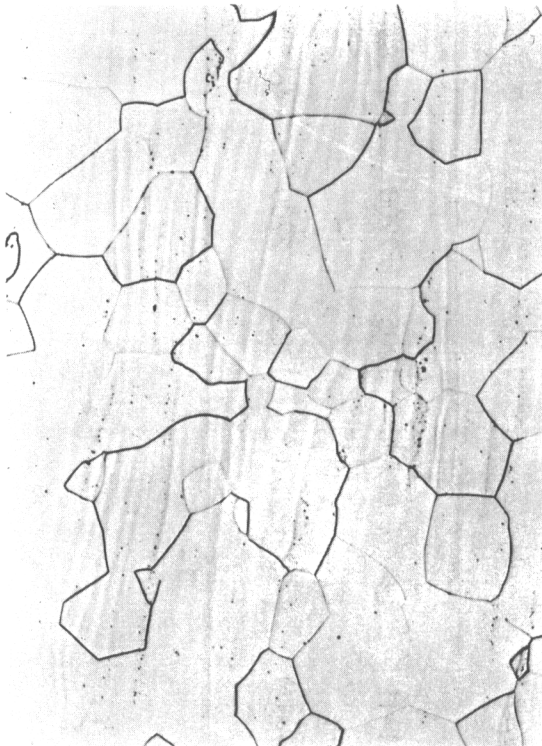
Stress-Rupture Data. Stress-rupture specimens were machined from sheet stock prepared from heats VAM-57, 61, and 69. Stress-rupture tests were carried out at 1205 °C (2200 °F) in vacuum at pressures below 5×10^{-5} Torr. Specimens were tested in two conditions: annealed one hour at 1095 °C (2000 °F); and annealed one hour at 1480 °C (2700 °F). The 1095 °C (2000 °F) anneal did not result in recrystallization of the carbon containing alloys. However, metallographic examination of the low carbon heat (VAM-57) showed this alloy to be approximately 90% recrystallized after the 1095 °C anneal. The microstructures of the material annealed 1 hour at 1480 °C (2700 °F) are shown in Figure 16. The low carbon B-77 was fully recrystallized with considerable grain growth after this annealing treatment. The intermediate and high carbon B-77 alloys were almost completely recrystallized but the grain size was quite small. It should be noted that the

TABLE 7. ELEVATED TEMPERATURE TENSILE DATA FOR B-77 ALLOYS

Specimen No.	Composition	Test. Temp.		0.2% Yield Strength	Ultimate Tensile Strength	Elongation (%)		Red. in Area (%)	Condition
		(°C)	(°F)			Unif.	Total		
VAM-57-4	B-77	260	500	60,600	80,600	19.5	25.5	62	Stress relieved one hour at 1095 °C. (2000 °F)
VAM-57-5	B-77	1095	1000	57,700	85,000	16.8	21.0	71	" "
VAM-57-8	B-77	1205	2200	32,200	35,000	1.8	52.0	72	" "
VAM-57-9	B-77	1315	2400	24,000	24,700	0.6	43.9	54	" "
VAM-61-Ti	B-77+0.077 C	1205	2200	47,800	49,300	--	36	46	Solution annealed two hours at 1800 °C.
VAM-69-Ti	B-77+0.15 C	1205	2200	46,500	47,600	--	18	24	He quenched " "



B-77 + 0.077 C (VAM-61)



B-77 + 0.0056 C (VAM-57)



B-77 + 0.15 C (VAM-69)

FIGURE 16 - MICROSTRUCTURE OF B-77 SHEET RECRYSTALLIZED 1 HOUR AT 2700 °F (1480 °C). 200X

prior working history of the three B-77 alloys was not identical, primarily because the carbon containing heats required intermediate recovery anneals during rolling. However, as can be seen from the flow charts of Figures 3, 5, and 6 (for the upset forged slabs) the low carbon B-77 heat (VAM-57) received somewhat less total reduction prior to final annealing than the carbon-containing heats. Thus, while the recrystallization characteristics of the three B-77 alloys cannot be compared precisely because of the variations in prior working, the data definitely indicate that carbon additions raise the recrystallization temperature range of B-77 and refine the as-recrystallized grain size.

Stress-rupture data for the alloys are shown in Figure 17 and summarized in Table 8. The data show, rather surprisingly, that carbon additions had no significant effect on the stress-rupture strength of B-77 at 1205 °C (2200 °F), at least for the two conditions of heat treatment evaluated. Furthermore, the strength data were essentially equivalent for both conditions of heat treatment. Significant differences were observed in the rupture strain exhibited by the various specimens. These observations may be summarized as follows:

- 1) Rupture strain was higher in the stress-relieved than the recrystallized condition for all alloys.
- 2) Rupture strain increased with increasing carbon content.
- 3) The 2700 °F recrystallization anneal resulted in a smaller decrease in rupture strain, with respect to the stress-relieved condition, the higher the carbon content.

The pronounced variation in rupture strain with prior heat treatments is illustrated by the photograph of the fractured stress-rupture specimens (Figure 18). It appears that the differences in rupture strain between the various alloys can be correlated with grain size. The microstructure of the fracture area of a low-carbon B-77 specimen is shown in Figure 19. As can be seen, the fracture is completely intergranular. Many grain boundary fissures can be seen adjacent to the fracture area. The observed fracture appears to be typical of a situation where grain boundary shearing is an important mode of deformation. The grain boundary shearing leads to the development of intergranular fissures originating at grain boundary junctions and the eventual linking of these fractures to cause failure. Fractures of this type are characterized by low total elongation values. The recrystallized alloys of intermediate and high carbon content showed much higher rupture strain at fracture than the low carbon heat (VAM-57). However, as shown in Figure 9, the grain size of the carbon containing B-77 heats was much smaller than the low carbon heat. The ratio ϵ_{gb}/ϵ_T (where ϵ_{gb} is the contribution of grain boundary sliding to the total creep strain, ϵ_T) has been found to increase with decreasing grain size.¹⁷ However, the controlling factor in the failure of the B-77 specimens does not appear to be the total amount of grain boundary shearing, but rather the fact that once a void or crack is initiated it usually grows to the full length of the grain boundary on which it lies. Thus, in the large grained material it is easier for a fissure network to grow and eventually connect to cause failure. An added or possibly alternative

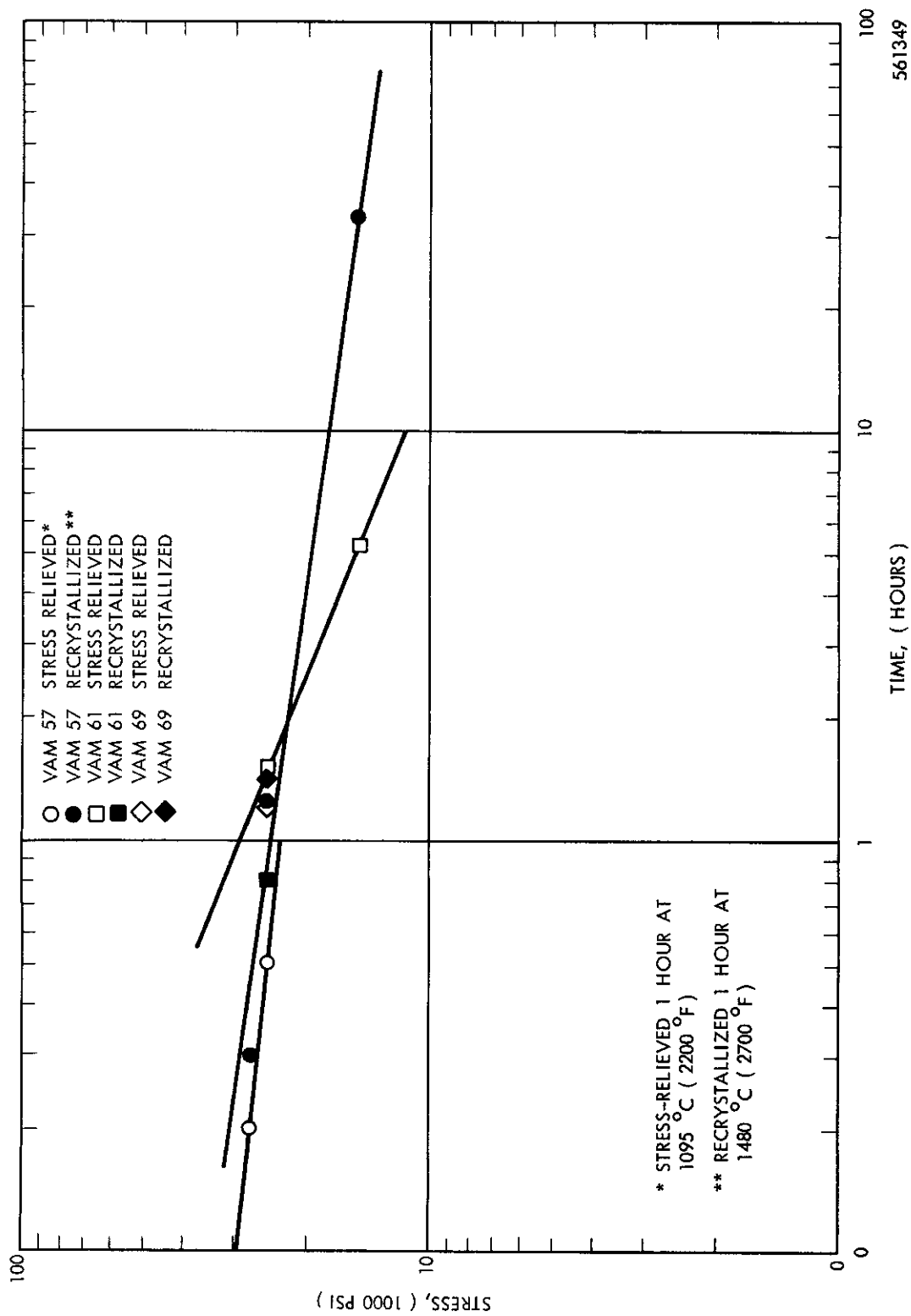


FIGURE 17 - 1205 °C (2200 °F) STRESS RUPTURE DATA FOR B-77 WITH VARYING CARBON LEVELS

TABLE 8. 1205° C (2200° F) STRESS RUPTURE DATA FOR B-77 WITH VARYING CARBON LEVELS

Specimen No.	Composition	Load (psi)	Rupture Time (hrs)	Rupture Strain (%)	Heat Treatment
VAM-57-1C	B-77 (low interstitial)	27,500	0.2	43.0	Stress-relieved*
VAM-57-2C	"	25,000	0.5	44.8	Stress-relieved
VAM-57-4C	"	27,500	0.3	7.2	Recrystallized**
VAM-57-5C	"	25,000	1.25	10.8	Recrystallized
VAM-57-6C	"	15,000	33.5	18.0	Recrystallized
VAM-61-6C	B-77 + 0.077C	25,000	1.5	71.9	Stress-relieved
VAM-61-2C	"	15,000	5.25	65.3	Stress-relieved
VAM-61-2C	"	25,000	0.8	36.1	Recrystallized
VAM-69-1C	B-77 + 0.15C	25,000	1.2	78.9	Stress-relieved
VAM-69-2C	"	25,000	1.4	51.0	Recrystallized

*Stress-relieved 1 hour at 1095° C (2000° F)

**Recrystallized 1 hour at 1480° C (2700° F)

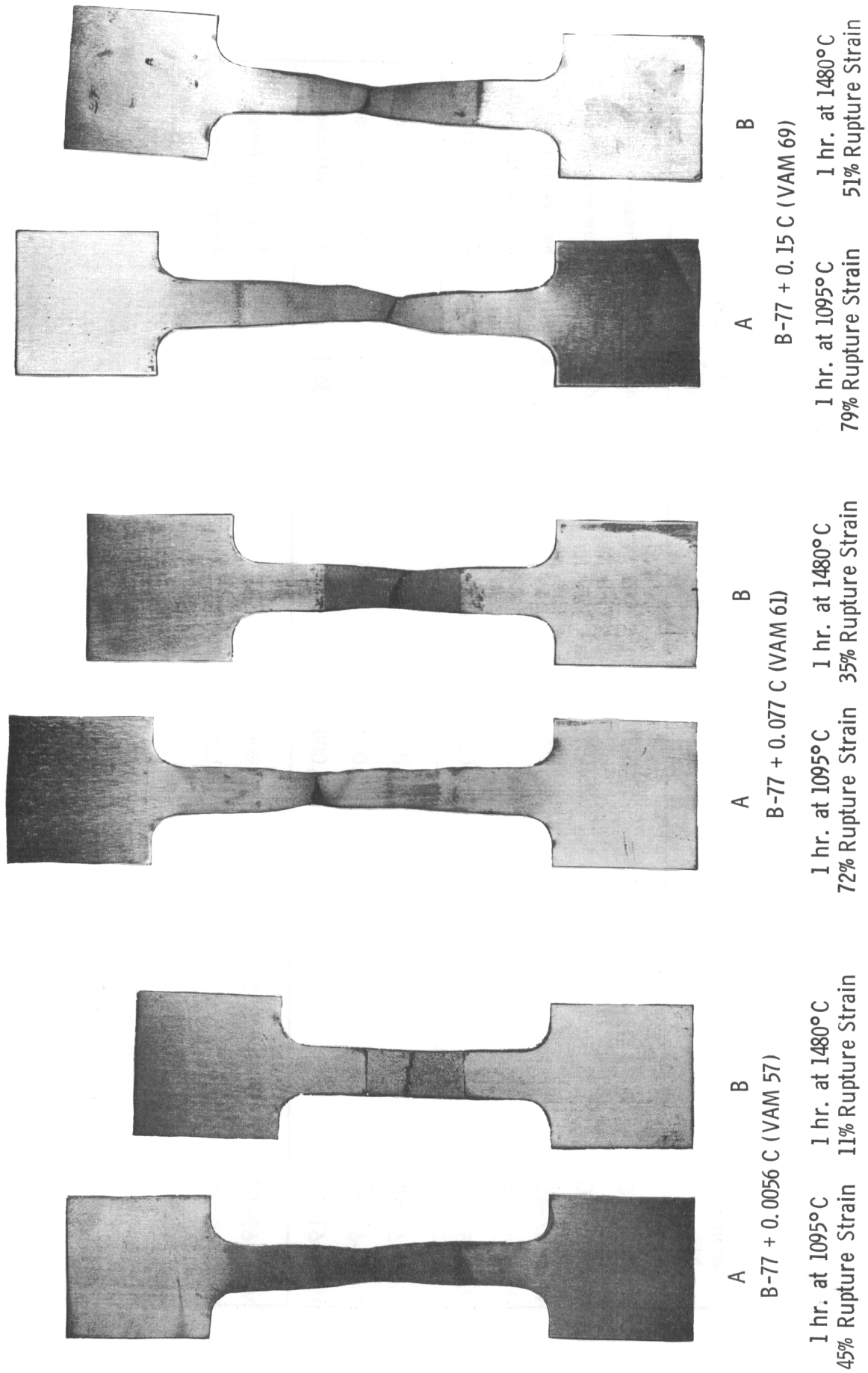


FIGURE 18 - PHOTOGRAPHS OF FRACTURED B-77 STRESS-RUPTURE SPECIMENS.
TEST TEMPERATURE 1205 °C. TEST LOAD 25,000 psi. 1X

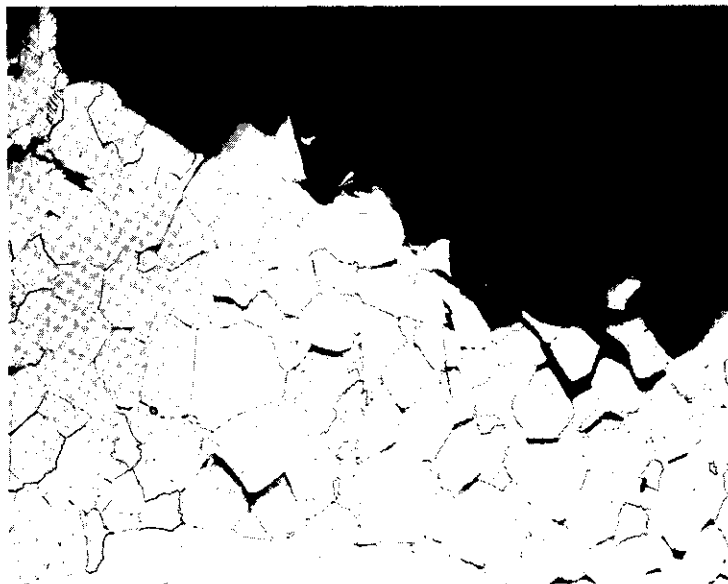


FIGURE 19 - MICROSTRUCTURE OF LOW CARBON B-77 (VAM-57).
ANNEALED 1 HR. AT 2700 °F (1480 °C) PRIOR TO STRESS
RUPTURE TESTING AT 2200 °F (1205 °C). 100X

explanation for the greater fracture strain of the carbon containing alloys is that carbides contribute to grain boundary strengthening.

The relationship between grain boundary shearing and the ductility minima exhibited by many metals has been explored by Rhines and Wray.¹⁸ The results of the present study, although quite limited, appear to be at least in qualitative agreement with their observations.

Grain Boundary Sliding

Much attention is currently being directed to potential applications of refractory metal alloys where creep strength rather than short time tensile properties is the important strength parameter. Consequently, many refractory metal alloy studies are being directed toward development of materials with attractive long-time creep properties. To satisfactorily achieve this goal, detailed information on the structural aspects of high temperature deformation is required. Unfortunately, little data in this area are available for the pure refractory metals, and data on refractory metal alloys are almost totally lacking.

The results of the stress-rupture tests conducted on the B-77 alloys suggested that studies of grain boundary sliding, both in its relation to total creep deformation and its effects on fracture characteristics, would be a fruitful area of study. Consequently, limited studies of grain boundary sliding were initiated. The initial objectives of this work were to establish qualitatively the existence of grain boundary sliding in a complex columbium alloy, and to obtain some indication of the effect of precipitates on this mode of deformation.

Background. The importance of grain boundary shearing as a mode of deformation at elevated temperatures has been shown by Grant and co-workers^{19, 20} and McLean¹⁷. A number of investigators^{21, 22} have reported that the ratio $\epsilon_{gb} / \epsilon_T$ increases with increasing temperature. McLean has shown that the relative contribution of grain boundary shearing to total creep strain increases as the stress is decreased in a series of constant temperature tests. Fazan, et al²³, has indicated that for a constant stress $\epsilon_{gb} / \epsilon_T$ was a constant independent of temperature. The effects of temperature reported by other investigators merely reflect the fact that lower stresses were used at the higher temperatures.

Several investigators have observed that grain boundary sliding is not uniform along the length of the boundary. Calculations by Brunner and Grant²⁴ show that the displacement is non-uniform over the length of the boundary, with the maximum displacement occurring at the mid-point of the shear plane. Their treatment shows that severe stress concentrations occur at the triple points whenever grain-boundary sliding takes place.

Experimental Procedure. Tensile specimens of low and intermediate carbon B-77 (heats VAM-68 and 61) were annealed 2 hours at 1800 °C and helium quenched. The tensile samples were then electrolytically polished in a bath of 10% H₂SO₄ - 5% HF - 85% methyl alcohol at -60 °C using a platinum wire cathode. Polishing was accomplished using 75 volts and 0.7 amps. The electropolished specimens were placed in the jig shown in Figure 20 and lightly scribed with a razor blade. Eight to ten lines were scribed along the gage length transverse to the stress axis of the specimen. No attempt was made to achieve a precise spacing of the scribe marks. Typical grooves intersecting a grain boundary can be seen in Figure 21.

Creep tests were conducted in vacuum at 1205 °C (2200 °F) using the test conditions summarized in Table 9. The tests were terminated after creep strain on the order of 1% was achieved, and the samples were examined metallographically to determine if grain boundary sliding could be observed.

TABLE 9. CREEP DATA FOR B-77 ALLOYS AT 1205 °C (2200 °F)

Heat No.	Stress (psi)	Test Duration (hrs.)	Creep Strain (%)	Minimum Creep Rate (%/hr)
VAM-68	12000	27.4	0.8	0.014
VAM-61	14000	26.3	1.5	0.043

Results. Examination of low interstitial B-77 after creep deformation showed that grain boundary shearing had occurred, as evidenced by the abrupt displacement of the scribe lines as they intersected grain boundaries (Figure 22). Figure 23 shows evidence of displacement of the triple point as a result of sliding along the grain boundary running from the lower right to upper left of the photomicrograph. Similar displacement at triple points has been observed by Chang and Grant²⁵ in Al-Zn alloys. It is interesting to note that distinct grain boundary sliding was observed at low total creep strains. In this initial study no attempt was made to establish the contribution of grain boundary sliding to total creep strain, or the relative displacement over the length of a single boundary. Qualitatively, it was observed that about half of the scribe lines showed evidence of displacement at grain boundaries.

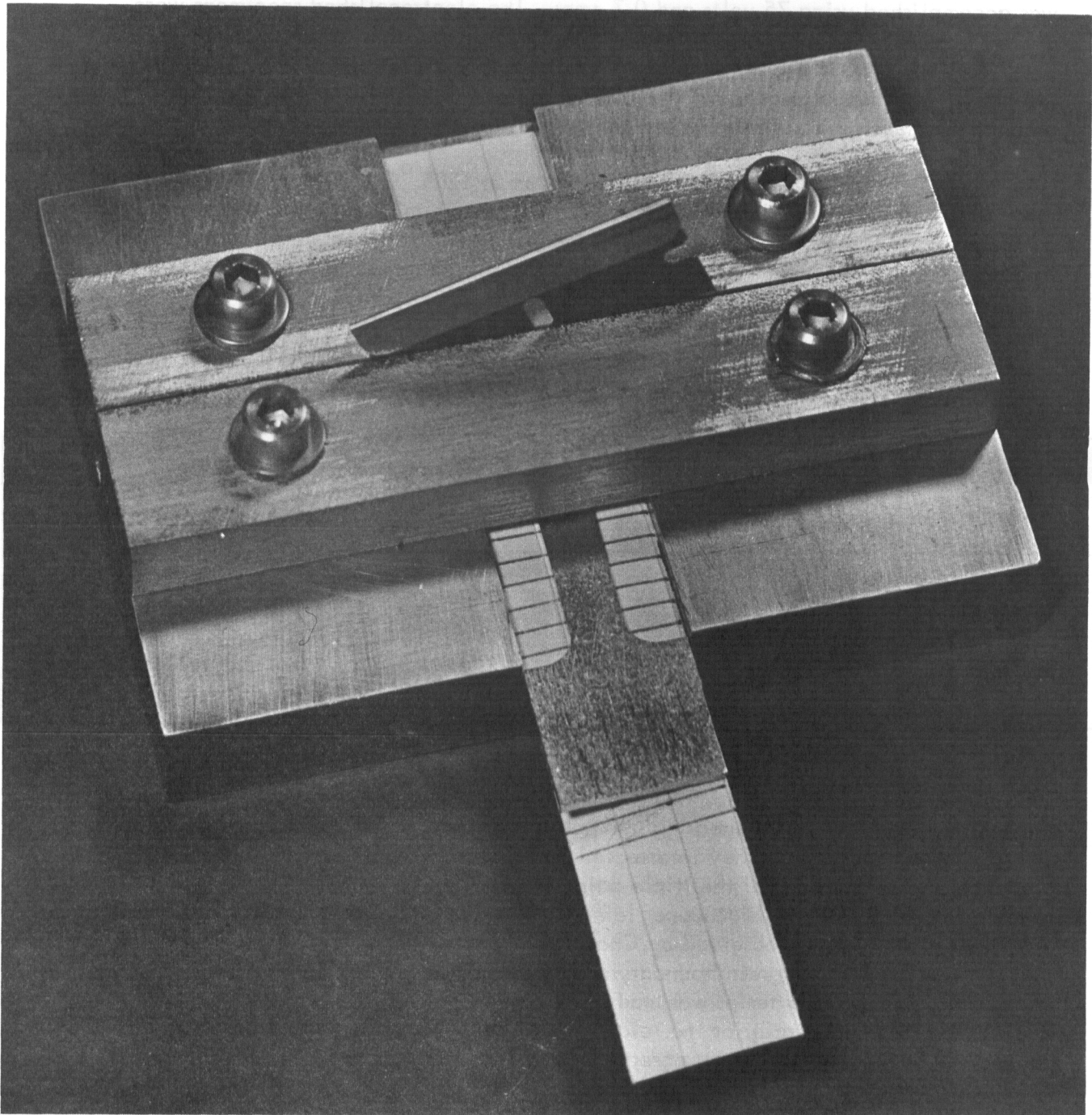


FIGURE 20 - FIXTURE USED TO SCRIBE LINES ON THE SURFACE OF CREEP SPECIMENS

Experimental Procedure. Tensile specimens of low and intermediate carbon B-77 (heats VAM-68 and 61) were annealed 2 hours at 1800 °C and helium quenched. The tensile samples were then electrolytically polished in a bath of 10% H₂SO₄ - 5% HF - 85% methyl alcohol at -60 °C using a platinum wire cathode. Polishing was accomplished using 75 volts and 0.7 amps. The electropolished specimens were placed in the jig shown in Figure 20 and lightly scribed with a razor blade. Eight to ten lines were scribed along the gage length transverse to the stress axis of the specimen. No attempt was made to achieve a precise spacing of the scribe marks. Typical grooves intersecting a grain boundary can be seen in Figure 21.

Creep tests were conducted in vacuum at 1205 °C (2200 °F) using the test conditions summarized in Table 9. The tests were terminated after creep strain on the order of 1% was achieved, and the samples were examined metallographically to determine if grain boundary sliding could be observed.

TABLE 9. CREEP DATA FOR B-77 ALLOYS AT 1205 °C (2200 °F)

Heat No.	Stress (psi)	Test Duration (hrs.)	Creep Strain (%)	Minimum Creep Rate (%/hr)
VAM-68	12000	27.4	0.8	0.014
VAM-61	14000	26.3	1.5	0.043

Results. Examination of low interstitial B-77 after creep deformation showed that grain boundary shearing had occurred, as evidenced by the abrupt displacement of the scribe lines as they intersected grain boundaries (Figure 22). Figure 23 shows evidence of displacement of the triple point as a result of sliding along the grain boundary running from the lower right to upper left of the photomicrograph. Similar displacement at triple points has been observed by Chang and Grant²⁵ in Al-Zn alloys. It is interesting to note that distinct grain boundary sliding was observed at low total creep strains. In this initial study no attempt was made to establish the contribution of grain boundary sliding to total creep strain, or the relative displacement over the length of a single boundary. Qualitatively, it was observed that about half of the scribe lines showed evidence of displacement at grain boundaries.

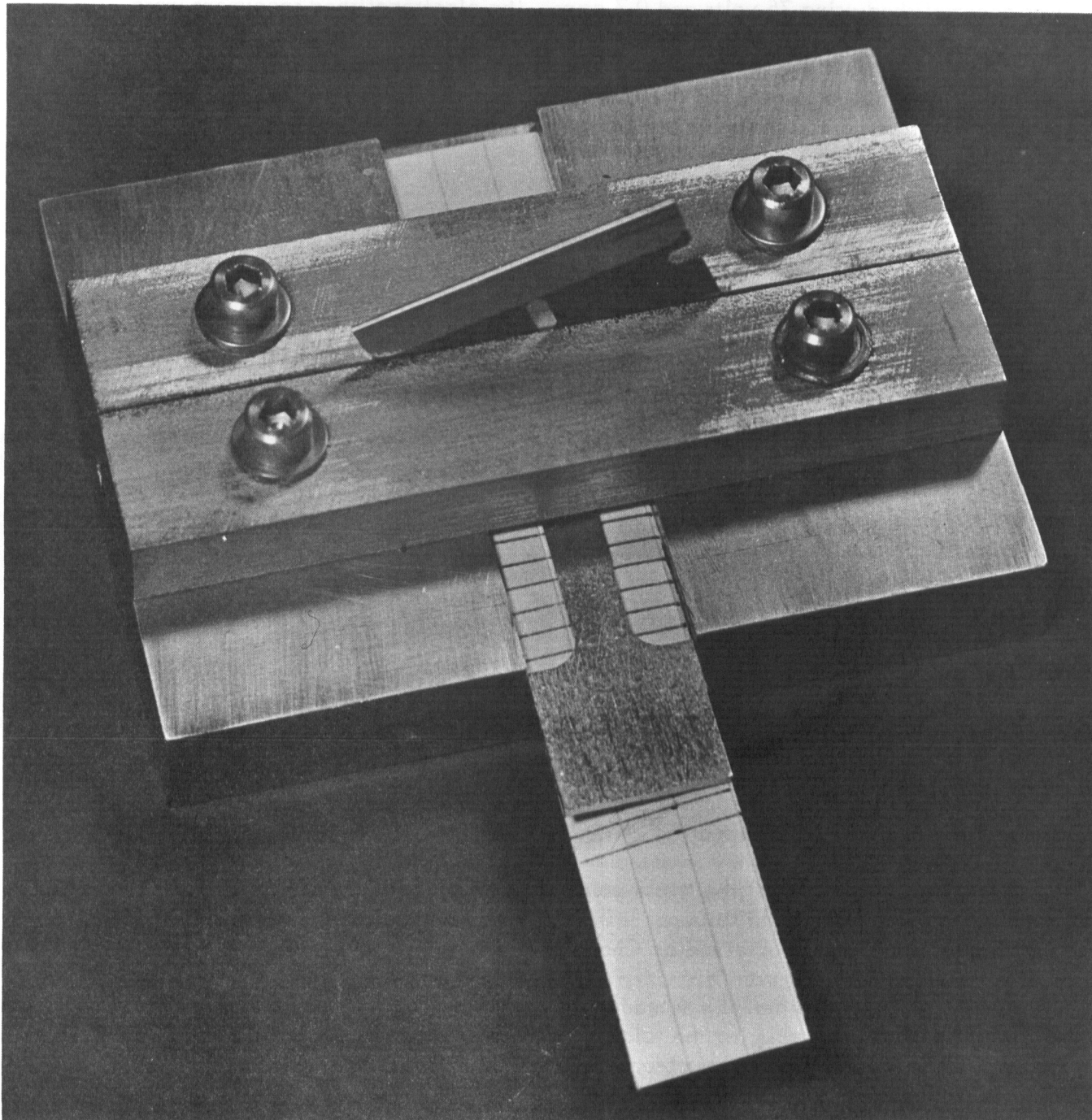


FIGURE 20 - FIXTURE USED TO SCRIBE LINES ON THE SURFACE OF CREEP SPECIMENS

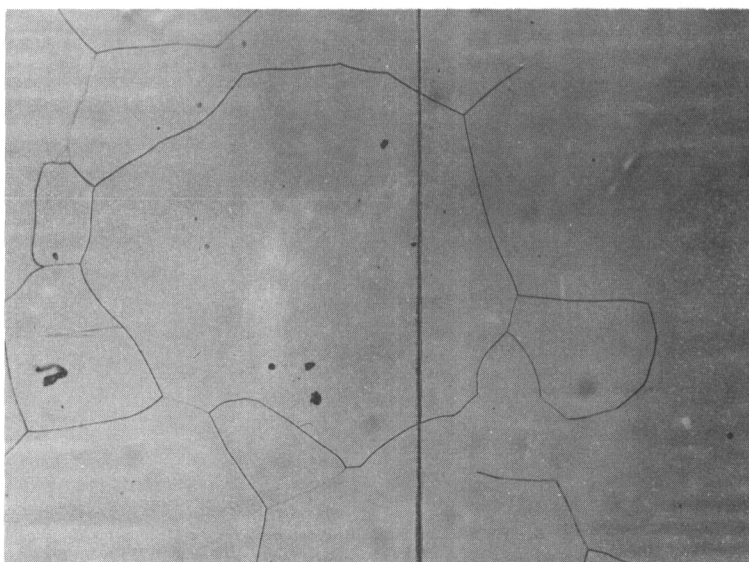
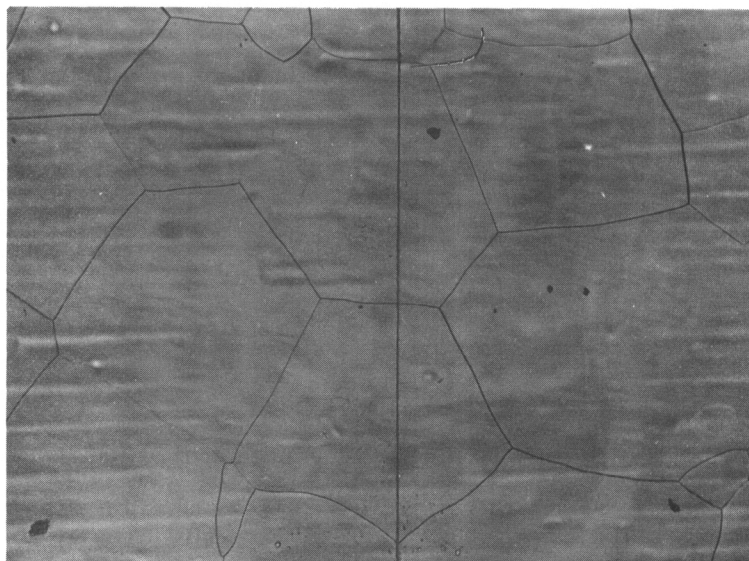


FIGURE 21 - MICROSTRUCTURE OF VAM 68 (B-77) SHOWING THE SCRIBE LINES INTERSECTING GRAIN BOUNDARIES. PRIOR TO CREEP STRAINING. 75X

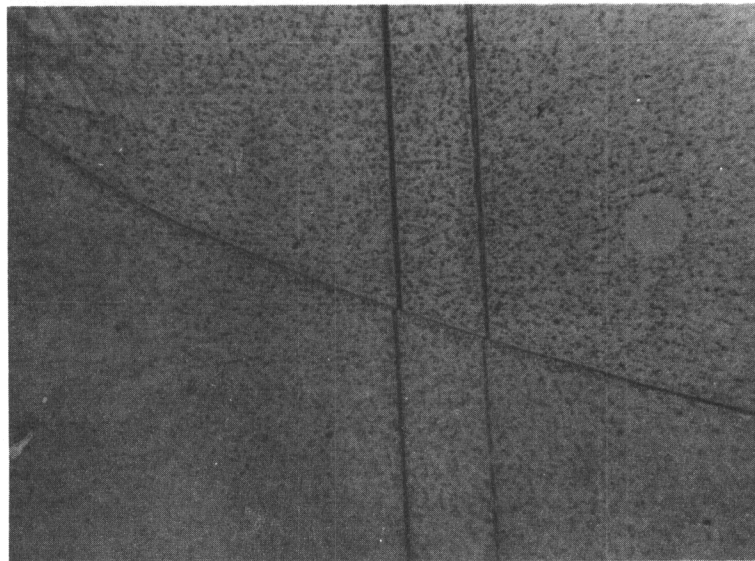
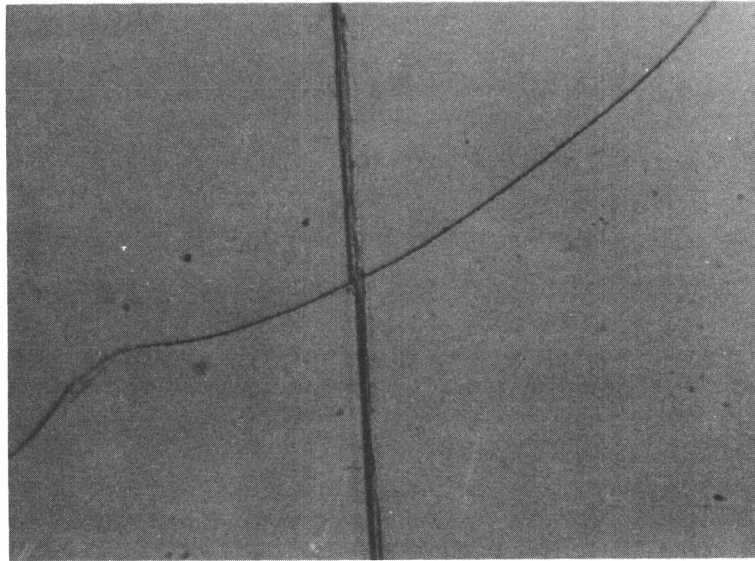


FIGURE 22 - MICROSTRUCTURE OF VAM 68 (B-77) SHOWING GRAIN BOUNDARY SLIDING. AFTER CREEP STRAINING AT 1205 °C (2200 °F). 500X

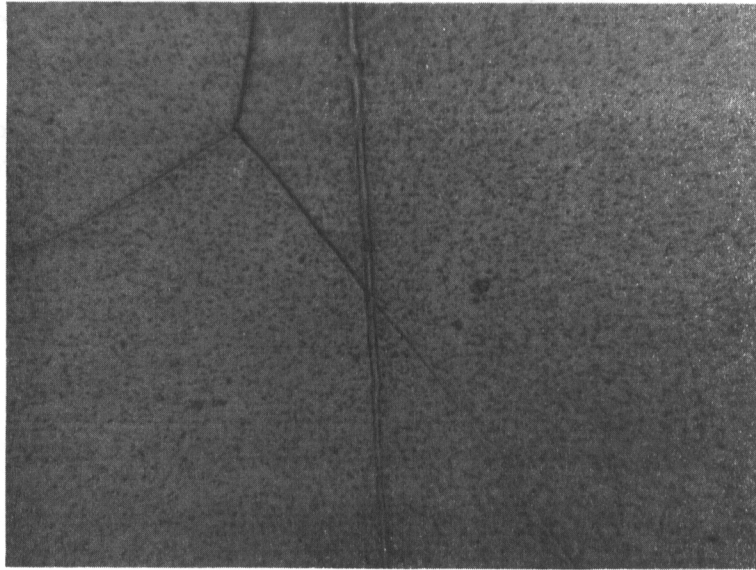


FIGURE 23 - MICROSTRUCTURE OF VAM 68 (B-77) SHOWING GRAIN BOUNDARY SLIDING AS EVIDENCED BY THE DISPLACEMENT AT THE TRIPLE POINT. AFTER CREEP STRAINING AT 1205 °C (2200 °F). 500X

Examination of the VAM-61 specimen (B-77 + 0.077 C) showed much less evidence of grain boundary sliding than the low carbon heat, despite the higher total elongation. Figure 24 shows the best example of grain boundary sliding in this alloy. It should be noted that a somewhat higher stress (14,000 psi) was used in straining the intermediate carbon alloy. While the observation of less grain boundary sliding in the carbon containing alloy is only qualitative, the results suggest that grain boundary sliding may have been inhibited by carbide precipitation on the boundaries. Previous heat treatment studies on the B-77 alloys have established that carbide precipitation will occur at 1205°C (2200°F), the test temperature used. The VAM-61 specimen was subsequently retested at 14,000 psi for an additional 152.8 hours (179.1 hours total). Total strain at this point was only 2.4%. Examination of the retested specimen is currently in progress.

These preliminary observations, while qualitative in nature, clearly show significant grain boundary shearing in a complex Cb alloy. More detailed studies of this mode of deformation in refractory metal alloys appear to be an area of fruitful investigation.



FIGURE 24 - MICROSTRUCTURE OF VAM 61 (B-77 + 0.077 C) SHOWING GRAIN BOUNDARY SLIDING. AFTER CREEP STRAINING AT 1205 °C (2200 °F) 500X

IV. CONSTITUTION AND PROPERTIES OF Cb-V-Mo ALLOYS

In a previous phase of this program, limited studies of the constitution of the Cb-rich corner of the Cb-V-Mo system were undertaken to provide base line data useful in investigations of the processing and mechanical properties of Cb-V-Mo and Cb-V-Mo-Zr alloys. During the current contract period, lattice parameter, melting point, and hot hardness data were obtained to complete studies of this alloy system.

Literature

No published data have been found in the literature concerning the constitution of the Cb-V-Mo ternary system. The columbium-vanadium binary phase diagram was determined by Wilhelm, Carlson, and Dickinson²⁶ to be a continuous solid solution. They observed a minimum in the liquidus and solidus at 1810 °C and approximately 35 w/o Cb. Lattice parameter data reported by Bückle²⁷ indicate that columbium and molybdenum also form an uninterrupted series of solid solutions. Molybdenum and vanadium are also reported to form a continuous solid solution.²⁸

Experimental Procedure

Alloy Preparation. Alloys were prepared in the form of 20 gram buttons by non-consumable arc melting. The columbium used in this investigation was obtained from the Union Carbide Metals Company in the form of small beads, approximately 1/8 inch in diameter. The chemical analysis of the columbium is as follows (in w/o): 0.045 oxygen, 0.011 nitrogen, 0.022 carbon, 0.5 tantalum, 0.01 titanium, <0.03 zirconium, <0.0001 boron. Vanadium and molybdenum sheet trimmings, of good commercial purity, were used for alloy additions. The vanadium was supplied by the Union Carbide Metals Company and had as the major impurity approximately 0.05 w/o oxygen. Molybdenum sheet was obtained from the Climax Molybdenum Company.

The melting charges were carefully weighed out and pressed in a die to provide 1/2 inch diameter compacts. The charges were placed in a multiple hearth arc furnace, which was evacuated to 5×10^{-5} Torr, flushed twice with high purity argon, and backfilled to 2/3 atmosphere argon pressure. Mass spectrometer analyses were obtained on the tank argon to insure a purity level of at least 99.99%. A titanium button was melted to getter any remaining impurities. The samples were then melted four times, the alloys being inverted after each melt. Weight losses incurred during melting were negligible, hence the nominal analyses were assumed correct. This assumption was verified by chemical analysis of several homogenized alloys, which showed very close agreement with the nominal compositions. Analysis did show a reduction in oxygen content to about 0.035 w/o as a result of arc melting, and a further reduction to approximately 0.02 w/o after vacuum annealing at 1900 °C.

Heat Treatment. Alloys were homogenized by annealing for various times (generally 24 hours) at 1900 °C. Annealing was carried out in a tungsten tube resistance furnace at pressures below 5×10^{-5} Torr. Each sample was wrapped in columbium foil and suspended within the furnace by a tungsten wire. Temperatures were measured with a calibrated optical pyrometer using procedures described in a later section of this report. The samples were radiation cooled after homogenization by turning off the power. Cooling was quite rapid, the specimen temperature falling below 1000 °C in approximately 30 seconds. Subsequently, sections of the homogenized alloys were sealed in evacuated quartz capsules and annealed 2 weeks at 1000 °C.

During the longer annealing treatments at 1900 °C, some loss of a constituent (presumably vanadium) occurred. Metallographic examination showed that the loss was confined to a thin surface layer. This depleted layer was removed prior to the preparation of samples for x-ray diffraction analysis, thus insuring lattice parameter data representative of the nominal compositions.

Melting Point Determinations. Melting point determinations were made on fully homogenized alloys by visually observing the first appearance of liquid. The alloys were supported on a columbium sling connected to a tungsten wire in the same furnace used for the homogenization treatments. The specimen could be observed from above through the open end of the furnace heater. Specimen temperature was measured with an optical pyrometer sighted through a small diameter hole drilled in the radiation shields and center of the heater tube, thus closely simulating ideal black body conditions. The pyrometer was calibrated against a standard lamp, and corrections were made for the reflection and absorption of the Pyrex sight glass using essentially the same technique described by Taylor, Doyle, and Kagle²⁹. In carrying out the melting point determinations a sharp edge of the specimen was observed from above while temperature was simultaneously determined by optical pyrometer readings taken through the sight hole in the mid length of the furnace tube. The furnace temperature was gradually raised until the first rounding of the sharp specimen edge was observed, at which point the sample was radiation cooled. This temperature was taken as the solidus temperature. Subsequent metallographic examination showed that melting had initiated when the rounding was observed. The melting points observed by this technique are probably somewhat higher than those obtained by metallographic incipient melting methods, but are considered to be substantially correct within ± 25 °C.

X-ray Diffraction. X-ray diffraction patterns were obtained in a Debye-Scherrer camera using filtered Co K α radiation. The lattice parameters were computed by extrapolating to 90° using the Nelson-Riley procedure. Powder samples were prepared by crushing or filing the homogenized alloys and placing the powder in cylindrical 3/8 inch diameter Cb crucibles. The powder was flash annealed by rapidly inserting the crucibles in the hot zone of a vacuum furnace evacuated to a pressure of about 1×10^{-5} Torr. The crucibles were held at 1200 °C for 5 to 10 minutes, and then removed from the hot zone. This recovery treatment provided sharp diffraction patterns for lattice parameter measurements.

Results

Constitution. Alloys containing 5, 10, 20, 30, and 40 weight per cent total alloy additions were investigated. Vanadium and molybdenum were added to the columbium base in the ratios 1:1, 1:3, and 3:1 at each alloy level, providing twelve Cb-V-Mo alloys. Metallographic examination of the alloys homogenized at 1900 °C showed them all to be single phase. Sections of the homogenized alloys annealed two weeks at 1000 °C were also single phase. X-ray diffraction data showed only the existence of a bcc solid solution. Although in this investigation compositions extending only from 100 to 60 w/o Cb were examined, it seems apparent that the Cb-V-Mo system is a continuous solid solution at all temperatures.

Lattice parameter data are shown in Figure 25. The alloys exhibit a continuous decrease in lattice parameter with increasing Mo and V level. The alloys with Mo/V solute ratios of 3 and 1/3 show a linear decrease in lattice parameter, while with a solute ratio of 1 a slight positive deviation from ideality was observed.

Melting points are plotted as a function of alloy addition in Figure 26. Alloys having Mo/V solute ratios of 1 and 1/3 showed a continuous decrease in solidus temperature with increasing alloy addition. As expected, vanadium had the most pronounced effect in depressing the melting point. An anomalously high melting point of 2520 °C was observed for the Cb-7.5Mo-2.5V alloy. This value is only 100 °C lower than the melting point of pure Mo and must be viewed with some reservation. However, the melting point was rechecked twice, and the observed values were all in agreement.

Hardness. Hardness data for the alloys in the as-cast and homogenized condition are shown in Figure 27. Annealing at 1900 °C resulted in a modest decrease in hardness with respect to the as-cast condition. Both molybdenum and vanadium additions have pronounced effects in increasing the hardness of Cb.

To provide some data on the high temperature properties of Cb-V-Mo alloys, hot hardness data were obtained for specimens having a Mo/V solute ratio of 1. The samples were homogenized by annealing 12 hours at 1800 °C prior to testing. Hot hardness measurements were conducted in a vacuum hot hardness machine described previously in this report. A load of either 5 or 2.5 Kg was used on the indenter, the higher load being used at temperatures below 1095 °C (2000 °F).

The effect of temperature on the hot hardness of the Cb-V-Mo alloys is shown in Figure 28. The data show Mo and V to be very effective solid solution strengtheners at temperatures as high as 1315 °C (2400 °F). The hardness-composition curves show a characteristic decrease in slope with increasing test temperature, following the pattern predicted for solid solution alloy strengthening. The hardness of the Cb-20Mo-20V alloy at 1205 °C (2200 °F) is approximately 165 VPN. Based upon a hot hardness-strength correlation established in previous work³⁰, this corresponds to a yield strength of 60,000 psi.

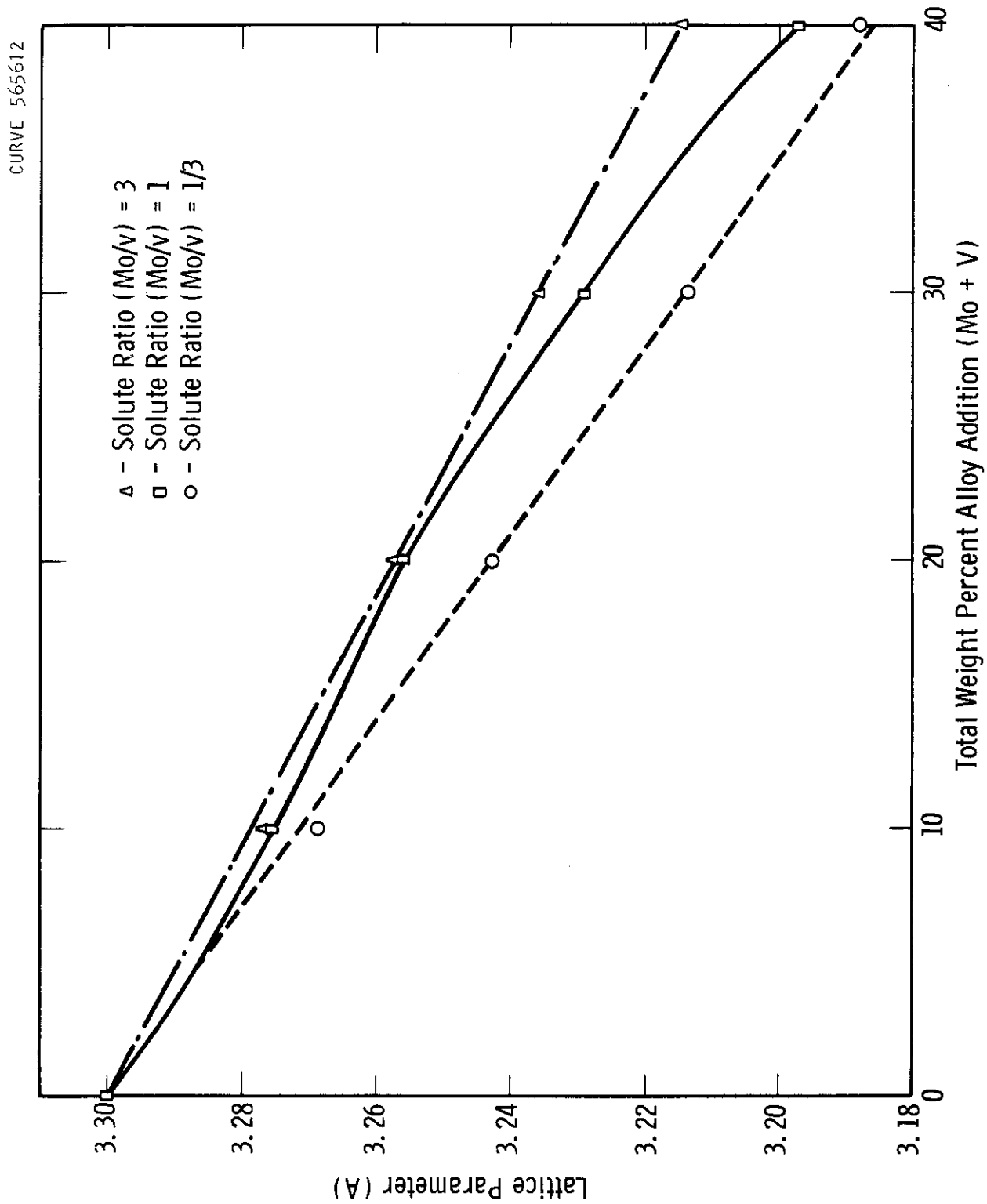


FIGURE 25 - VARIATION OF LATTICE PARAMETER WITH COMPOSITION FOR Cb-V-Mo ALLOYS

CURVE 565611

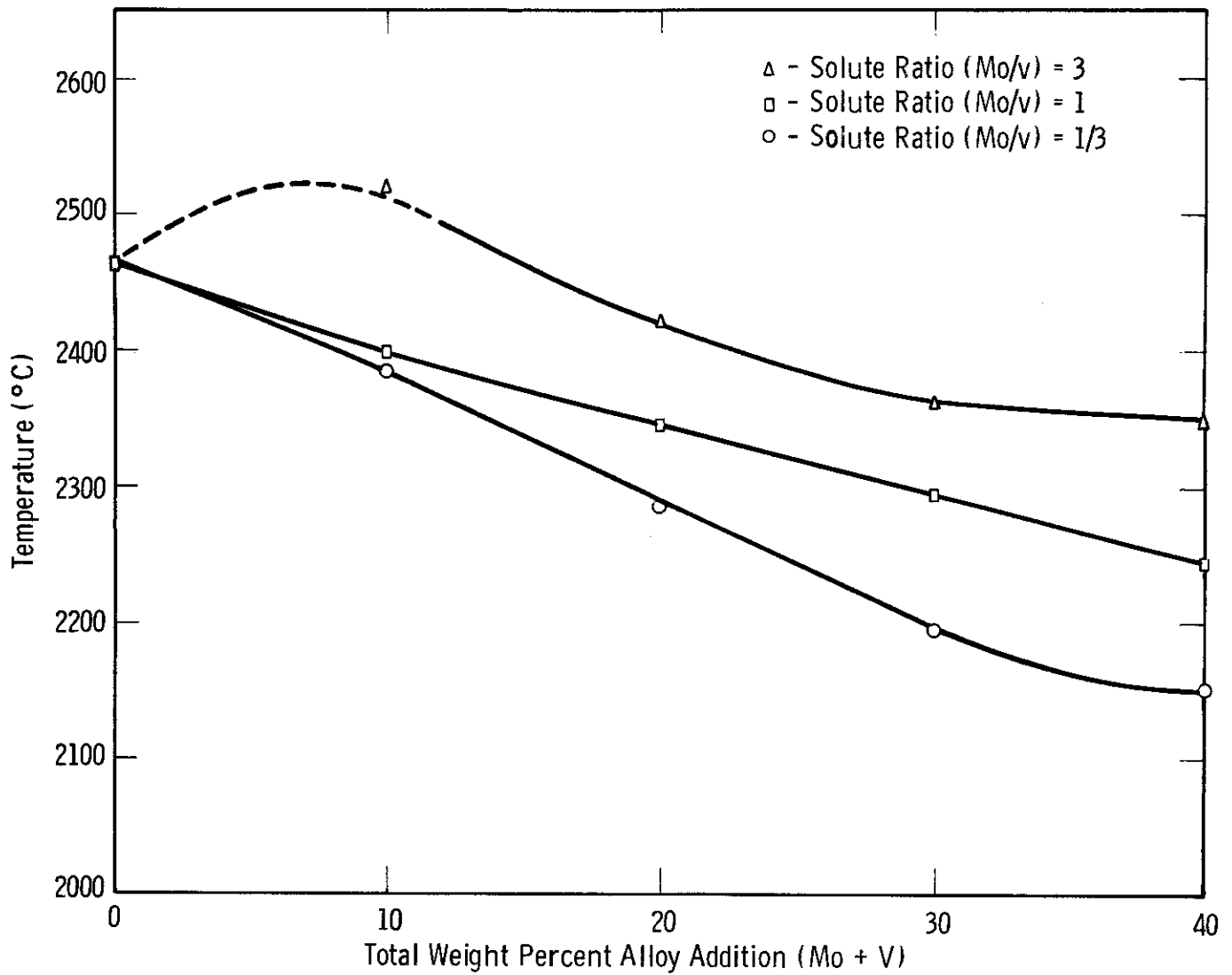


FIGURE 26 - VARIATION OF MELTING POINT WITH COMPOSITION FOR Cb-V-Mo ALLOYS

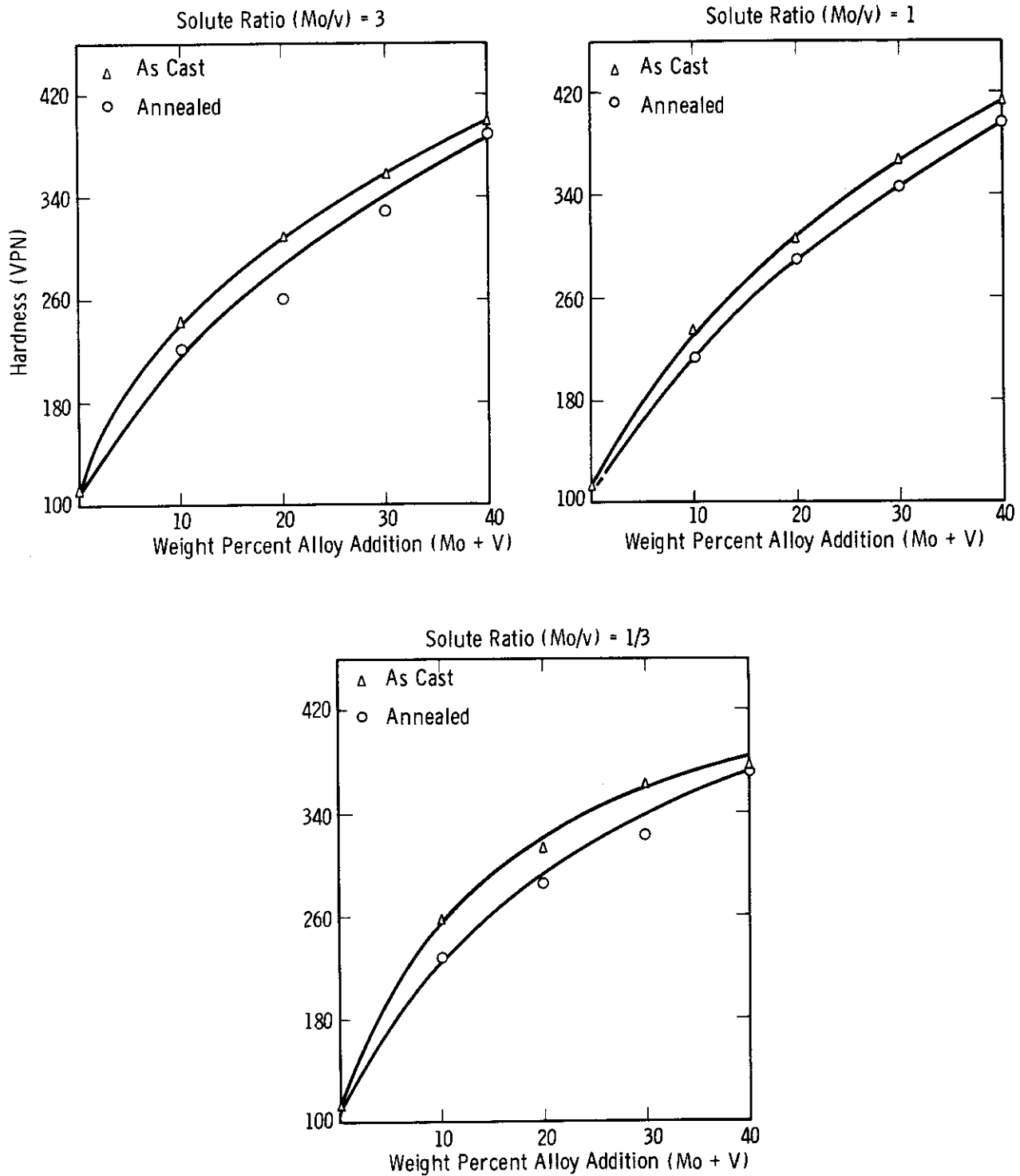


FIGURE 27 - EFFECT OF COMPOSITION ON THE HARDNESS OF Cb-V-Mo ALLOYS

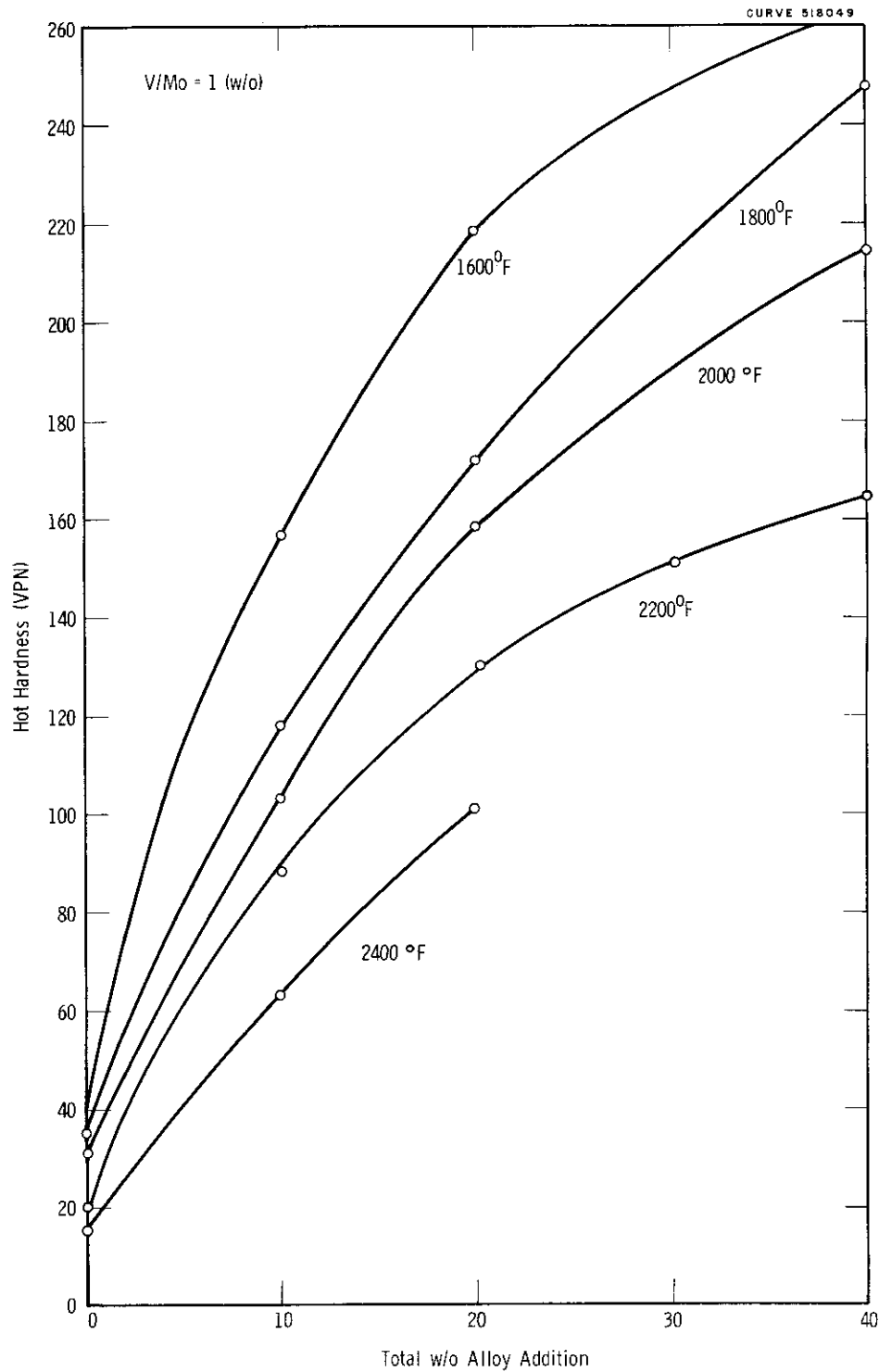


FIGURE 28 - HOT HARDNESS OF Cb-V-Mo ALLOYS

Evidence of an approximate correlation between room temperature strength and change in lattice parameter for dilute alloys has been shown by French and Hibbard³¹, as well as a number of other investigators. In the refractory metals, Chang³² has summarized the data of several investigators who also show a rough correlation between high temperature tensile strength and lattice parameter change for Cb, Ta, and Mo alloys containing binary additions of various solutes. The relationship between hot hardness and change in lattice for Cb-V-Mo alloys obtained in the present investigation is shown in Figure 29. Hot hardness data obtained at 1095 °C (2000 °F) and 1205 °C (2200 °F), when plotted against change in lattice parameter, give a curve which is approximately parabolic in shape. However, the data points for Mo + V concentrations up to 20 w/o can be fitted to a straight line. The approach of considering only the size factor in solute strengthening can only provide a crude first approximation, for it ignores electrical and chemical interactions, as well as local order (Fisher interaction). A detailed treatment of solid solution strengthening has recently been presented by Flinn³³.

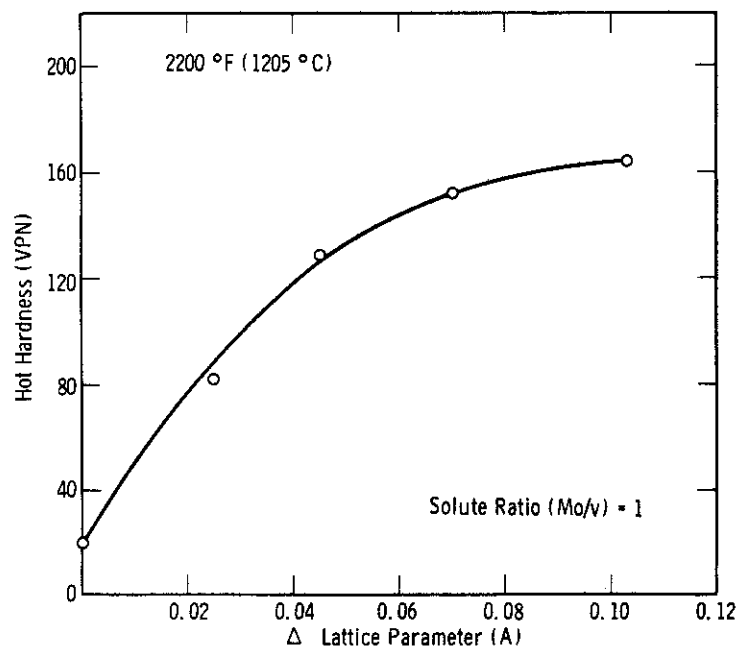
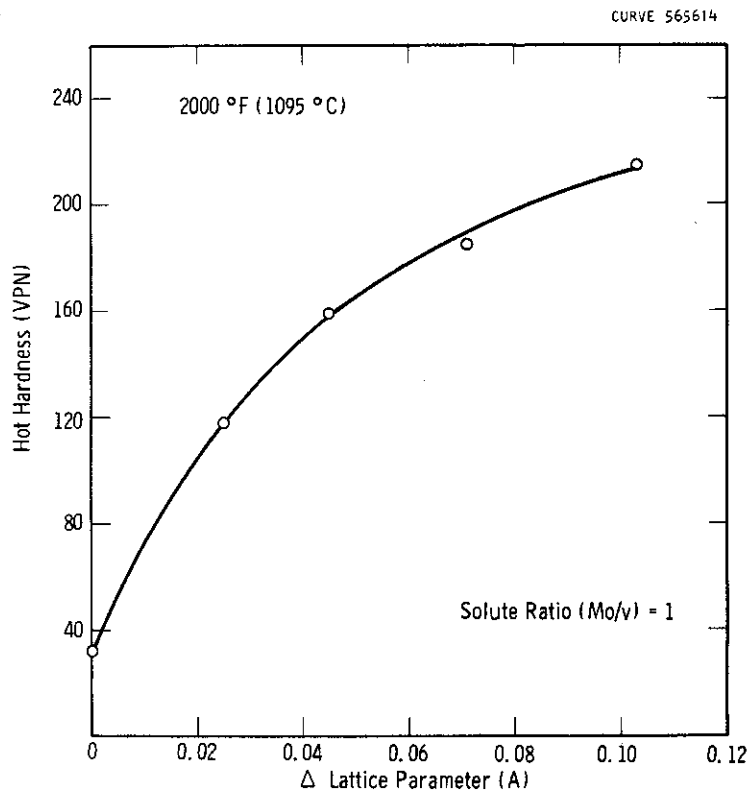


FIGURE 29 - CORRELATION OF HOT HARDNESS WITH CHANGE IN LATTICE PARAMETER FOR Cb-V-Mo ALLOYS

V. STUDIES OF Cb-Hf-N ALLOYS

Experimental work in an earlier phase of this program⁴ had shown that Cb-Hf alloys containing additions of approximately 0.1 w/o nitrogen exhibited very high hot hardness values at temperatures up to 1095 °C - 1205 °C (2000-2200 °F). The attractive hot hardness values were apparently associated with the precipitation of a nitride phase. In view of the interesting preliminary results, more detailed studies of Cb-Hf-N alloys were initiated, since this system appeared to be particularly attractive for the study of precipitation phenomena in columbium alloys.

Alloy Preparation. A Cb-5Hf-0.2 N alloy was prepared by consumable electrode arc melting to provide material for detailed studies of heat treatment effects. A low interstitial Cb-5Hf alloy was also melted to provide base line data. It was originally intended to prepare a Cb-5Hf-0.1 N alloy for investigation. Since it was anticipated that considerable loss of nitrogen would occur during vacuum arc melting, the electrode was prepared with approximately 100% excess nitrogen. However, relatively little loss of nitrogen occurred, hence the final nitrogen level was close to 0.2 w/o.

Melting. The Cb-5Hf heat (VAM-71) was melted using an electrode fabricated from high purity columbium and crystal bar hafnium strip. The analysis of the base material is listed in Table I (Lot 1074). A 3/4 inch square composite electrode, with the hafnium strip contained in the center of the electrode assembly was vacuum arc melted into a 1-7/8 inch diameter crucible. The ingot weight was approximately four pounds. To prepare the nitrogen containing heat (VAM-73), two sections of columbium rod, 14 inches long and 11/16 inch in diameter, were nitrided to achieve the desired nitrogen level. The base material was the same as that used for VAM-71. The rods were placed in a vacuum induction furnace, which was evacuated to 1×10^{-5} Torr and back-filled to 2/3 atmosphere nitrogen pressure. The bars were reacted with nitrogen for one hour at 1700 °C. The time required to bring the furnace to temperature was 50 minutes. The bars were carefully weighed before and after nitriding. The observed weight increase corresponded to a nitrogen level of 0.22 w/o. After nitriding, the two bars were joined mechanically and strips of hafnium were tack welded along the sides. The electrode was consumably arc melted into a 1-7/8 inch water-cooled, copper crucible, using 30 volts and 1200 amps AC. Earlier work had established that excellent homogeneity is achieved by single AC melting composite electrodes. The pressure during melting did not exceed 8×10^{-4} Torr, indicating that very little nitrogen was lost during melting. Chemical analyses and as-cast hardness values of the Cb-5Hf and Cb-5Hf-0.2 N alloys are listed in Table 10. The nitrogen analysis of heat VAM-73 was 0.193 w/o, fairly close to the initial nitrogen level of the electrode.

Fabrication. A one inch thick section of the Cb-5Hf alloy (VAM-71) was cut from the ingot and upset forged to approximately 50% reduction in thickness at 1200 °C. Heating for forging was accomplished in a retort with a flowing argon atmosphere to

minimize contamination. The forged slab was conditioned to remove the contaminated surface and then annealed one hour at 1370 °C (2500 °F). The annealed material was subsequently cold rolled to 0.05 inch sheet, a reduction of approximately 90%.

Ingot breakdown of the Cb-5Hf-0.2 N alloy was accomplished by Dynapak extrusion. After the as-cast billet was conditioned by machining, a 7/8 inch thick molybdenum nose plug was attached to the billet to minimize the danger of a nose burst. The billet was coated with Corning glass 7052 and heated in an argon atmosphere induction furnace to 1650 °C (3000 °F). The billet was rapidly transferred to a container and extruded to a sheet bar configuration using a fire pressure of 2000 psi. The extrusion ratio was 4:1. The die was coated with alumina to minimize die washout. The basic Dynapak extrusion techniques were very similar to those described in an earlier report.⁴ As shown in Figure 30, the results of extrusion were excellent. No cracking was observed, and the as-extruded surface was very good considering the relatively high extrusion temperature.

The sheet bar was surface conditioned and then vacuum annealed one hour at 1500 °C. The bar was then rolled at 260 °C (500 °F) from 0.43 inch thick to 0.26 inch thick (40% reduction). The bar was then reannealed one hour at 1500 °C and given an additional 75% reduction by rolling at 260 °C. The rolling characteristics of the material were excellent. No evidence of cracking whatsoever was observed. As will be shown later in this report, the 1500 °C annealing treatment provided an overaged structure which was quite soft and easily fabricable.

TABLE 10. CHEMICAL ANALYSES OF Cb-Hf AND Cb-Hf-N ALLOYS

Heat No.	Nominal Composition (w/o)	Analysis (w/o)				As-cast Hardness (VPN)
		O	N	C	Hf	
VAM-71	Cb-5Hf	0.012	0.005	0.0005	4.61	170
VAM-73	Cb-5Hf-0.2 N	0.021	0.193	0.0023	4.71	364
NC-370	Cb-5Hf-0.1 N	0.018	0.09	---	--	290

Effects of Heat Treatment.

The effects of thermal treatment on room temperature hardness, microstructure and hot hardness of the Cb-5Hf-0.2 N were evaluated.

Solutioning and Aging Reactions. Initial aging studies were conducted on a 20 gram Cb-5Hf-0.1 N alloy button prepared by non-consumable arc melting (heat NC-370, Table 10). Sections of the as-cast button were aged one hour at temperatures ranging from 600-1800 °C. The hardness data are shown in Figure 31. The as-cast condition for the small

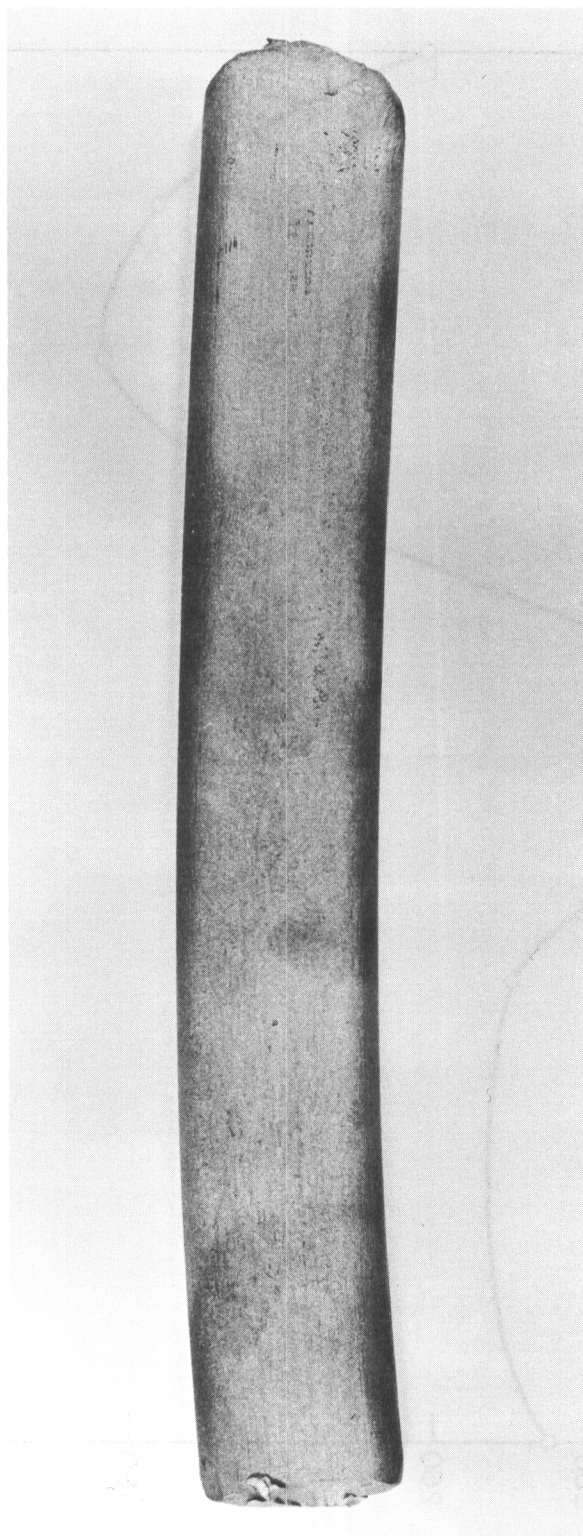


FIGURE 30 - DYNAPAK EXTRUDED Cb-5Hf-0.2N ALLOY. 1X

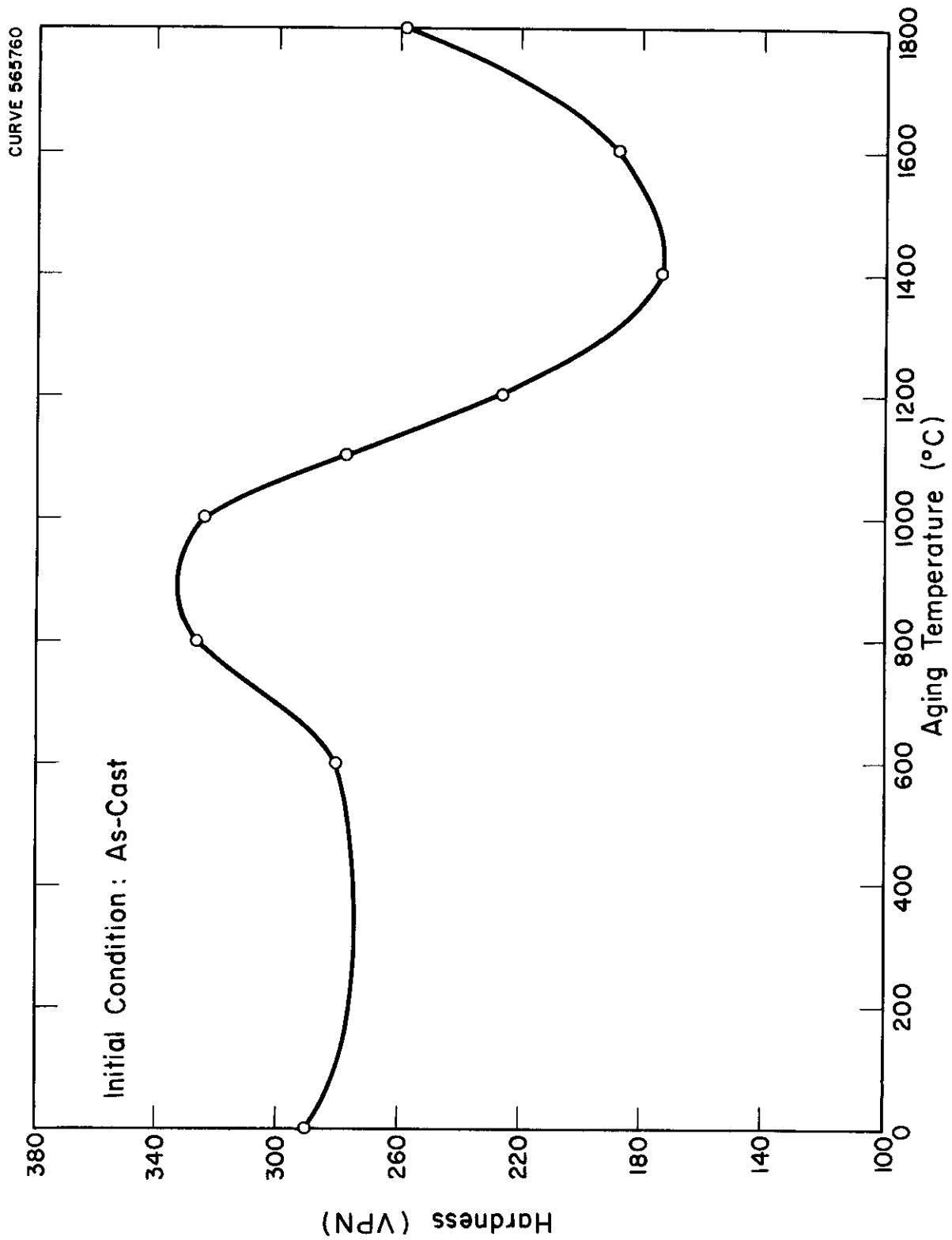


FIGURE 31 - EFFECT OF AGING TEMPERATURE ON THE HARDNESS OF A Cb-5Hf-0.1N₂ ALLOY

button corresponds to a fairly rapid quench, since the sample cools from the melt in a water-cooled, copper crucible. As can be seen from Figure 31, aging one hour at 800 and 1000 °C resulted in a significant hardness increase. Hardness thereafter decreased rapidly with increasing aging temperature, until a hardness minimum was reached at 1400 °C. Hardness then increased with increasing aging temperature, evidently as a result of resolution of a nitride phase. Metallographic examination showed no evidence of a second phase at aging temperatures up to 1400 °C. Material aged one hour at 1400 °C showed matrix hardening. The sample aged at 1600 °C showed a very fine precipitate distributed throughout the grain volumes. The precipitate could barely be resolved at a magnification of 500 X. Aging four hours at 1600 °C resulted in a coarsening of the precipitate, as shown in Figure 32.

Sections of the as-rolled VAM-73 sheet, 0.055 inches thick, were subsequently solution annealed two hours at 1800 °C in vacuum at pressures below 1×10^{-5} Torr. To determine the effect of cooling rate on the solution annealed hardness, samples were quenched by dropping them from the hot zone of a vertical tungsten tube furnace onto a liquid nitrogen cooled copper plate. Other samples were cooled by turning off the furnace power and admitting helium to the furnace chamber. In the latter case, the specimens cooled to below red heat in less than 1-1/2 minutes. The as-solution annealed hardness values are listed in Table 11.

TABLE 11. HARDNESS OF SOLUTION ANNEALED Cb-5Hf-0.2 N ALLOY

Heat No.	Nominal Composition (w/o)	Hardness (VPN)	
		Annealed 2 hours at 1800°C and Quenched	Annealed 2 hours at 1800°C and Helium Cooled
VAM-73	Cb-5Hf-0.2 N	390	223

As can be seen, the quenched samples had a much higher hardness than those cooled in helium, evidently because of a much greater nitrogen supersaturation in the case of the quenched material. Subsequently, additional material was solution annealed two hours at 1800 °C, quenched, and aged one hour at temperatures ranging from 600 to 1600 °C. The effect of aging temperature on the hardness of the Cb-5Hf-0.2 N alloy is shown in Figure 33. Hardness initially decreased moderately, and then abruptly increased on aging at 800 °C. Hardness then decreased rapidly with increasing aging temperature, reaching a minimum after a one hour aging anneal at 1400 °C. Optical photomicrographs of material aged at 600, 1200, 1400 and 1600 °C are shown in Figure 34. The microstructure after aging at 600 and 1200 °C is essentially single phase, although some grain boundary precipitation and random matrix precipitation can be observed. However, after aging one hour at 1400 °C general precipitation within the grain volumes occurs. This appears as general

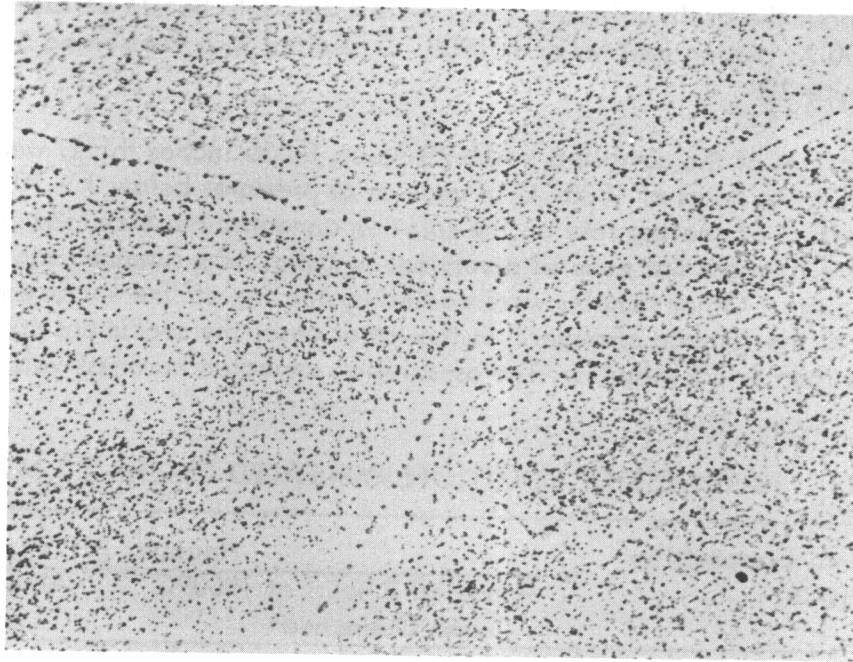


FIGURE 32 - MICROSTRUCTURE OF Cb-5Hf-0.1N ALLOY (NC-370)
AGED 4 HOURS AT 1600°C. 500X

CURVE 565838

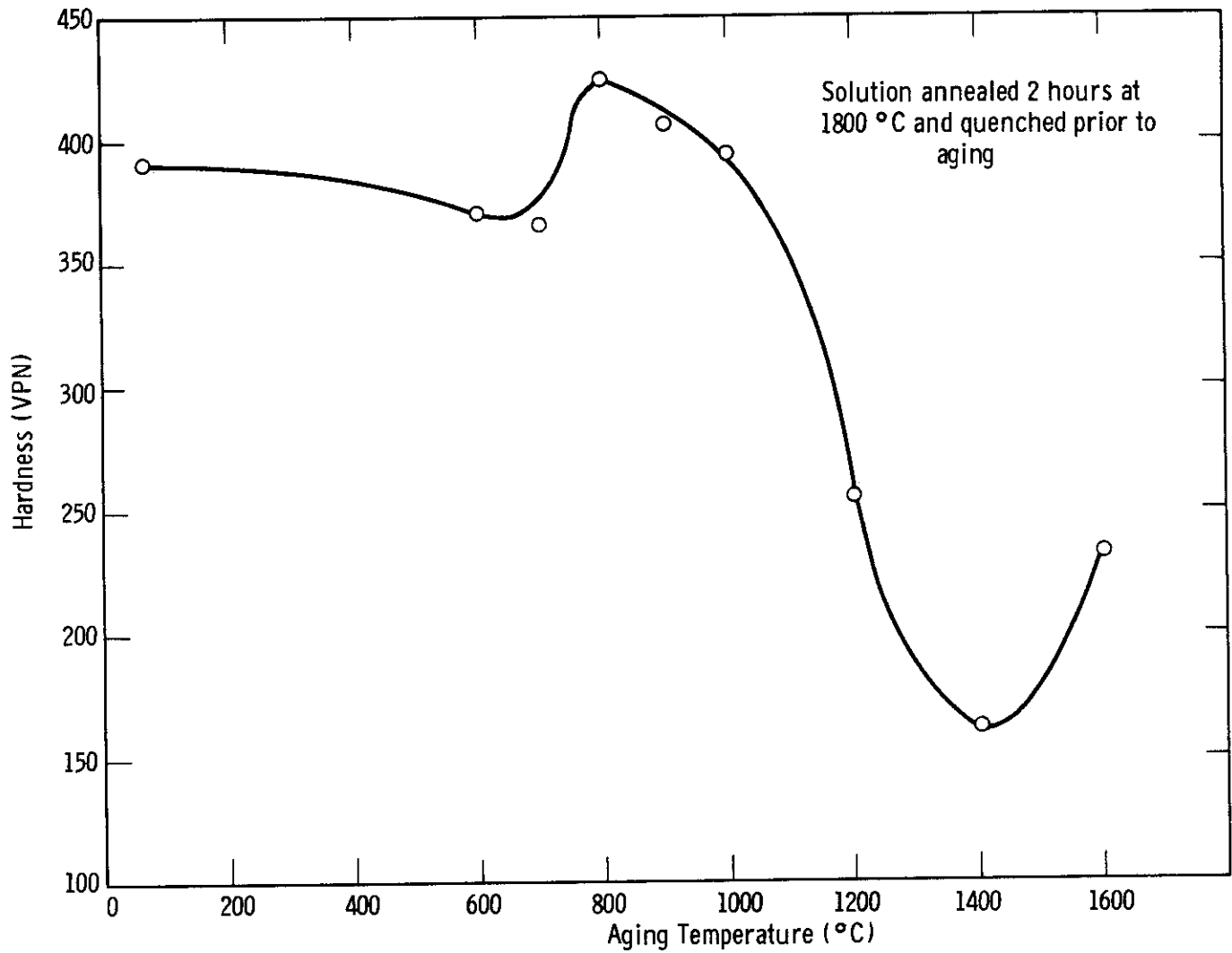
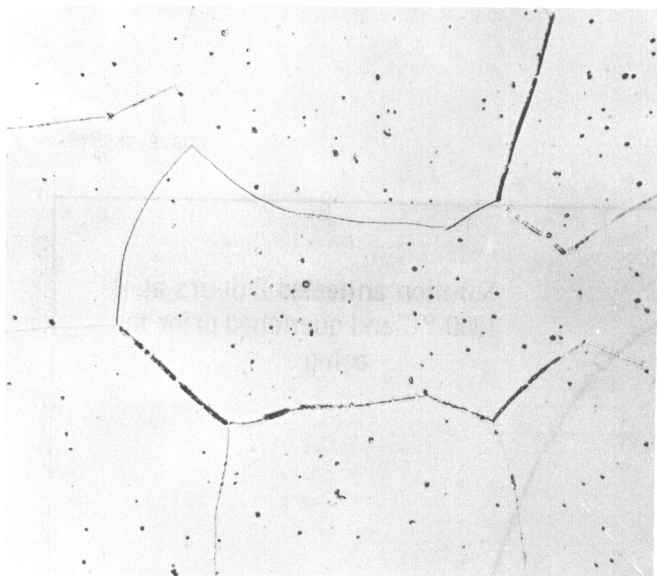
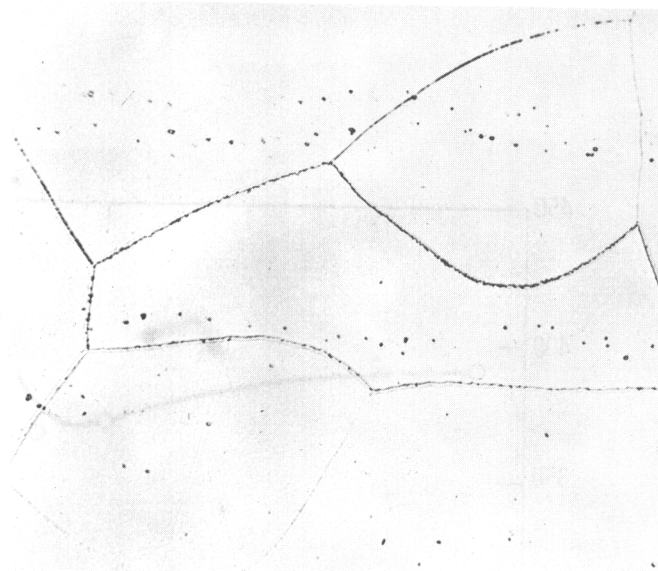


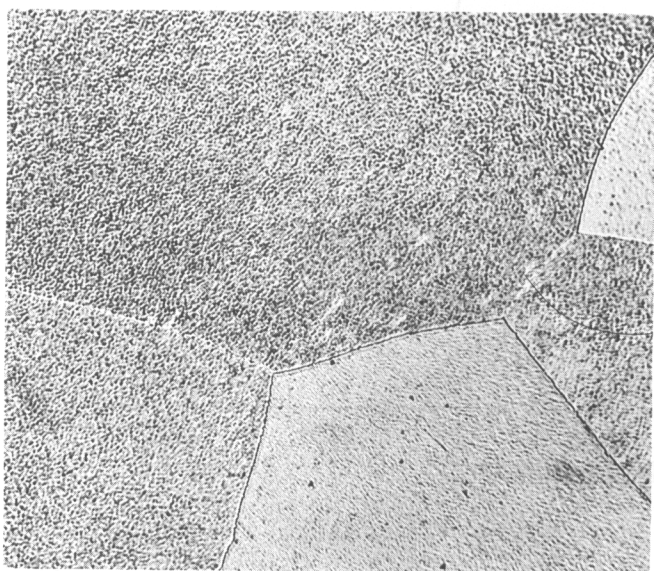
FIGURE 33 - EFFECT OF AGING TEMPERATURE ON THE HARDNESS
OF Cb-5Hf-0.2N ALLOY (AGED 1 HOUR)



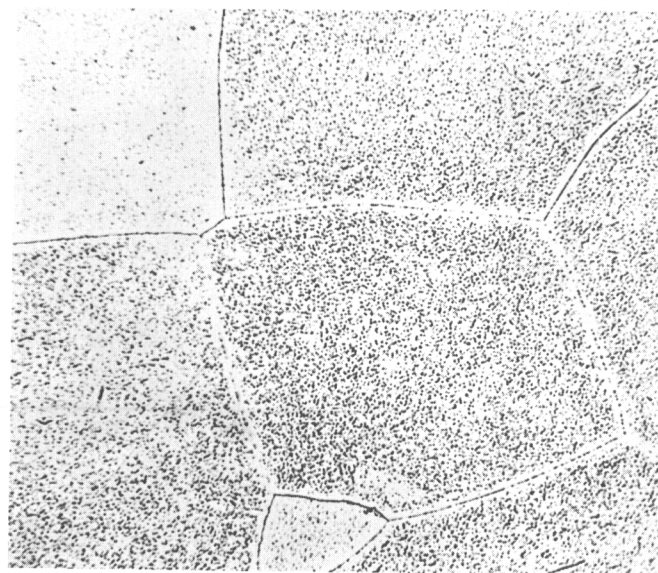
(a)
Aged 1 hour at 600 °C



(b)
Aged 1 hour at 1200 °C



(c)
Aged 1 hour at 1400 °C



(d)
Aged 1 hour at 1600 °C

FIGURE 34 - MICROSTRUCTURE OF Cb-5Hf-0.2N ALLOY (VAM-73)
SOLUTION ANNEALED 2 HOURS AT 1800°C AND
QUENCHED. 500X

matrix darkening when observed metallographically at a magnification of 500 X (Figure 34). Aging at 1600 °C results in a coarsening of the precipitate, which can be fairly easily resolved at a magnification of 500 X. Some re-solutioning apparently also occurs on annealing at 1600 °C, as indicated by the increase in hardness with respect to the 1400 °C aging anneal.

Solution annealed specimens were aged for 48 hours at 700 °C and 900 °C. This aging treatment gave a single phase structure as shown in Figure 35.

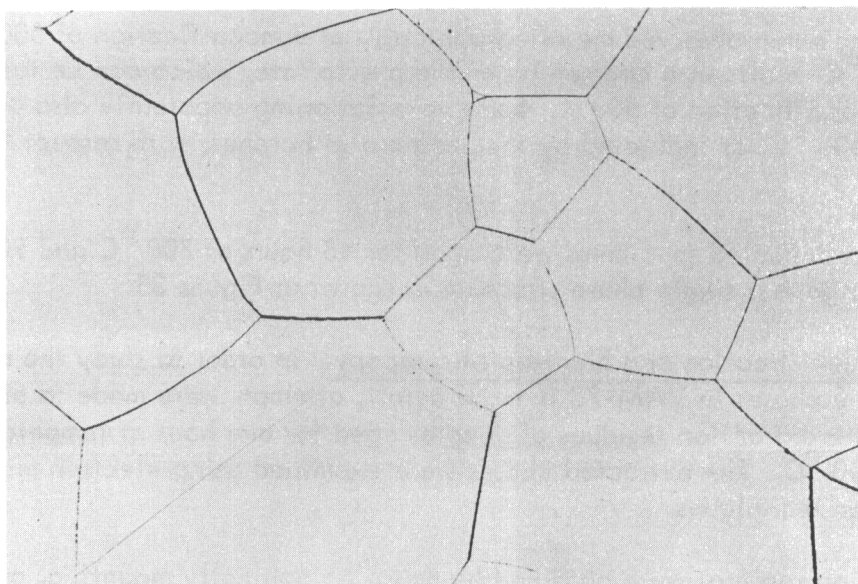
Phase Identification and Electron Microscopy. In order to study the morphology of the precipitating phases in VAM-73 in more detail, attempts were made to analyse extraction replicas and bulk extraction residues of samples aged for one hour at temperatures ranging from 600 to 1600 °C. The extracted phases were examined using electron microscopic and x-ray diffraction techniques.

Extraction replicas were obtained by metallographically mounting, polishing, and etching the specimens, vapor depositing a carbon film (↪ 300 Å thick) and etching in a 10g tartaric acid-10ml bromine-90ml methanol solution at room temperature until the carbon film with the adhering precipitate floated free. These extraction replicas were then examined in the electron microscope to obtain electron micrographs and selected area diffraction patterns.

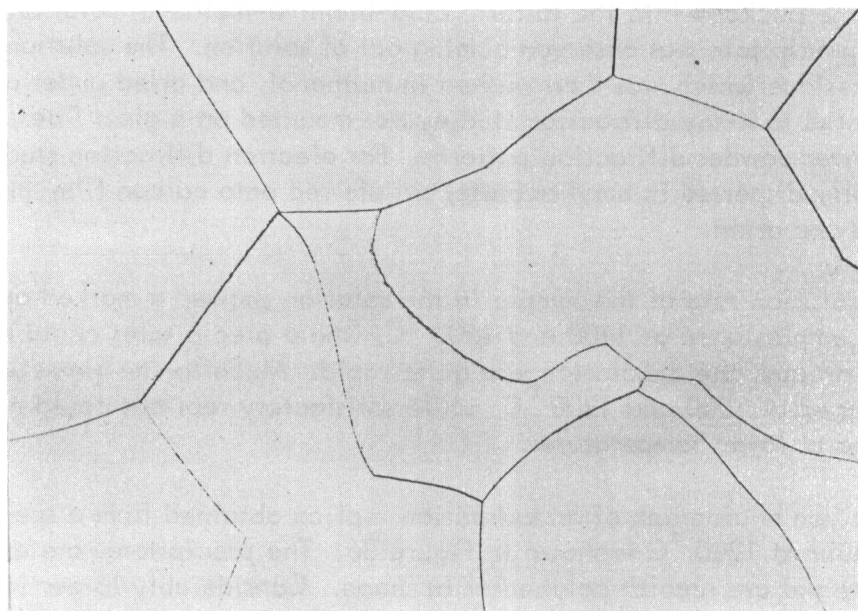
Bulk extraction residues were obtained by wrapping the specimen in platinum wire and immersing the package into the tartaric acid-bromine-methanol solution until a substantial amount of precipitate was observed coming out of solution. The solution was centrifuged to remove the residue which was then washed in methanol, and dried under a partial vacuum. Material subjected to x-ray diffraction studies was mounted on a glass fiber, and identified by Debye-Scherrer powder diffraction patterns. For electron diffraction studies, the material was ultrasonically dispersed in amyl acetate, transferred onto carbon film mounted on specimen grids, and dried.

The dissolution rate of the sample in the solution showed a marked dependence on the structure. For samples aged at 1400 and 1600 °C, where precipitates could be easily resolved by optical microscopy, the dissolution was quite rapid. Much longer times were required for the specimens aged at 1000 and 1200 °C, while satisfactory replicas could not be obtained from alloys aged at lower temperatures.

An electron micrograph of an extraction replica obtained from a specimen annealed and aged one hour at 1200 °C is shown in Figure 36. The precipitates are extremely fine (↪ 0.1 micron) and are regular polyhedral in shape. Considerably larger irregular shaped particles can also be seen in Figure 36a. Increasing the aging temperature to 1400 °C resulted in the formation of larger precipitates (0.3 to 0.6 microns), and a marked increase in the extent of precipitation (Figure 37). Widely scattered larger precipitates, similar to those seen after the 1200 °C aging treatment resulted in the formation of still larger precipitates which tended to be acicular in shape (Figure 38). A band or cluster of precipitates on a grain boundary or sub-boundary is shown in the left side of Figure 38. No orientation relationship of the precipitates with the matrix is evident from these photomicrographs.

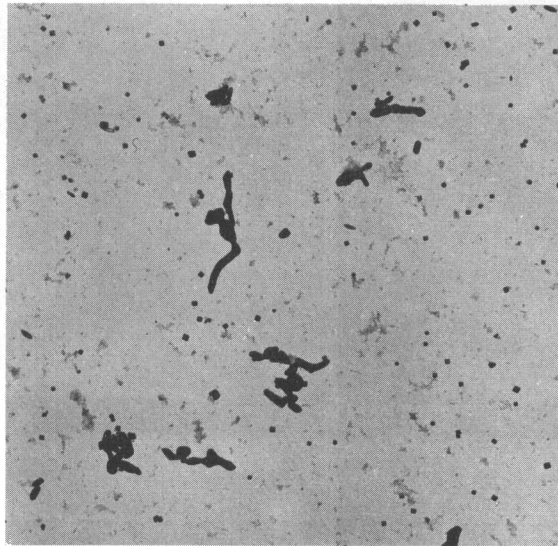


(a) Aged 48 hours at 700° C.

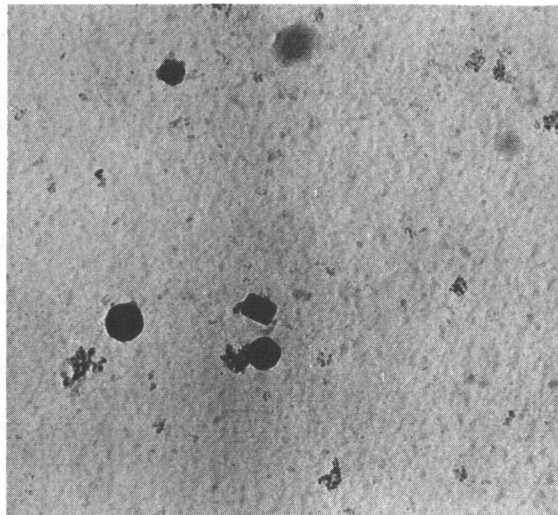


(b) Aged 48 hours at 900° C.

FIGURE 35 - MICROSTRUCTURE OF Cb-5Hf-.2N (VAM 73).
SOLUTION ANNEALED 2 HOURS AT 1800 °C
AND QUENCHED. AGED 48 HOURS. 100X



(a) 8500 X



(b) 30,000 X

FIGURE 36 - EXTRACTION REPLICA OF Cb-5Hf-0.2N ALLOY.
AGED ONE HOUR AT 1200 °C.

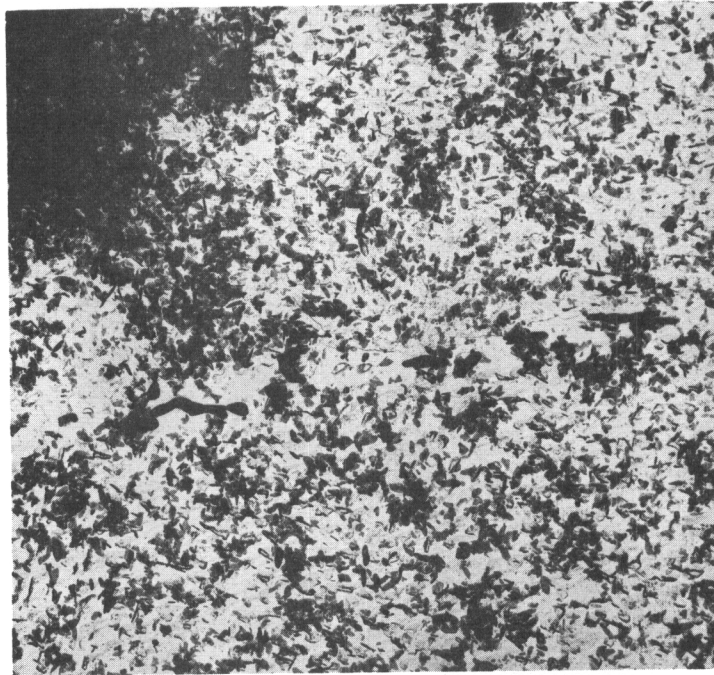


FIGURE 37 - EXTRACTION REPLICA OF Cb-5Hf-0.2N ALLOY.
AGED 1 HOUR AT 1400 °C. 5500X

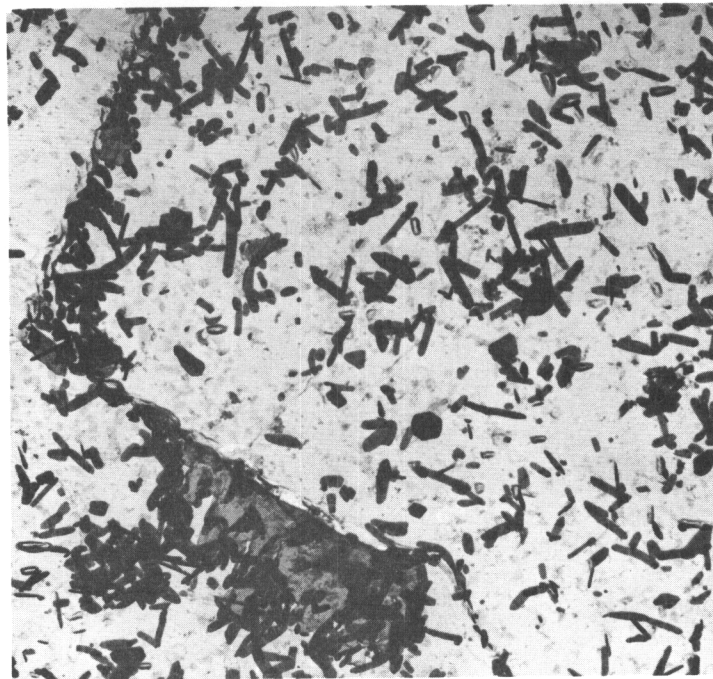


FIGURE 38 - EXTRACTION REPLICA OF Cb-5Hf-0.2N ALLOY.
AGED 1 HOUR AT 1600 °C. 5500X

Electron diffraction patterns obtained from the extracted and bulk residues showed that the HfN phase was the major precipitate. Diffraction data obtained by electron diffraction and x-rays are shown in Table 12 and 13 respectively. The data show excellent agreement with the published data for the HfN phase. A summary of the diffraction data is shown in Table 14. While the data indicate that HfN is the primary precipitating phase, there is also some evidence of a CbC phase. It is interesting to note that the carbide phase was not apparent in the 1400 °C aged specimen held in the dissolution solution for 71 hours.

The morphology of the precipitating phases was determined through the electron micrograph and diffraction patterns. The specimen which was aged at 1200 °C showed fine precipitates of HfN with massive platelike precipitates of CbC (Figure 39). Increasing the aging temperature to 1400 °C did not change the patterns for dissolution times of 23 hours. However, when the specimen was held in the solution for 71 hours no massive precipitates of CbC showing the characteristic streaked spot pattern could be detected (Figures 40 and 41). The additional time in solution also appears to have altered the nitrides from the previous fine shape to a lenticular design. Further increasing the aging temperature to 1600 °C retained the lenticular design but again showed the pattern for CbC (Figure 42).

The results of this portion of the investigation show conclusively that the HfN phase is precipitated in extremely minute particle sizes. Thermodynamic data for the possible nitrides in this alloy system indicate that HfN is the most stable phase. A combination of maximum stability and extremely fine particle size with moderate dispersion is believed to be the mechanism of second phase strengthening operative in this alloy system to produce the high temperature strength values observed.

Hot Hardness Data. Hot hardness tests were conducted on sheet samples of VAM-73, using the testing techniques described previously for the B-77 alloys. Material was tested in two conditions of heat treatment:

- A. Annealed two hours at 1800 °C and quenched.
- B. Annealed two hours at 1800 °C and quenched. Aged one hour at 800 °C.

The hot hardness tests were run in order of increasing temperature, and each specimen was exposed to the complete thermal cycle from 650 to 1315 °C (1200 to 2400 °F). Hot hardness data are plotted as a function of testing temperature in Figure 43. Comparative results for the Cb-5Hf binary alloy are also included. The hot hardness data show the remarkable effect of nitrogen additions in increasing the hot hardness of the alloy. The aged VAM-73 sample shows higher values at temperatures up to 1095 °C (2000 °F). Above this temperature the hardness values were essentially identical. The solution treated alloy shows an increase in hot hardness with increasing temperature up to 982 °C (1800 °F), resulting from precipitation during the testing thermal cycle. Extrapolation of the hot hardness tensile strength correlation shown in Figure 13 indicates that the Cb-5Hf-0.2 N alloy should have a tensile strength in excess of 80,000 psi at 1095 °C (2000 °F).

TABLE 12. TRANSMISSION ELECTRON DIFFRACTION DATA
Cb-5Hf-0.2 N ALLOY (VAM-73)*

Specimen d meas.	HfN (ASTM 11-479)	
	d	hkl
2.585	2.59	111
2.235	2.24	200
1.58	1.59	220
1.345	1.357	311
1.29	1.299	222
1.122	1.128	400
1.03	1.035	331
1.00	1.008	420

*Solution annealed two hours at 1800 °C. Aged one hour at 1400 °C.

TABLE 13. X-RAY DIFFRACTION DATA
Cb-5Hf-0.2 N ALLOY (VAM-73)*

Specimen d meas.	I	HfN (ASTM 11-479)	
		d	hkl
2.622	S	2.59	111
2.264	S	2.24	200
1.605	S	1.59	220
1.365	S	1.357	311
1.312	W	1.299	222
1.135	W	1.128	400
1.041	M	1.035	331
1.012	M	1.008	420
0.926	M		
0.872	M		
0.810	W		

*Solution annealed two hours at 1800 °C. Aged one hour at 1400 °C.

TABLE 14. DIFFRACTION RESULTS ON BULK EXTRACTED RESIDUES OF AGED Cb-5Hf-0.2N ALLOY (VAM-73)*

Aged for 1 hr. at Temp. °C	Dissolution Time in Solvent** at R.T., hrs	Extracted Phases Identified by	
		X-Ray	Electron
1200	71	--	HfN + CbC
1400	23	HfN	HfN + CbC
1400	71	HfN	HfN
1600	28	HfN	HfN + CbC

*Solution annealed two hours at 1800 °C

**10g Tartaric Acid -
10ml Br₂ - 90ml CH₃OH

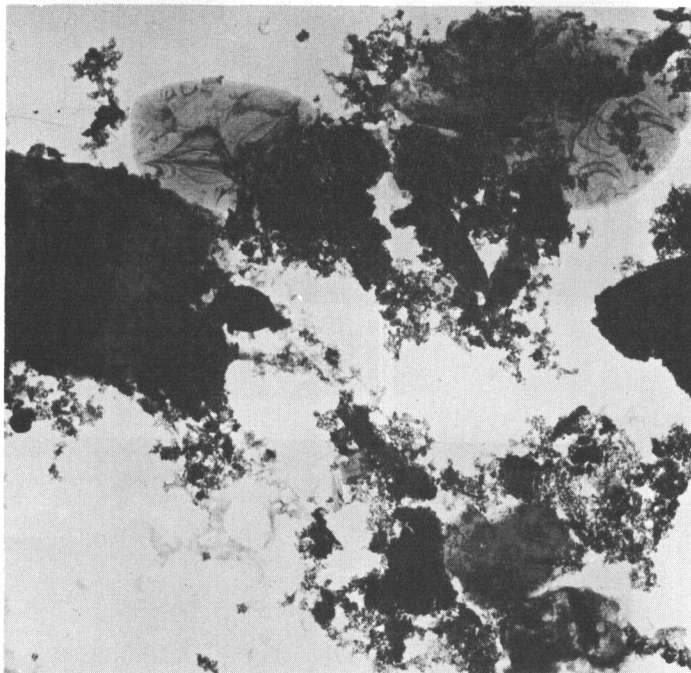


FIGURE 39 - ELECTRON MICROGRAPH OF BULK EXTRACTED
RESIDUE FROM Cb-5Hf-0.2 N ALLOYS. AGED
1 HOUR AT 1200 °C. 8000X

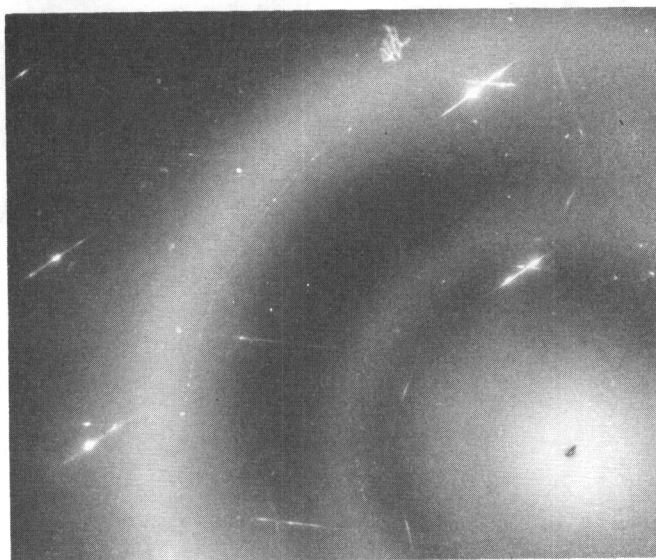
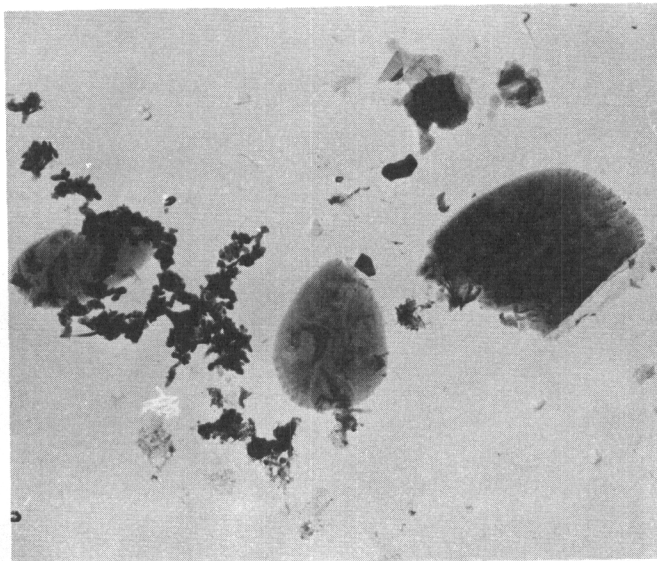


FIGURE 40 - ELECTRON MICROGRAPH AND DIFFRACTION PATTERN OF BULK EXTRACTED RESIDUE FROM Cb-5Hf-0.2 N ALLOYS IN SOLUTION FOR 23 HOURS. AGED 1 HOUR AT 1400 °C. 8000X

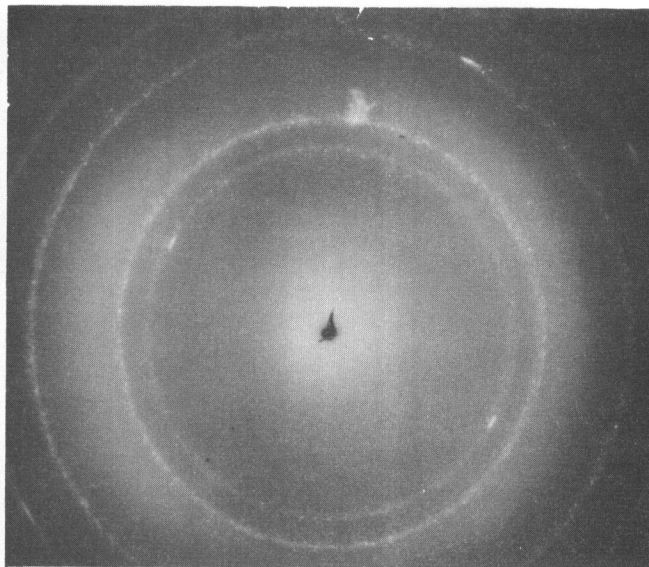
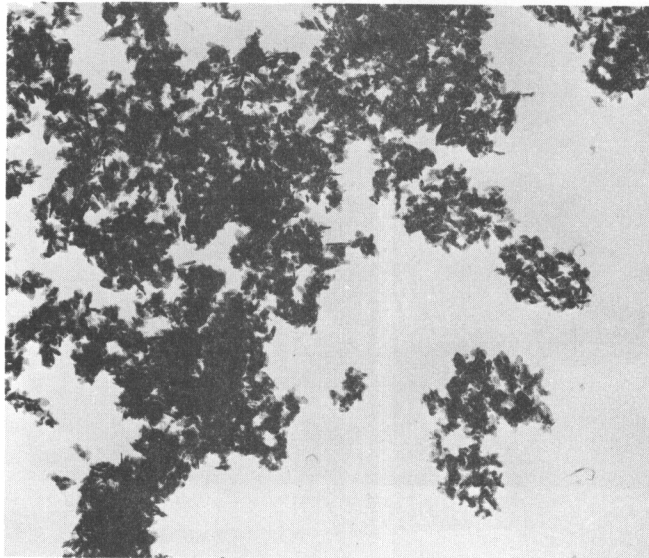


FIGURE 41 - ELECTRON MICROGRAPH AND DIFFRACTION PATTERN OF BULK EXTRACTED RESIDUE FROM Cb-5Hf-0.2 N ALLOYS IN SOLUTION FOR 71 HOURS. AGED 1 HOUR AT 1400 °C. 8000X

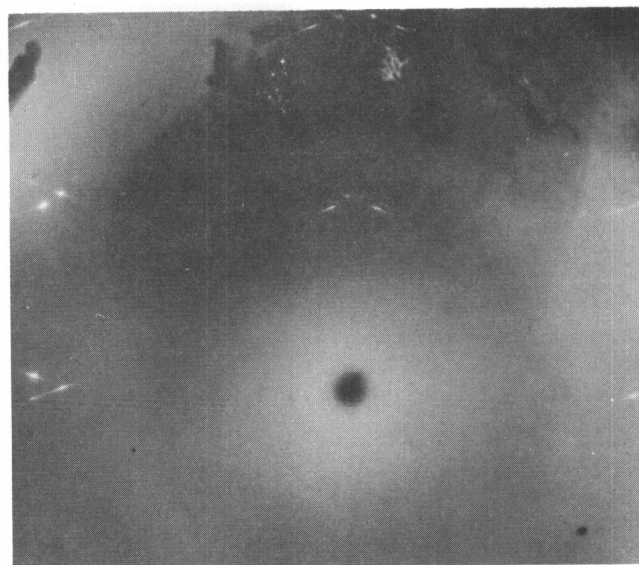
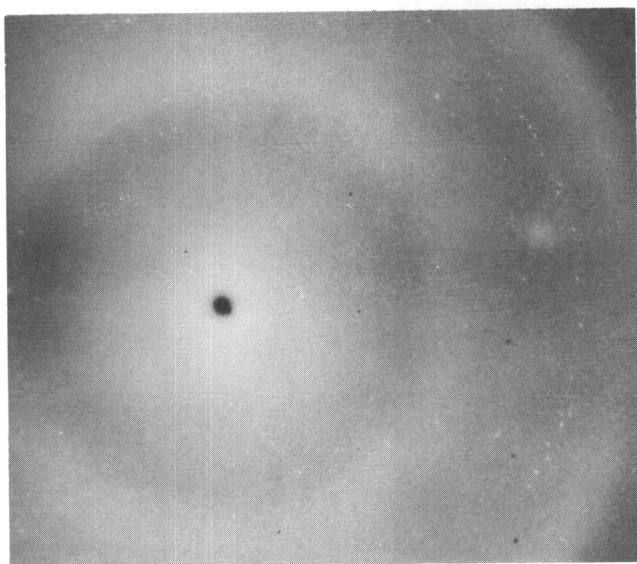
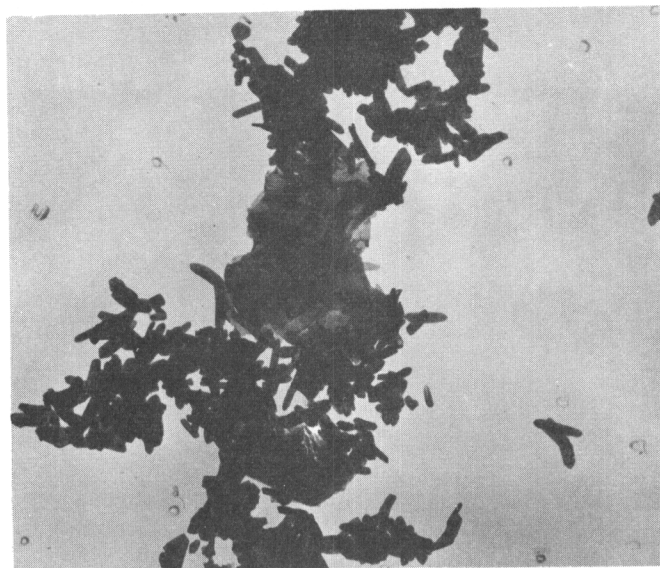
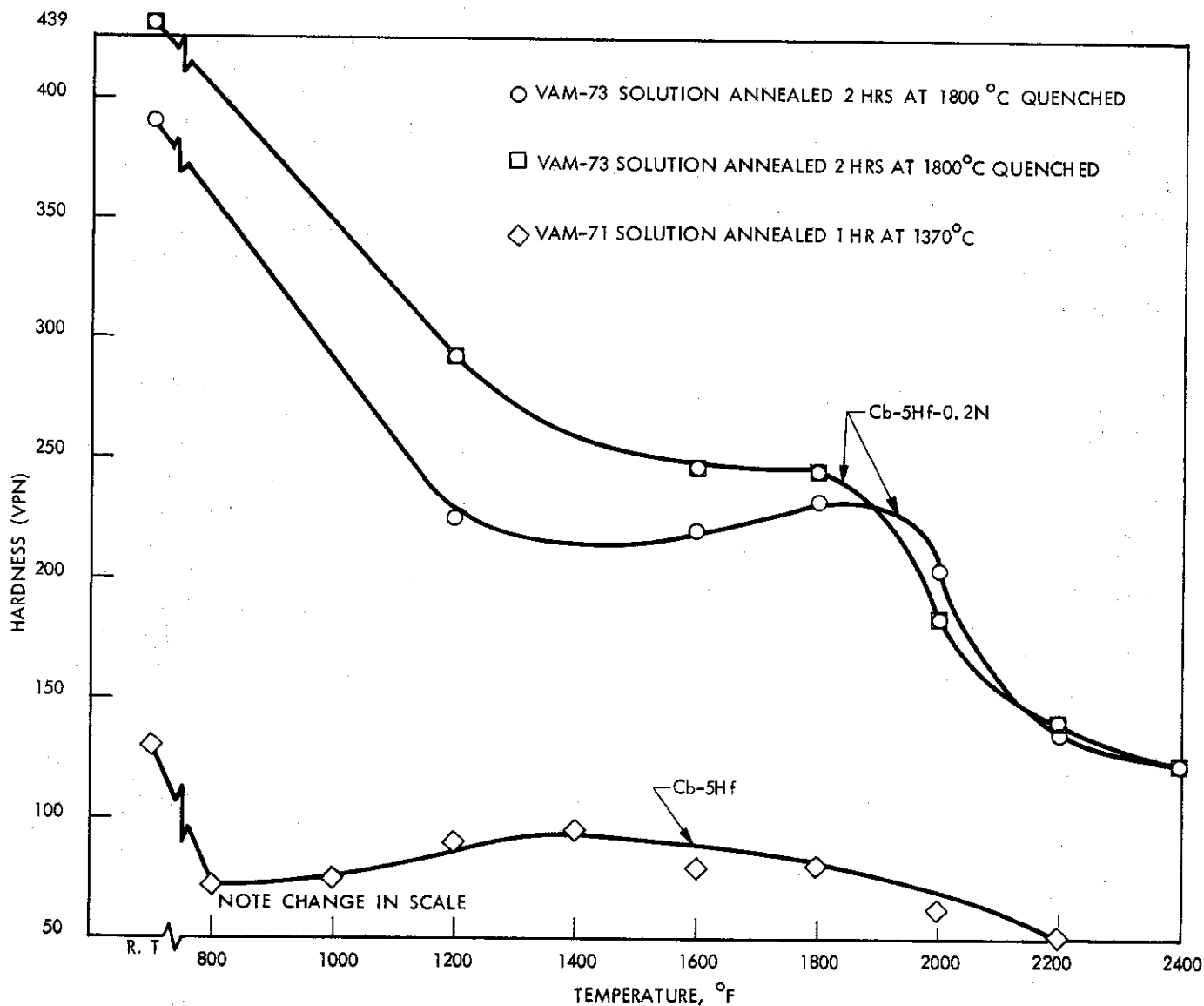


FIGURE 42 - ELECTRON MICROGRAPH AND DIFFRACTION PATTERN
OF BULK EXTRACTED RESIDUE FROM Cb-5Hf-0.2 N
ALLOYS. AGED 1 HOUR AT 1600 °C. 8000X



560852

FIGURE 43 - EFFECT OF TEMPERATURE ON THE HOT HARDNESS OF Cb-5Hf AND Cb-5Hf-0.2N ALLOYS

Discussion. The response to heat treatment of the Cb-5Hf-0.2 N alloy appears to follow classical precipitation hardening behavior, and can be rationalized as discussed below. The high as-quenched hardness would seem to be primarily due to a high supersaturation with respect to nitrogen, although, considering the rapid over aging in this system, it is possible that some precipitation occurs during the quenching treatment. Attempts to obtain extraction replicas from the as-quenched samples to determine if HfN precipitates are present in the microstructure have not as yet been successful. On aging the Cb-Hf-N alloy, precipitation of a coherent nitride phase (HfN) occurs, giving rise to a significant hardness increase. At temperatures above 800 - 900 °C, loss of coherency and coalescence of the precipitate occurs, resulting in pronounced softening. Further increase in aging temperature above 1400 °C resulted in both growth of the precipitates and resolution of nitrogen in the matrix.

The Cb-Hf-N system is particularly interesting from the standpoint of studying dispersed phase strengthening phenomena in columbium alloys, since the changes occurring as a result of heat treatment are very pronounced. The nitride hardened alloys also have intriguing engineering potential, since in the overaged condition they are soft and fabricable yet they can be strengthened by heat treatment to very high strength levels. As noted previously, the hot hardness data for both aged and unaged VAM-73 indicate that strength levels in excess of 80,000 psi at 1095 °C (2000 °F) are possible. The hardness data do not, however, provide any information concerning ductility. Attempts are currently being made to heat treat tensile samples, so that both high and low temperature tensile properties may be determined. It is interesting to note that the as-quenched VAM-73 showed no sign of cracking on quenching, and the as-quenched material could be attached to the hot hardness mounts without failure.

The obvious difficulty with this alloy system is the fairly rapid overaging at relatively low temperatures. Despite the early onset of overaging, hot hardness tests indicated that the Cb-5Hf-0.2 N alloy had excellent short time strength at temperatures up to 1315 °C (2400 °F). It is quite possible that the kinetics of the aging reaction can be altered substantially by further alloying.

Cb-W-Hf-N Alloys

In view of the rapid overaging at low temperatures encountered with Cb-Hf-N alloys, attempts were made to modify the aging kinetics by the addition of 10 w/o tungsten. The tungsten additions were also intended to provide additional solid solution strengthening.

Alloy Preparation. Two Cb-W-Hf-N alloys, weighing 250 grams, were prepared by non-consumable arc melting. High purity electron beam melted columbium, crystal bar hafnium, and tungsten sheet trimmings were used as the base materials. Nitrogen was added as a Cb-N master alloy. Available chemical analysis data are listed in Table 15. The as-melted buttons were coated by hot dipping in an Al-12 Si bath to provide protection from contamination during processing. The coated buttons were forged at 1205 °C (2200 °F) to approximately 50% reduction in thickness. Considerable edge cracking occurred during the forging operation. The forgings were trimmed and surface conditioned, canned in

stainless steel, and rolled at 1200 °C. Alloy NC-385-1 was rolled an additional 70% to provide sheet stock 0.047 inches thick. During rolling NC-385-2, the stainless steel can fractured and rolling was terminated at this point. This alloy received only 55% reduction resulting in a final sheet thickness of 0.081 inch.

TABLE 15. CHEMICAL ANALYSIS OF Cb-W-Hf-N ALLOYS

Heat No.	Nominal Composition (w/o)	Analysis (w/o)		
		O	N	C
NC-385-1*	Cb-10W-5Hf-0.1 N	0.015	0.15	--
NC-385-2*	Cb-10W-5Hf-0.05 N	0.018	0.07	--

*Samples were not analyzed for metallic elements since prior work had shown good recovery during non-consumable arc melting.

Effects of Heat Treatment. Portions of the tungsten containing alloys were solution annealed two hours at 1800 °C and quenched. Aging treatments of one hour were subsequently carried out in the temperature range 900 to 1400 °C, and the data are shown in Figure 49. As in the case of the Cb-5Hf-0.2 N alloy, a pronounced hardness peak occurred after aging at approximately 900 °C. The as-quenched hardness values for the Cb-W-Hf-N alloys were lower than those of the Cb-Hf-N alloy, reflecting the lower nitrogen supersaturation of the former. However, a comparison of the data of Figures 33 and 49 show that the tungsten containing samples had a higher hardness in the overaged condition as a result of solid solution strengthening by the tungsten.

The microstructures of the Cb-10W-5Hf-0.15 N and Cb-10W-5Hf-0.07 N alloys shown in Figure 44 and 45 indicate a small amount of precipitate present in the as-quenched specimens. Aging the solution annealed alloys one hour at 1100 °C did not result in any increase in the extent of precipitation (Figure 46). However, increasing the aging temperature to 1400 °C caused much more general precipitation within the matrix, and the formation of larger precipitates, as shown in Figure 47 and 48. The microstructures were very similar to those of the Cb-W-Hf-N alloy, but it appears that the predominant strengthening mechanism in this system is the precipitation of HfN on aging.

Hot Hardness Data. Hot hardness data were obtained for the Cb-W-Hf-N alloys in the following conditions of heat treatment:

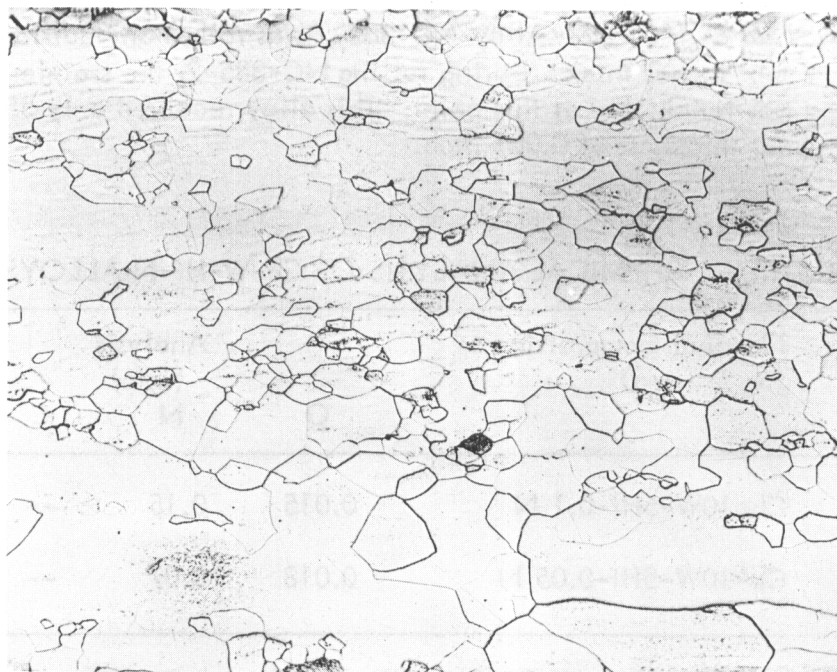


FIGURE 44 - MICROSTRUCTURE OF Cb-10W-5Hf-.15N (NC 385-1).
SOLUTION ANNEALED 2 HOURS AT 1800 °C AND
QUENCHED. 100X

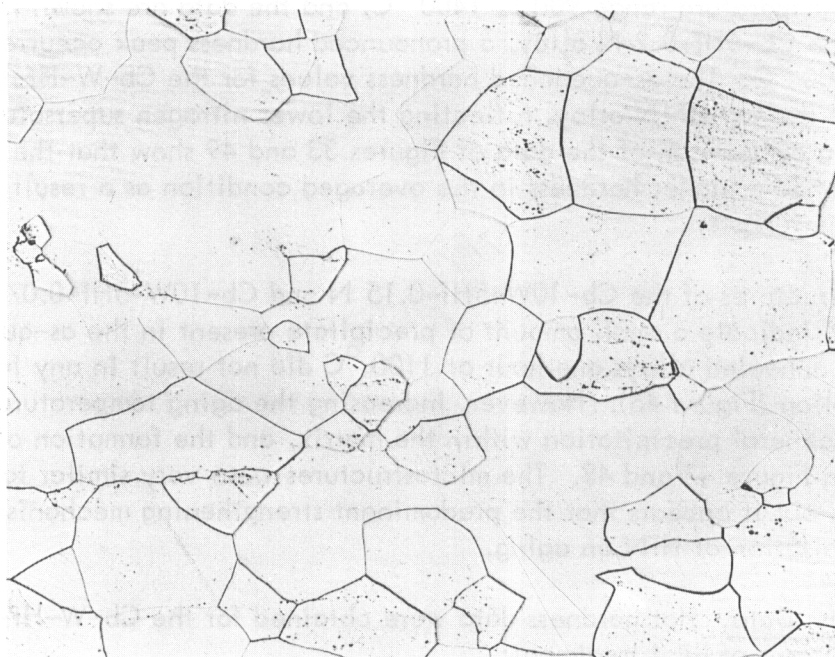
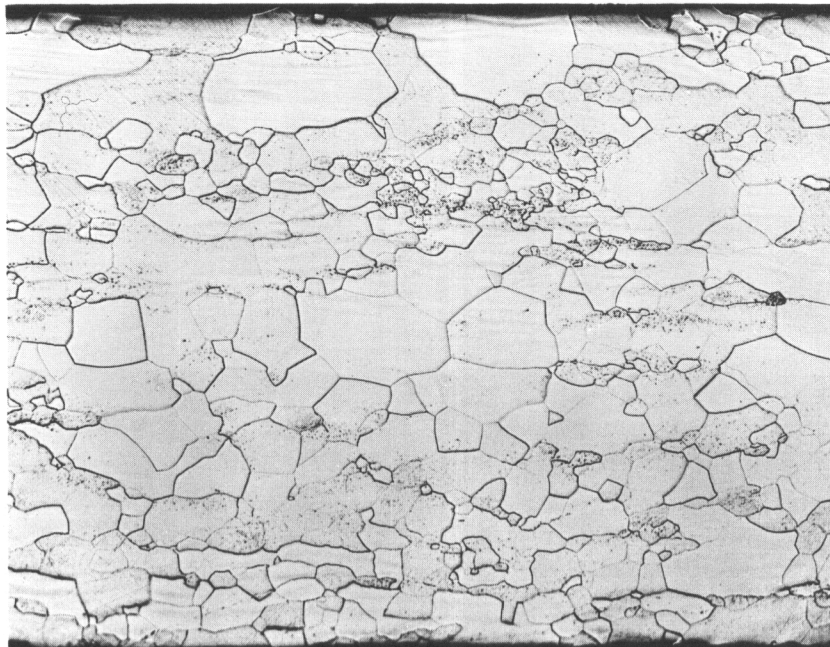
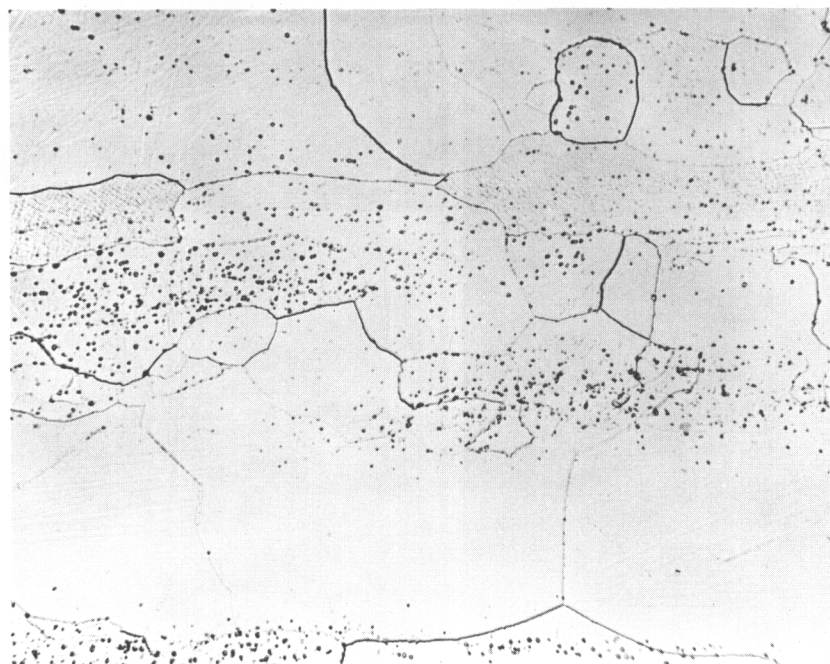


FIGURE 45 - MICROSTRUCTURE OF Cb-10W-5Hf-.07N (NC 385-2).
SOLUTION ANNEALED 2 HOURS AT 1800 °C AND
QUENCHED. 100X



(a) 100X



(b) 500X

FIGURE 46 - MICROSTRUCTURE OF Cb-10W-5Hf-.15N (NC 385-1).
SOLUTION ANNEALED 2 HOURS AT 1800 °C AND
QUENCHED. AGED 1 HOUR AT 1100 °C.

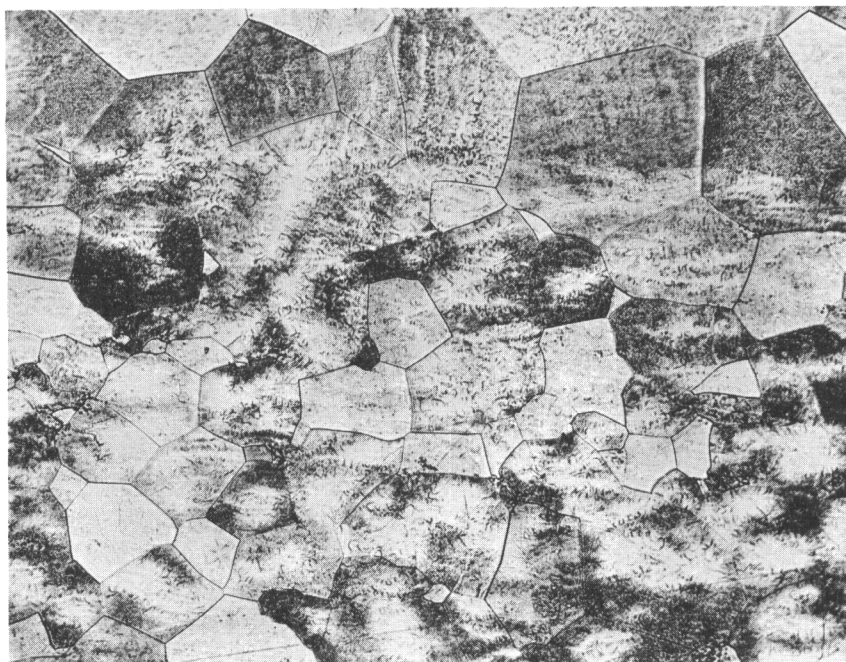
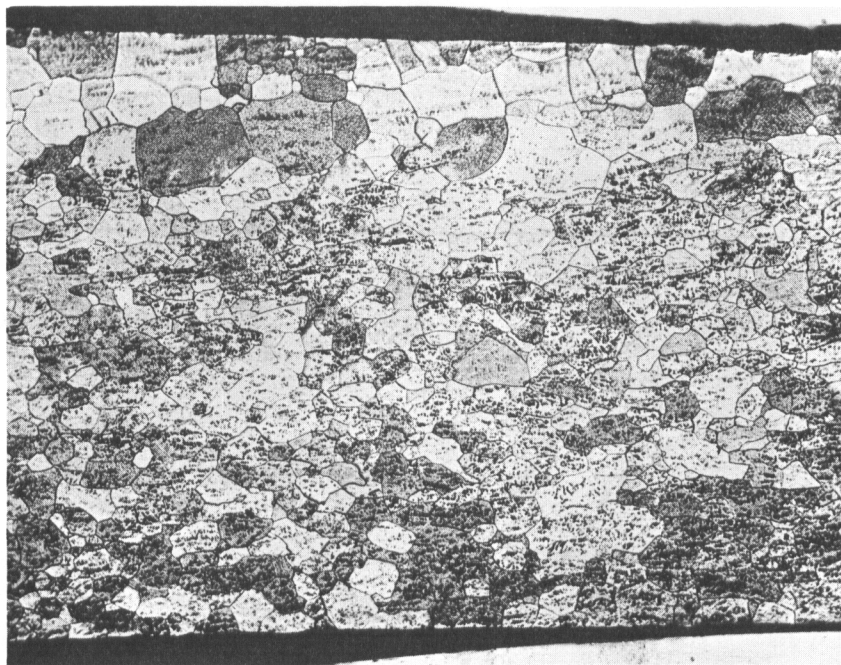


FIGURE 47 - MICROSTRUCTURE OF Cb-10W-5Hf-.07N (NC 385-2).
SOLUTION ANNEALED 2 HOURS AT 1800 °C AND
QUENCHED. AGED 1 HOUR AT 1400 °C. 100X



(a) 100X



(b) 500X

FIGURE 48 - MICROSTRUCTURE OF Cb-10W-5Hf-.15N (NC 385-1).
SOLUTION ANNEALED 2 HOURS AT 1800 °C AND
QUENCHED. AGED 1 HOUR AT 1400 °C.

CURVE 565833

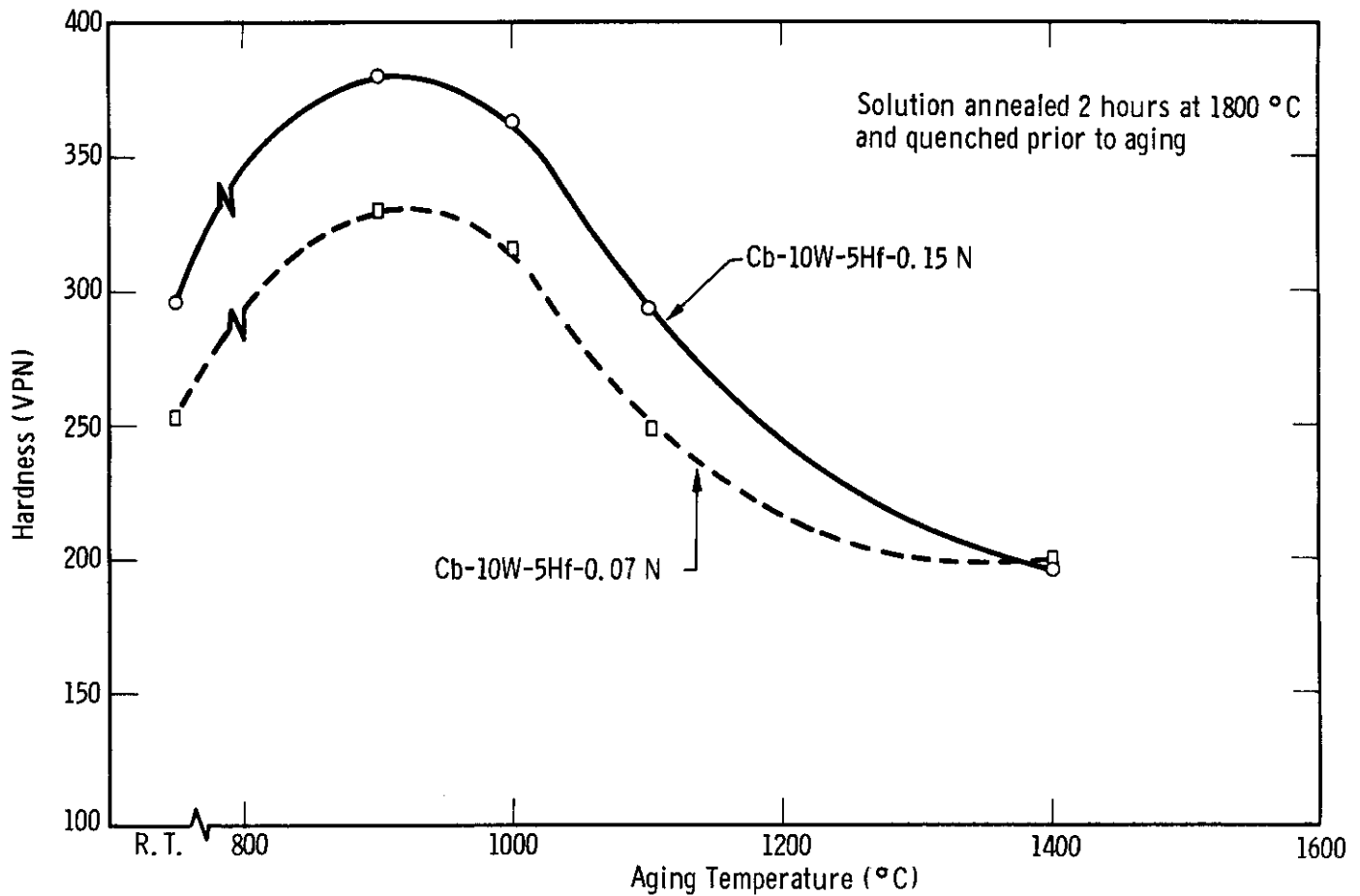


FIGURE 49 - EFFECT OF AGING TEMPERATURE ON THE HARDNESS OF Cb-W-Hf-N ALLOYS. (AGED 1 HOUR)

- A. Annealed two hours at 1800 °C and quenched.
- B. Annealed two hours at 1800 °C and quenched. Aged one hour at 900 °C.
- C. Annealed two hours at 1800 °C and radiation cooled. Aged one hour at 900 °C.

Material was radiation cooled by dropping it from the hot zone of the furnace into the bottom of the furnace chamber. Hot hardness data for alloys in the quenched, radiation cooled plus aged, and quenched plus aged conditions are shown as a function of temperature in Figures 50, 51, and 52 respectively. Reference data for B-66, one of the strongest fabricable Cb alloys, are also shown on the curves. The Cb-10W-5Hf-0.15 N alloy had the highest hot hardness values over the entire temperature range from 870 to 1315 °C (1600 to 2400 °F), in all conditions of heat treatment. The hot hardness of the as-quenched material increased significantly as the test temperature was raised from 870 to 980 °C (1600 to 1800 °F), as a result of aging during the testing thermal cycle. The effects of prior heat treatment on hot hardness are summarized in the bar graphs of Figures 53 and 54. The aged samples show superior hot hardness values up to 1095 °C (2000 °F). However, at 1205 °C (2200 °F) the hot hardness values for the quenched and quenched plus aged conditions are identical. The hardness data for the alloy containing 0.15 w/o N are markedly superior to those of B-66, particularly at the higher temperatures. The 1205 °C (2200 °F) values for NC-385-1 (Cb-10W-5Hf-0.15N) correspond to a yield strength of approximately 50,000 psi. The data for these alloys are quite encouraging and warrant more detailed studies of mechanical properties.

CURVE 565839

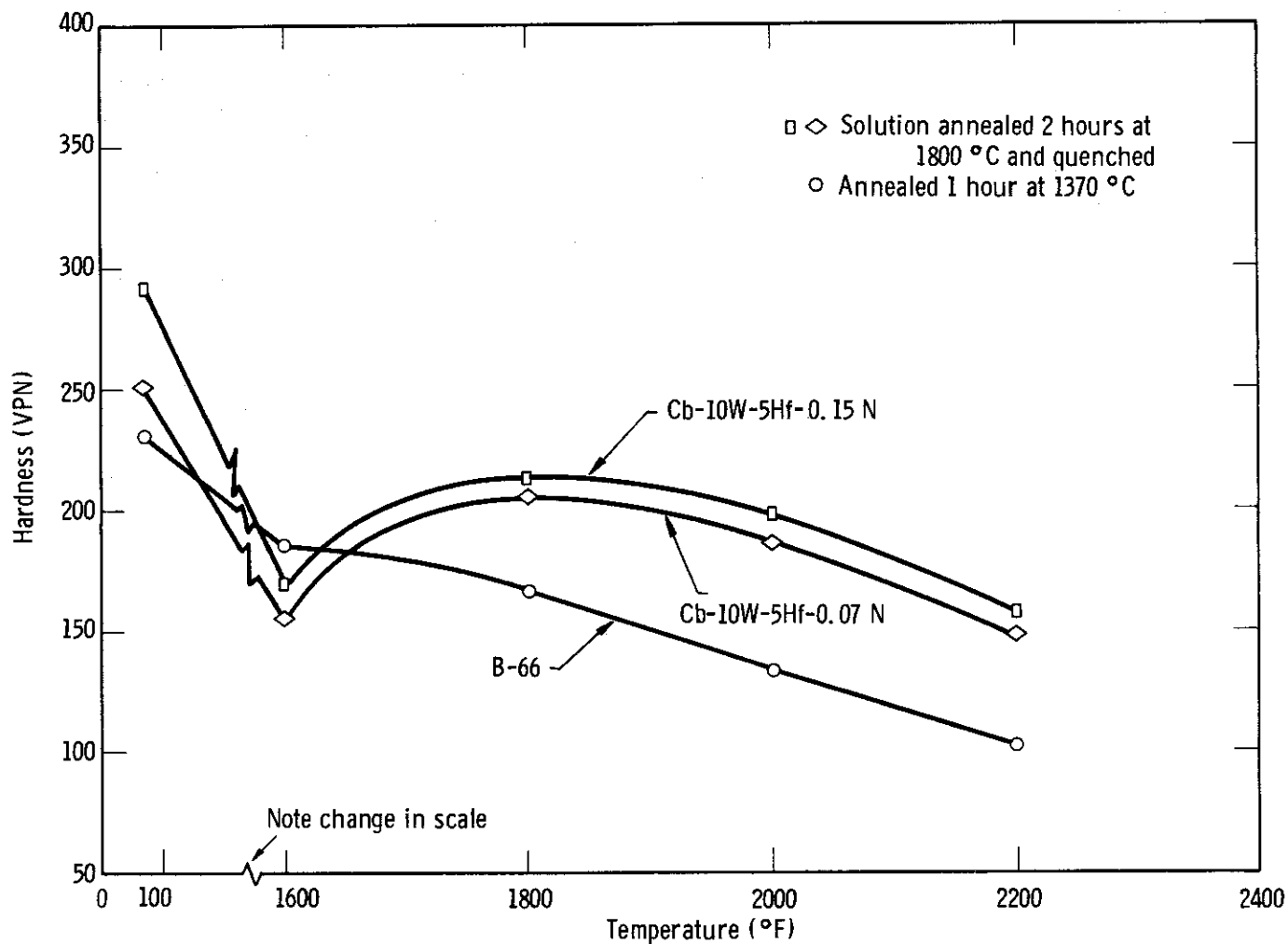


FIGURE 50 - EFFECT OF TEMPERATURE ON THE HOT HARDNESS OF Cb-W-Hf-N ALLOYS

CURVE 565836

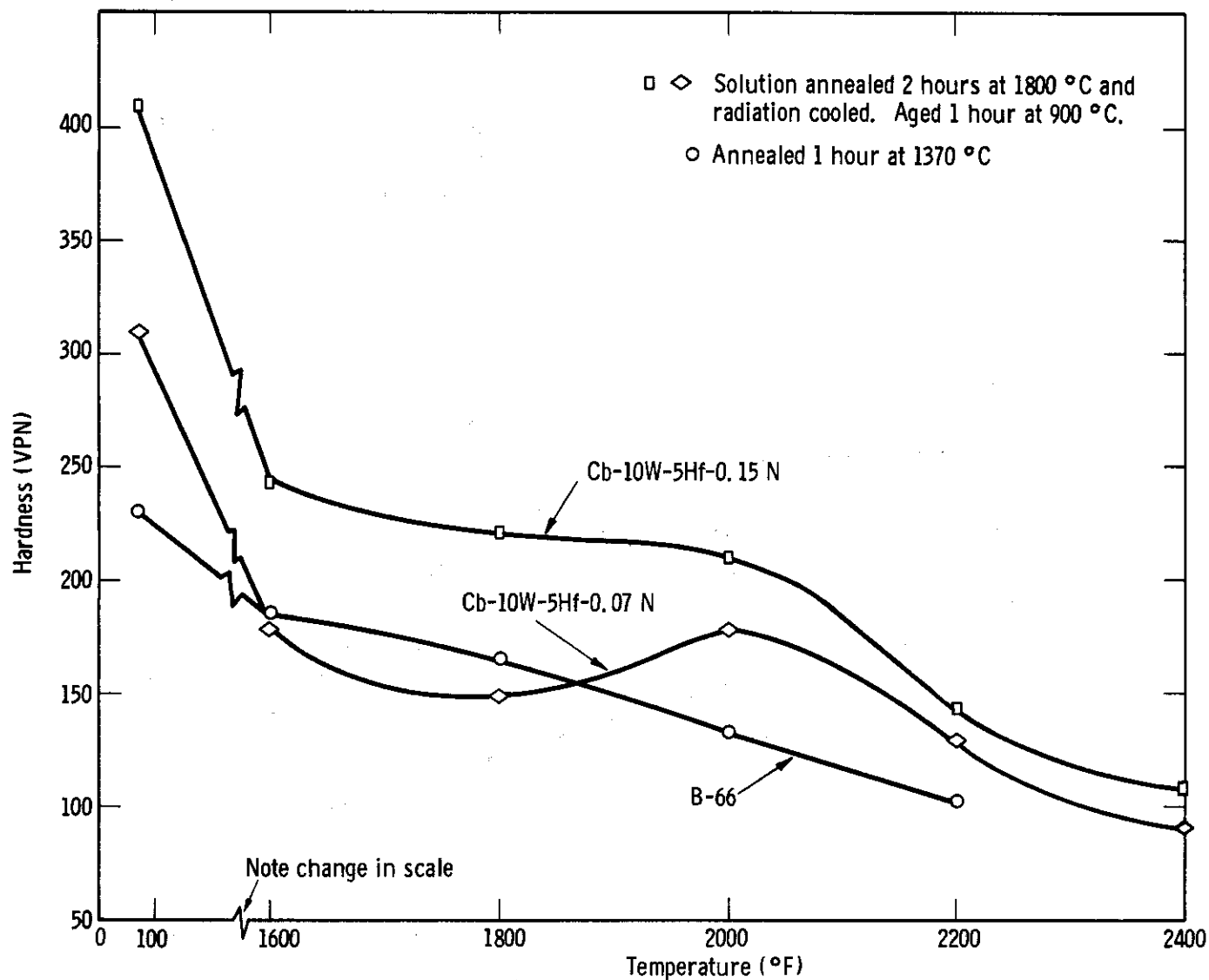


FIGURE 51 - EFFECT OF TEMPERATURE ON THE HOT HARDNESS OF Cb-W-Hf-N ALLOYS

CURVE 565837

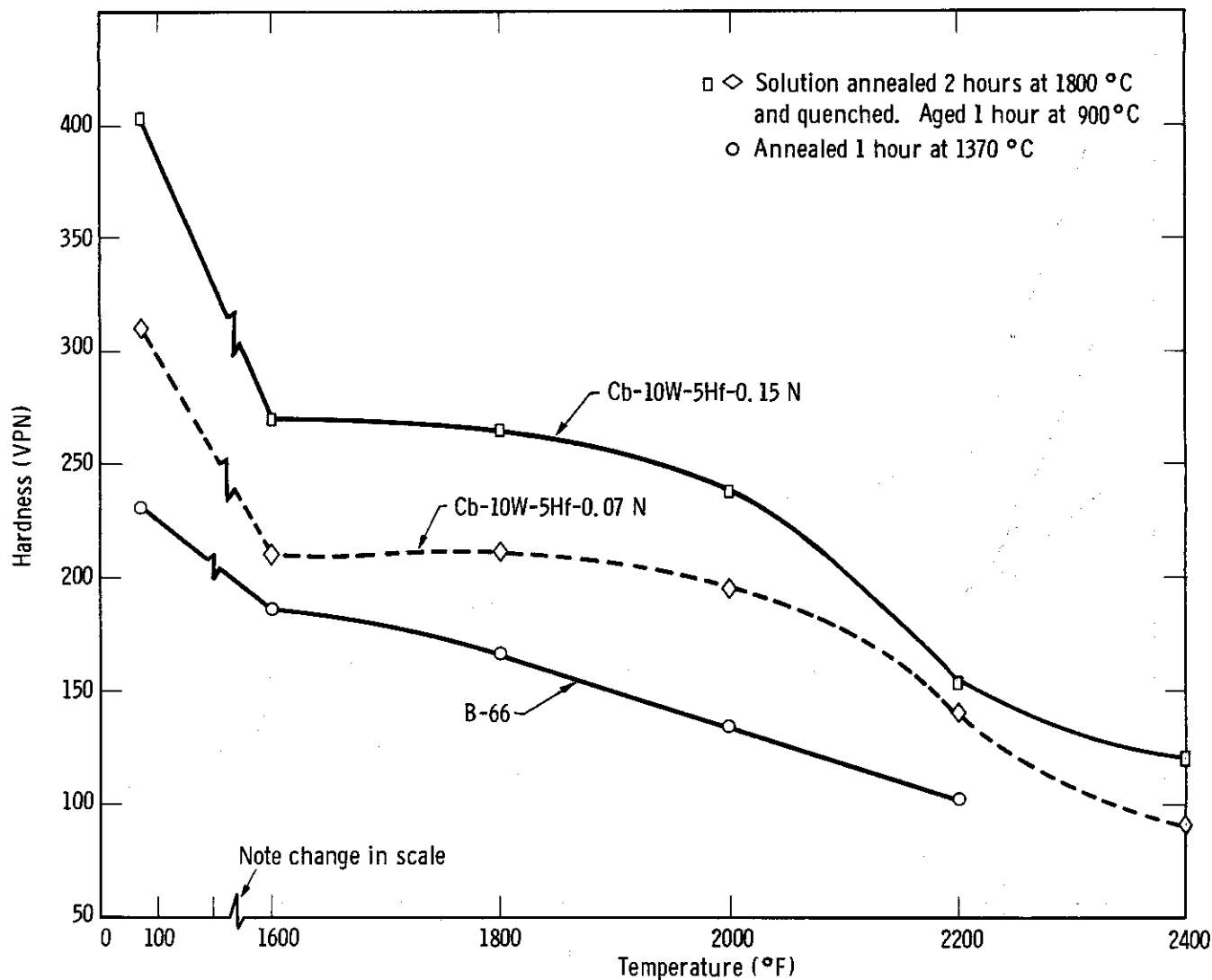


FIGURE 52 - EFFECT OF TEMPERATURE ON THE HOT HARDNESS OF Cb-W-Hf-N ALLOYS

CURVE 565834

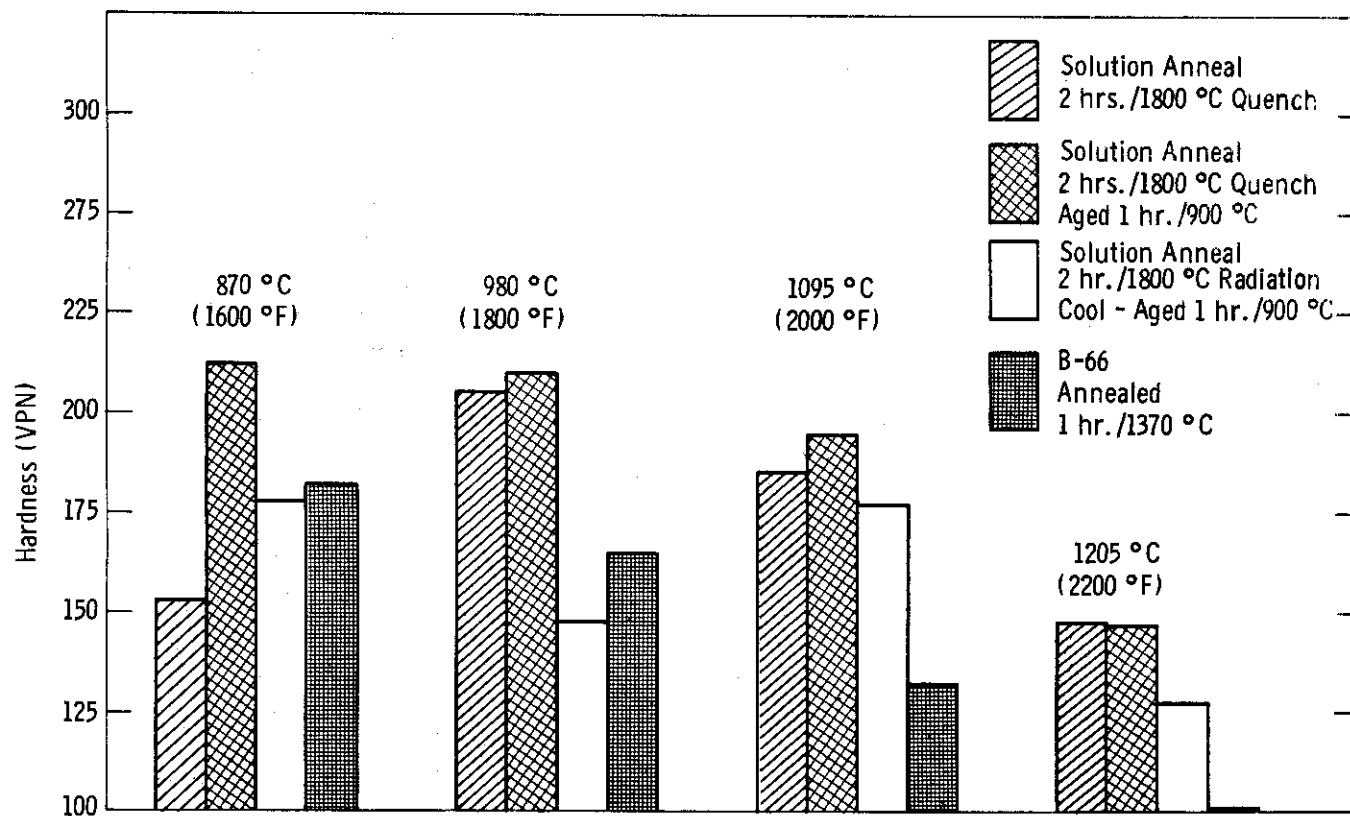


FIGURE 53 - EFFECT OF HEAT TREATMENT ON THE HOT HARDNESS OF A Cb-10W-5Hf-0.07N ALLOY

CURVE 565835

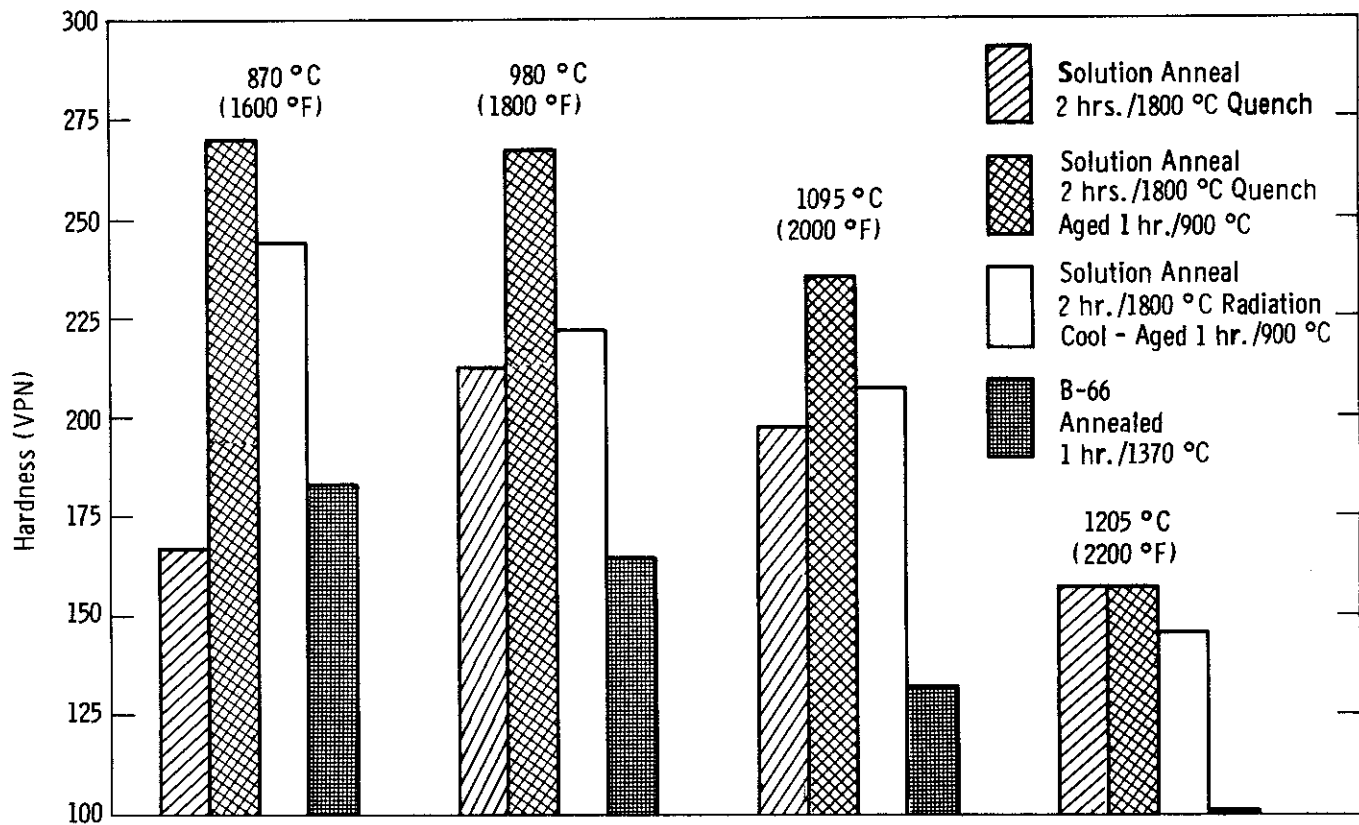


FIGURE 54 - EFFECT OF HEAT TREATMENT ON THE HOT HARDNESS OF A Cb-10W-5Hf-0.15N ALLOY

REFERENCES

1. R. T. Begley, et al, Development of Niobium-Base Alloys, WADC-TR-57-344.
2. R. T. Begley, et al, Development of Niobium-Base Alloys, WADC-TR-57-344, Part II, December, 1958.
3. R. T. Begley and W. N. Platte, Development of Niobium-Base Alloys, WADC-TR-57-344, Part IV. April, 1960
4. R. T. Begley, W. N. Platte, R. L. Ammon, and A. I. Lewis, Development of Niobium-Base Alloys, WADC-TR-57-344, Part V. January, 1961.
5. R. T. Begley, R. L. Ammon, and R. Stickler. Development of Niobium-Base Alloys, WADC-TR-57-344, Part VI. August, 1962.
6. M. J. Manjoine, E. T. Wessel, and W. H. Pryle, "Constant Strain Rate Testing Machine with Instantaneous Speed Change". ASTM Bulletin No. 226, December, 1957, p. 31.
7. E. T. Wessel and R. D. Olleman, "Apparatus for Tensile Testing at Sub-Atmospheric Temperatures". ASTM Bulletin No. 187, January, 1953, p. 56.
8. D. D. Lawthers and M. J. Manjoine, "The Effect of Testing Atmospheres on the Creep-Rupture Properties of Molybdenum-Base Alloy" in High Temperature Materials, John Wiley and Sons, New York, 1959, pp. 486-497.
9. W. H. Chang, A Study of the Influence of Heat Treatment on Microstructure and Properties of Refractory Alloys. ASD-TDR-62-211, February, 1962.
10. F. F. Schmidt, et al, Investigation of Tantalum and Its Alloys, ASD-TDR-62-594, October, 1962.
11. R. L. Ammon and R. T. Begley, Third Quarterly Report on Contract NOw-62-0656-d, Westinghouse Astronuclear Laboratory Report WANL-PR-M-003, February 16, 1963.
12. F. B. Cuff, Research to Determine the Composition of Dispersed Phases in Refractory Metal Alloys, ASD-TDR-62-7.

13. E. T. Wessel, L. L. France, and R. T. Begley. "Flow and Fracture Characteristics of Electron-Beam Melted Columbium", in Columbium Metallurgy, AIME Metallurgical Society Conferences, Vol. 10, Interscience, N. Y., 1961, p. 459.
14. L. L. France, R. T. Begley, and H. G. Kohute. "Apparatus for Hardness Testing at Low Temperatures", Materials Research and Standards, Vol. 1, No. 3, March, 1961, p. 192.
15. M. A. Adams, H. C. Roberts, and R. E. Smallman. Acta Metallurgica, Vol. 8, 1960, p. 328.
16. R. T. Begley and R. W. Buckman, Unpublished data.
17. D. McLean. J. Inst. of Metals, Vol. 81, 1952-53, p. 293.
18. F. N. Rhines and P. J. Wray. "Investigation of the Intermediate Temperature Ductility Minimum in Metals". ASM Transactions Quarterly, Vol. 54, No. 2, June, 1961.
19. H. C. Chang and N. J. Grant. Transactions AIME, Vol. 194, 1962, p. 619.
20. H. C. Chang and N. J. Grant. Transactions AIME, Vol. 197, 1953, p. 1175.
21. F. N. Rhines and A. W. Cochardt. NACA Technical Note 2746, July, 1957.
22. C. S. Roberts. Transactions AIME, Vol. 197, 1953, p. 1121.
23. B. Fazan, O. D. Sherby, and J. E. Dorn, Transactions AIME, Vol. 200, 1954, p. 920.
24. H. Brunner and N. J. Grant, Journal of Institute of Metals, Vol. 85, 1956-57, p. 77.
25. H. C. Chang and N. J. Grant. Journal of Metals, February, 1956, p. 177.
26. H. A. Wilhelm, O. N. Carlson, and J. M. Dickinson. Transactions AIME, Vol. 200, 1954, p. 915.
27. H. Bückle, Z. Metallkunde, Vol. 37, 1956, p. 53.
28. M. Hansen. Constitution of Binary Alloys, McGraw-Hill, N. Y., 1958, p. 980.

29. A. Taylor, N. J. Doyle, and B. J. Kagle. "Constitution Diagram of the Mo-Hf System", J. Less Common Metals, Vol. 3, 1961, p. 265.
30. R. T. Begley, R. W. Buckman, J. L. Godshall. 7th Quarterly Progress Report, Contract AF 33(616)-6258, October 1, 1962.
31. R. S. French and W. R. Hibbard. "Tensile Deformation of Copper", Trans. AIME, Vol. 188, 1950, p. 53.
32. W. H. Chang. "Strengthening of Refractory Metals", in Refractory Metals and Alloys, AIME Metallurgical Society Conferences, Vol. 11, Interscience, N. Y., 1961, p. 83.
33. P. A. Flinn. "Solid Solution Strengthening", in Strengthening Mechanisms in Solids, ASM, Metals Park, Ohio, 1962, p. 17.